Louisiana State University
LSU Digital Commons

2013

Fluorescent Materials for Chemical Sensing

Brian Gerard Imsick
Louisiana State University and Agricultural and Mechanical College

FLUORESCENT MATERIALS FOR CHEMICAL SENSING

A Dissertation

Submitted to the Graduate Faculty of the
Louisiana State University and
Agricultural and Mechanical College
in partial fulfillment of the
requirements for the degree of
Doctor of Philosophy

in

The Department of Chemistry

by
Brian Gerard Imsick
B.S., Randolph-Macon College, 2008
August 2013

In memory of

Michael F. Imsick

1954-1998

ACKNOWLEDGMENTS

I would like to acknowledge, first and foremost, Professor Evgueni E. Nesterov for his advice, guidance, and support. I value him as an excellent mentor and friend from whom I have learned a great deal while at Louisiana State University. I am grateful for having an advisor who has constantly challenged me while at LSU, whilst having a great deal of patience.

A special thanks to my committee, Drs. George Stanley, Graça Vicente, and William Crowe for their kindness, humor, and encouragement.

To group members, past and present (Carlos Chavez, Sourav Chatterjee, Sang Gil Youm, Chien-Hung Chiang Deepa Pangeni, Rajib Mondal, Drs. Jiba Raj Acharya, Jinwoo Choi, and Euiyong Hwang): Thanks for making Choppin 727 and Annex 460 great places to work.

Most importantly, I would like to recognize my wife, Anne Rabalais Imsick as a constant source of love and encouragement during my tenure at LSU. Her kindness and support kept me working when reactions were not.

I would also like to acknowledge the special efforts of Dr. George Stanley and Dr. Zakiya Wilson for securing funding via the US Department of Education for the Graduate Assistant for Areas of National Need (GAANN) program as financial support for the majority of my graduate career.

TABLE OF CONTENTS

LIST OF FIGURES

LIST OF SCHEMES

ABBREVIATIONS AND ACRONYMS

Cys	-Cysteine
D_{HV}	-Dichroic ratio
DDQ	-2,3-dichloro-5,6-dicyano-1,4-benzoquinone
DMF	-*N,N*-dimethylformamide
DMSO	-Dimethylsulfoxide
DPPA	-Diphenylphosphoryl azide
ET	-Energy Transfer
HOMO	-Highest Occupied Molecular Orbital
I	-Intensity
ITO	-Indium-tin oxide
K_{SV}	-Stern-Volmer quenching constant
LUMO	-Lowest Unoccupied Molecular Orbital
ODMS	-Octadecyldiethoxymethylsilane
PE	-Penta(*p*-phenylene ethynylene)
TBAF	-Tetrabutylammonium fluoride (Bu_4NF)
THF	-Tetrahydrofuran
TIPS	-Triisopropylsilyl

ABSTRACT

Materials incorporating fluorescent π-electron conjugated molecular species for sensing and imaging are advantageous over other detection or identification methods such as colorimetric reporters. Fluorescent materials offer easy recognition of binding events due to the highly sensitive nature of fluorescence techniques down to the single molecule level. The properties of fluorescent molecules allow for rapid attenuation of observable readout due to the facile transport of excited state energy *via* both inter- and intramolecular pathways.

This dissertation primarily focused on the development and study of a general platform for ratiometric fluorescent chemosensing using surface-immobilized oligomers, as well as in depth explorations of the unique properties of the chemosensors utilizing this platform. It encompasses bichromophoric fluorescent energy transfer cassettes consisting of a mono-disperse conjugated oligomer and a red-shifted energy transfer acceptor that is specifically reactive on the presence of a chosen analyte. Molecular organization of these cassettes into a surface-immobilized monolayer lends excellent and advantageous properties to the devices for sensing purposes primarily due to enhanced efficiency of intermolecular energy transfer within the monolayer. Several intriguing properties of this class of sensing devices are described, as well as how these properties, such as the effect of exciton delocalization and spatial control of energy transfer efficiency can be harnessed to generate practical chemosensing films that undergo significant emission wavelength (color) shift upon analyte exposure. The fundamental properties of this strategy toward ratiometric fluorescent chemosensing are described as applied to the measurements of acidity (pH) and fluoride ion concentration as practical examples.

A smaller project that is part of this dissertation involves the synthesis of a semi-napthofluorescein fluorescent dye with a reactive handle for bioconjugation. This new dye

exhibits an unusually large Stokes shift due to its broad absorption spectrum, and also shows highly bathochromically-shifted emission. The properties of this dye compound were studied and fully characterized and included as a chapter of this dissertation.

CHAPTER 1 π-CONJUGATED ORGANIC MATERIALS FOR FLUORESCENT CHEMOSENSING: AN INTRODUCTION

1.1 Fluorescent Sensing With Conjugated Polymers

Conjugated polymers are a vibrant research field with many potential materials applications. This class of polymers is characterized by extended conjugation throughout the length of the polymer chain through incorporation of only sp and/or sp^2 carbon centers, as well as similarly hybridized heteroatoms possessing lone electron pairs. Polymers of this type, such as poly-*p*-phenylene (PPP)[1], polythiophene (PT)[2], poly (*p*-phenylene vinylene) (PPV)[3], and poly(*p*-phenylene ethynylene) (PPE)[4] (Figure 1.1) have been applied to sensors, solar cells, field-effect transistors, and light-emitting diodes.[5]

PPP   PT   PPV   PPE
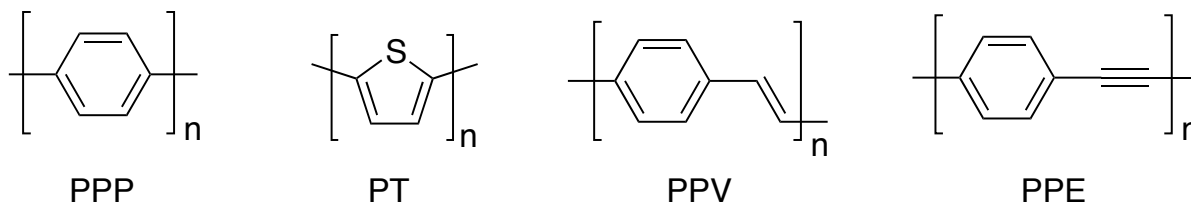
Figure 1-1. Representative examples of commonly used conjugated polymers for organic materials applications.

Transition from conjugated small molecules into oligomers or polymers transforms discrete HOMO-LUMO levels into progressively more diffuse band structures resembling valence and conduction bands akin to organic semiconductors.[6] The low-lying conduction band in a conjugated polymer results in relatively easy transport of excitons along the polymer conjugated backbone. A perturbation in this band structure caused by the presence of an analyte interaction along the polymer backbone inserts a quenching site (or a lower energy bathochromically-shifted site), resulting in the "funneling" of excitons generated over the length of the backbone into these analyte-dependent quenching sites by insertion of quencher LUMO into the polymer intergap space (Figure 1-2).[7]
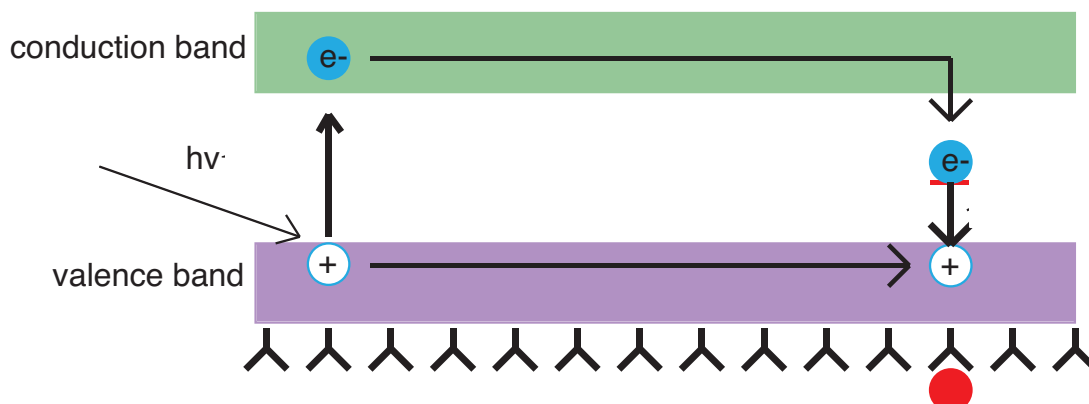
Figure 1-2. Diagram illustrating exciton migration towards a band gap perturbation caused by receptor-analyte interaction, resulting in quenched polymer emission due to insertion of quencher LUMO into the band structure of the polymer backbone.

The dramatic effect of electronic perturbations in a conjugated polymer results in easily observable fluorescent output changes, making conjugated polymers excellent fluorescent sensors due to the high signal amplification caused by the facility of exciton migration.[8] An example of an amplifying conjugated polymer that incorporates side groups acting as a receptor for fluoride ion is shown in Figure 1-3.[9] The presence of fluoride ion initiates a tandem desilylation-cyclization to form a coumarin species (red-colored in Figure 1-3) that acts as a low-energy acceptor of excited state energy from the polymer backbone, resulting in "turn-on" signal amplification.
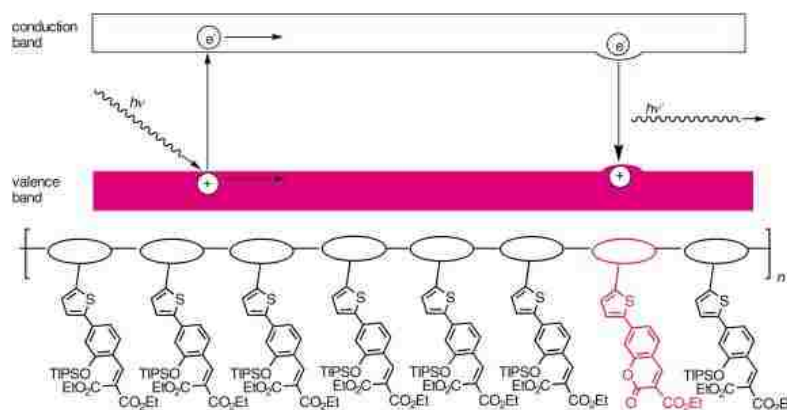
Figure 1-3. Diagram illustrating exciton migration towards a band gap perturbation caused by chemical reaction of analyte through the formation of a low energy chromophore on the polymer chain. Reproduced with permission from Ref. 9. Copyright © 2003 Wiley-VCH.

Due to the high sensitivity of devices fabricated from conjugated polymers, sub-stoichiometric amounts of analyte need only be present in a sample in order to achieve significant response, resulting in high optical gain in fluorescent detection. The most notable of this type of fluorescent polymer sensor utilizes the powerful quenching effects of nitroaromatics on conjugated polymers (Figure 1.4).[10,11]
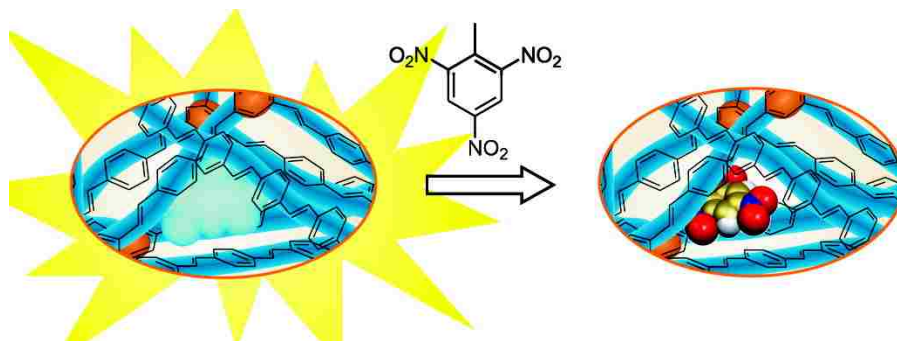
Figure 1-4. Amplifying conjugated polymer with a molecularly imprinted cavity capable of binding trinitrotoluene where it behaves as a quencher of the polymer fluorescence. Reproduced with permission from Ref. 11. Copyright © 2007 American Chemical Society.

1.2 Fluorescent Sensing With Small Molecules

Small fluorescent molecules do not possess the optical gain that is characteristic of conjugated polymers. Therefore, in order to achieve maximum response from a small molecule fluorescent sensor, the probe must react in a stoichiometric manner with the sensing molecule. The degree of reaction between analyte and sensor is dictated by the equilibrium or association constant of the transformation. Thus, transformations that occur to a poor extent or are thermodynamically unfavorable are not useful for small molecule chemosensing.[12] In addition, most small fluorescent probes are insoluble in aqueous environments. Aqueous sensing is the most desirable use of small molecule probes for practical purposes for applications towards real-time *in vitro* detection.

Enhancing the sensitivity of a single molecule fluorophore sensor is not without pitfalls. An increase in association constant of analyte and probe binding can cause irreversibility, and prevents the reuse of fluorescent probes on solid support, if desired.[13] In addition, it may be impossible to increase the association constants for particularly unreactive analytes due to their inherent poor reactivity or lack of suitable fluorescent probes. Based on these disadvantages, well-defined fluorescent probes are needed that harness sensitivity of conjugated polymers and convenience of small molecules for practical fluorescent chemosensing.

1.3 Latent Fluorophores as Components in Energy Transfer Cassettes and Ratiometric Sensing

A popular motif in the design of fluorescent probes relies on non-covalent interactions.[14] Examples of such interactions are hydrophobic π-π stacking, hydrogen bonding, or the formation of metal ion complexes to modify the spectral properties of the fluorophore.[15] Unfortunately, such minor modifications have relatively insignificant spectroscopic effects on the fluorophore itself,[16] making it difficult to discern the presence of analyte without the aid of sophisticated instrumentation. Thus, more substantial covalent interactions are required, such as the formation or breaking of bonds caused by chemical reaction of the analyte to release the indicator. The structural modification of the probe by a chemical reaction offers dramatic spectral changes, usually the generation of a colored or fluorescent dye.[17] It is important to note at this stage that a probe that operates via chemical reaction is formally a dosimeter, since the probe usually cannot be reset due to the chemical transformation being irreversible.[18] A further benefit of utilizing covalent interactions to generate a fluorescent molecule as an output is diminished potential for false-positives (as the selectivity is dictated by structure-reactivity relationships) or background interference, due to the initial state of the sensor being completely non-fluorescent. These "turn-on" sensors are known as reactive probes, or latent fluorophores.[19] Development of new,

selective fluorescent probes for reactive analytes is a burgeoning field and offers many options for incorporation into energy transfer cassettes to generate ratiometric fluorescent sensors.

Two fluorophores can be covalently linked to assemble a molecular cassette that operates on an energy transfer principle. Photoexcitation of a higher energy fluorophore covalently linked to a latent, "turn-on" receptor in the absence of analyte will result in solely the emission from the higher energy fluorescent moiety. As analyte is introduced, an increasing amount of lower energy bathochromically-shifted fluorescent moieties will accept excited state energy from the higher energy donor fluorophore (Figure 1-5).
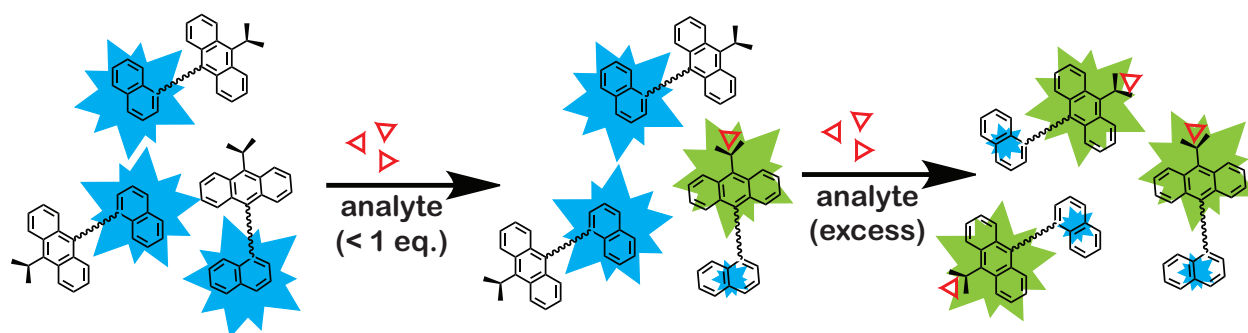
Figure 1-5. Cartoon illustrating the origin of ratiometric fluorescent response in energy transfer casettes, when the higher energy fluorophore is excited in the presence of varying amounts of analyte (red triangles) that activate a lower energy fluorophore.

From a spectroscopic standpoint, this results in dual fluorescent output with a decrease of the intensity of the higher energy band as well as concomitant intensity enhancement in the lower energy band, which ideally pivots around an isoemissive point (Figure 1-6).[20] Molecular systems that exhibit such variations in dual emission bands upon increasing analyte concentration are formally known as "ratiometric sensors." Plots of the concentration dependence on the ratios of either peak intensity or area generated are then interpolated with a trend line, and sensing devices are then used for field measurements of unknown concentrations of the analyte. Ratiometric fluorescent sensors are considered more reliable and more convenient for a few reasons: (1) Higher reproducibility due to presence of intrinsic reference

signal; (2) independence of environmental factors, such as light source intensity, dye concentration, and film thickness; and (3) avoidance of the need for "pre-calibration" of sensing devices prior to performing field experiments, which may not be possible for reactive probes. [21-23]
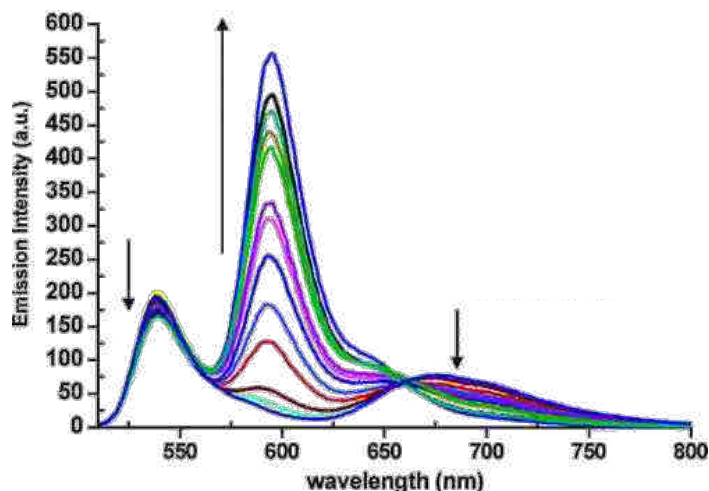
Figure 1-6. Representative example of the fluorescent ratiometric response of a bichromophoric ET cassette caused by "masking" the acceptor fluorophore by analyte binding. The band at ~700 nm decreases with simultaneous appearance and growth of the 600 nm band upon increasing analyte concentration. The spectrum features a well-defined isoemissive point at ~660 nm. Reproduced with permission from Ref. 22. Copyright © 2006 American Chemical Society.

1.4 Mechanisms of Energy Transfer[24]

The transport of excitation energy can occur through two pathways known as the through-space Förster and through-bond Dexter mechanisms. The Förster mechanism is a radiationless transition occurring through Coulombic interactions between electronic transition dipoles of donor and acceptor moieties. Several factors were shown to be important in this process. Although there is no requirement for chemical bonding between the donor and acceptor, there needs to be considerable overlap between donor emission and acceptor absorption. The Coulombic interactions between the transition dipoles also dictate the efficiency of this process. Dipole-dipole interactions, according to the classical treatment of charged bodies, decay at an

inverse-cubed relationship. With respect to energy transfer, two Coulombic bodies are being treated, which results in an inverse-sixth relationship between intermolecular distances being incorporated into the efficiency of such a process. In addition, relative orientation between the dipoles is also important. The dependence of the efficiency of "through-space" energy transfer on these variables according to Förster theory is described by Equation 1.1:

$$k_{ET} = C \frac{\kappa^2 k_D^o}{R_{DA}^6} J \tag{1.1}$$

In this equation, k_{ET} is the efficiency (rate constant) of Förster-type energy transfer; C is a constant that corrects for variables in experimental conditions, such as solvent index of refraction and concentration. Orientation of molecular transition dipoles is represented by κ^2, where in isotropic conditions, such as in solution or a spin-coated film, it is assigned a value of 2/3 and increased to 1 when these dipoles are in parallel alignment (this value is maximized to 4 when transition dipoles are parallel *and* co-linear). J represents the spectral overlap integral, which is the overlap between donor emission and acceptor absorption.

The Dexter mechanism of energy transfer,[25] also known as an electron exchange mechanism, can be visualized as a simplified cartoon in Figure 1-7.
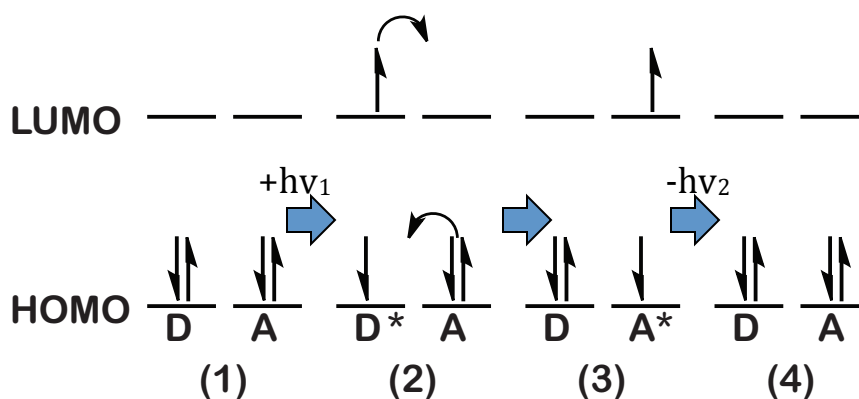
Figure 1-7. Simplified graphical representation of the Dexter mechanism of energy transfer explaining the origin of the acceptor emission upon donor excitation.

In a simplified description of the Dexter mechanism, a ground state donor-acceptor cassette (1) has its donor unit preferentially photoexcited by careful choice of excitation wavelength (2). Next, the electron that has been promoted to the LUMO of the donor "hops" to the LUMO of the acceptor. In either a concerted or stepwise mechanism, an electron from the acceptor HOMO is transferred to the HOMO of the donor, resulting in the excited state (3). The overall consequence of this electron exchange is transferring the excited state to the acceptor chromophore. Finally, the acceptor relaxes and emits a photon (4) and the whole molecule returns to the ground state. The presence of separately localized HOMO and LUMO in different regions of a long molecule (as predicted by computational experiments) is evidence that this exchange mechanism is likely to occur.[26] This exchange mechanism is not necessarily related to spectral overlap; however, it is even more closely related to the distance and molecular orbital interactions between the donor and acceptor. This essentially forces the donor and acceptor unit to be electronically conjugated *via* π-bonds in organic molecules. The efficiency of Dexter energy transfer is determined by Equation 2.2:

$$k_{ET} = KJe^{-\frac{2R_{DA}}{L}}$$

(1.2)

The overlap integral, *J*, is repeated in the Dexter theory of energy transfer; however, unlike the overlap integral in equation (1.1), it is normalized in this case as only an energetic match is necessary. The distance dependence on the efficiency of Dexter energy transfer is an exponential decay, related to separation of donor and acceptor relative to their van der Waals radii, *L*.

Upon comparison of these two theories of energy transfer, it is evident that the Förster mechanism is essentially a long range process, while the Dexter mechanism is short range due to the exponential dependence on donor-acceptor distance. However, π-electron conjugation results in attenuation of the Dexter energy transfer toward lesser dependence on the interchromophore distance, as far as the strong electronic coupling is preserved.

1.5 Research Focus

The main focus of this dissertation is the development of thin film ratiometric fluorescent sensors generated by the covalent immobilization of bichromophoric energy transfer cassettes based on π-electron conjugated oligomers, as well as the in-depth investigations into the photophysical and sensing properties of these materials. These energy transfer cassettes consist of a "universal" donor moiety, utilizing a penta(p-phenylene)ethynylene (PE) chromophore coupled with a lower energy acceptor as an "end-cap" that is designed to specifically react with analyte *via* a chemical reaction which releases or "activates" the terminal acceptor. The general operating principle is that the interaction with the analyte attenuates the energy gap of the end-cap receptor, making it higher or lower than the energy gap of the PE donor unit. This energy gap modification either enables or prohibits energy transfer to the end cap receptor group. The extent of reaction on the surface is related to the proximity of unreacted sensor molecules to reacted acceptor sites which results in varying intensities of the donor and acceptor emission bands due to increasing/decreasing efficiency of energy transfer processes. The fundamental explaination of the origin of this ratiometric emission is displayed as a cartoon in Figure 1-8 (next page).
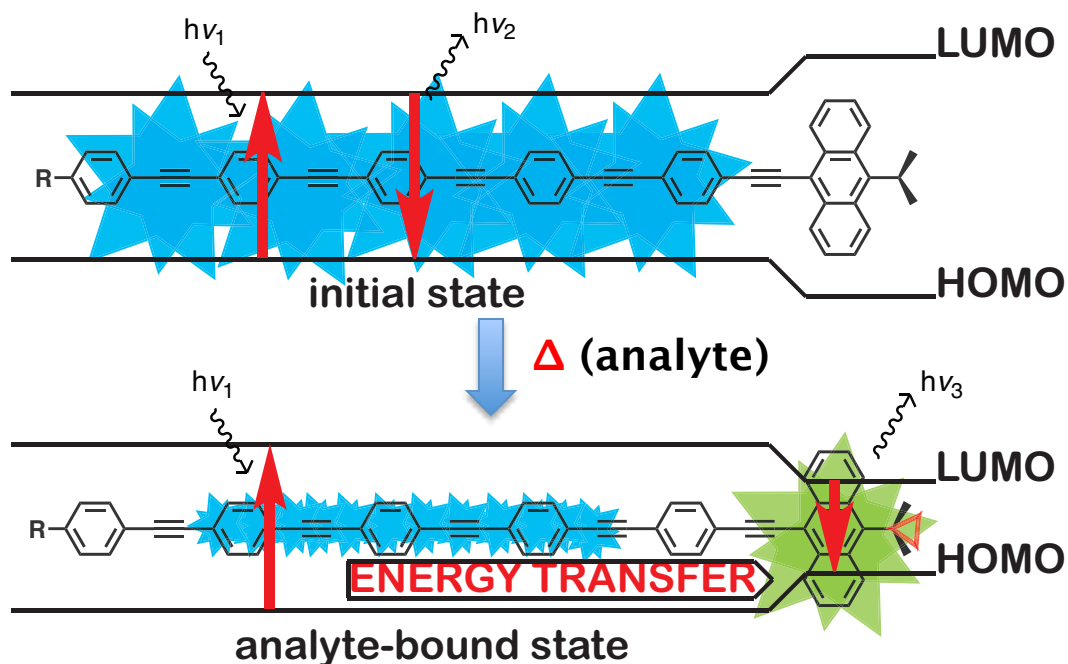
Figure 1-8. Simplified energy diagram representation of the origin of ratiometric response of fluorescent sensors described in this dissertation.

This project originated with the initial development of a ratiometric fluorescent monolayer sensor for cysteine as a proof of concept example (Figure 1.9).[27] Prior work has confirmed that the 9-anthracenyl functionality was an excellent energy acceptor for photoexcited PE donor.[28] In the proof-of-concept example, conversion of the electron-withdrawing 9-anthraldehyde functional group to a more electron donating substituent had a dramatic effect on the electronic properties of the end cap receptor. The effect of such a transformation was to provide sufficient energy gap modification to the anthracenyl receptor upon conversion to thiazolidine when the sensor was exposed to cysteine.
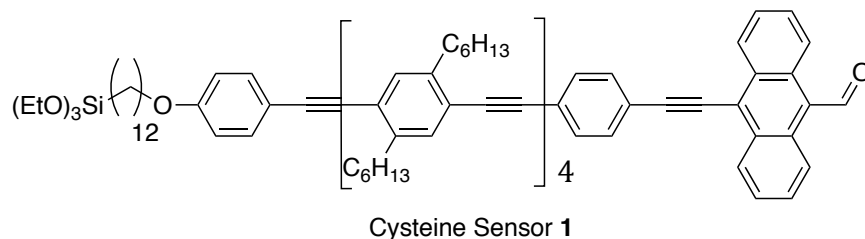
Cysteine Sensor **1**

Figure 1.9. Molecular structure of cysteine (Cys) sensor **1**.

10
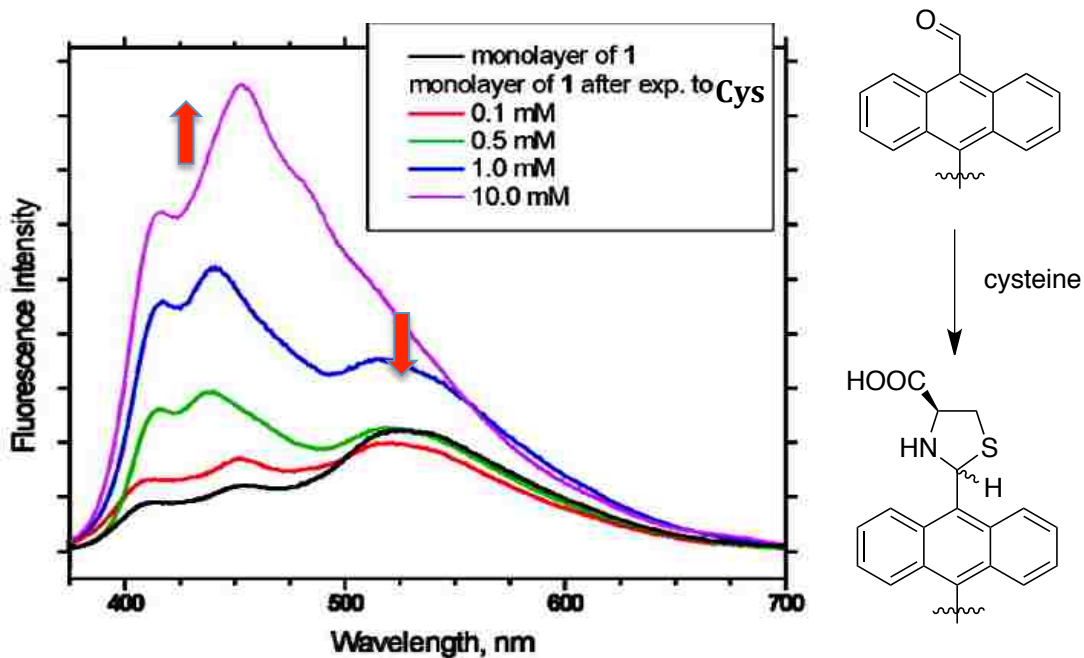
Figure 1-10. Ratiometric response of the surface-immobilized monolayer of **1** upon exposure to increasing concentrations of the amino acid. Reproduced with permission from Ref. 27. Copyright © 2009 American Chemical Society.

In the absence of cysteine, excitons initially formed by photoexcitation of the PE unit migrate to the lower energy anthraldehyde chromophore resulting in emission from the receptor at approximately 540 nm. However, when the monolayer was exposed to aqueous solutions of cysteine, the energy gap of the anthracene receptor was increased to the point where the energy transfer was hindered, resulting in only PE emission at 420 nm (Figure 1-10). While this reaction was clearly evident in the monolayer using fluorescence studies, and could be reversed after exposure of the monolayer-functionalized slides to dilute HCl causing thiazolidine hydrolysis to restore the receptor emission, the corresponding reaction was found not to occur in solution. It was hypothesized that there was significant optical gain in the sensing of analytes using surface immobilized monolayers due to the substantial exciton delocalization within the monolayer. However, this hypothesis was mainly unproven and required further investigation as

to the extent and effect of this delocalization prompting further studies to be described in this dissertation.

In Chapter 2, a ratiometric fluorescent thin-film sensor for pH is described. The intermolecular exciton delocalization phenomenon discovered in the case of the cysteine sensor was harnessed to transform fluorescein, a narrow-range threshold fluorescent pH sensor, to a broad-range pH sensor. In addition, the covalently immobilized monolayers were compared in sensing ability to a random spin cast film and the difference in behavior between the two was explained. An in-depth study of the extended two-dimensional exciton delocalization on sensing performance of these monolayers to be used as a new and superior method of fluorescent detection is also described.

In Chapter 3, tuning the signal amplification in the monolayer-based sensing platform exemplified by a thin-film ratiometric fluorescent sensor for fluoride ion concentration is described. It was observed that the initially prepared device was too sensitive and reached saturation much too rapidly to be useful as a ratiometric fluorescent sensor due to extremely narrow operating range. A simple method of tuning the photonic amplification through attenuation of the intra-monolayer exciton migration was developed that is applicable to all sensing materials of this class. Additional experiments are also described in Chapter 3 that probe the nature of the monolayers in an attempt to further explain this unusual and exciting high level of exciton delocalization previously found in these materials.

The concluding Chapter 4 describes the design and synthesis of a regioisomerically pure, broad absorption fluorescent dye. This dye, with an unusually large Stokes shift, can be potentially utilized as a universal FRET tag for biological and biomedical experiments.

1.6 References

(1)   Ambrosch-Draxyl, C.; Majewski, J. A.; Vogl, P.; Leising, G. First-Principles Studies of the Structural and Optical Properties of Crystalline poly(*para*-Phenylene). *Phys. Rev. B*, **1995**, *51*, 9668-9676.

(2)   McCullough, R. D. The Chemistry of Conducting Polythiophenes. *Adv. Mater.* **1998**, *10*, 93-116.

(3)   Skotheim, T. A; Elsenbaumer, R. L.; Reynolds, J. R. *Handbook of Conducting Polymers, 2nd ed.*; CRC Press, **1997**.

(4)   Bunz, U. H. F. poly(Aryleneethynylene)s: Syntheses, Properties, Structures, and Applications. *Chem. Rev.* **2000**, *100*, 1605-1644.

(5)   Dai, L. *Intelligent Macromolecules for Smart Devices*; Springer, **2004**.

(6)   Skolheim, T. A.; Elsenbaumer, R. L.; Reynolds, J. R., Eds. *Handbook of Conducting Polymers, 2nd ed;* Marcel Dekker, **1998**.

(7)   Swager, T. M.; Gil, C. J.; Wrighton, M. S. Fluorescence Studies of poly(*p*-Phenyleneethynylene)s: The Effect of Anthracene Substitution. *J. Phys. Chem.* **1995**, *99*, 4886-4893.

(8)   Thomas III, S. W.; Guy, D. J.; Swager, T. M. Chemical Sensors Based on Amplifying Fluorescent Conjugated Polymers. *Chem. Rev.* **2007,** *107*, 1339-1386.

(9)   Kim, T.-H.; Swager, T. M. A Fluorescent Self-Amplifying Wavelength-Responsive Sensor Polymer for Fluoride Ions. *Angew. Chem. Int. Ed.* **2003**, *42*, 4803-4806.

(10)   Yang, J.-S.; Swager, T. M. Porous Shape Persistent Fluorescent Polymer Films: An Approach to TNT Sensory Materials. *J. Am. Chem. Soc.* **1998**, *120*, 5321-5322.

(11)   Li, J.; Kendig, C. E.; Nesterov, E. E. Chemosensory Performance of Molecularly Imprinted Fluorescent Conjugated Polymer Materials. *J. Am. Chem. Soc.* **2007**, *129*, 15911-15918.

(12)   Zhou, Q.; Swager, T. M. Methodology for Enhancing the Sensitivity of Fluorescent Chemosensors: Energy Migration in Conjugated Polymers. *J. Am. Chem. Soc.* **1995***, 117*, 7017-7018.

(13)   Callan, J. F.; de Silva, A. P.; Magri, D. C. Luminescent Sensors and Switches in the Early 21st Century. *Tetrahedron* **2005**, *61*, 8551-8588.

(14)   de Silva, A. P.; Gunaratne, H. Q. N.; Gunnlaugsson, T.; Huxley, A. J. M.; McCoy, C. P.; Rademacher, J. T.; Rice, T. E. Signal Recognition Events with Fluorescent Sensors and Switches. *Chem. Rev.* **1997**, *97*, 1515-1566.

(15)   Valeur, B.; Leray, I. Design Principles of Fluorescent Molecular Sensors for Cation Recognition. *Coord. Chem. Rev.* **2000**, *205*, 3-40.

(16)   Jun, M. E.; Roy, B.; Ahn, K. H. "Turn-on" Fluorescent Sensing with "Reactive" Probes. *Chem Commun.*, **2011**, *47*, 7853-7601.

(17)   Kobayashi, H.; Ogawa, M.; Alford, R.; Choyke, P. L.; Urano, Y. New Strategies for Fluroescent Probe Design in Medical Diagnostic Imaging. *Chem. Rev.* **2010**, *110*, 2620-2640.

(18)   Cho, D.-G.; Sessler, J. L. Modern Reaction-Based Indicator Systems. *Chem. Soc. Rev.*, **2009**, *38*, 1647-1662.

(19)   Janata, J. Introduction: Modern Topics in Chemical Sensing. *Chem. Rev.* **2008**, *108*, 327-328.

(20)   Grynkiewicz, G.; Poenie, M.; Tsien, R. Y. A New Generation of Ca^{2+} Indicators with Greatly Improved Fluorescence Properties. *J. Biol. Chem.* **1985**, *260*, 3440-3450.

(21)   Schäferling, M.; Duerkop, A. Intrinsically Referenced Fluorimetric Sensing and Detection Methods. *Springer Ser. Fluoresc.* **2008**, *5,* 373-414.

(22)   Coskun, A.; Akkaya, E. U. Signal Ratio Amplification via Modulation of Resonance Energy Transfer: Proof of Principle in an Emission Ratiometric Hg(II) Sensor. *J. Am. Chem. Soc.* **2006**, *128*, 14474-14475.

(23)   Takausa, H.; Kikuchi, K.; Urano, Y.; Kojima, H.; Nagano, T. A Novel Design Method of Ratiometric Fluorescent Probes Based on Fluorescence Resonance Energy Transfer Switching by Spectral Overlap Integral. *Chem. Eur. J.* **2003**, *9*, 1479-1485.

(24)   Turro, J. N. *Modern Molecular Photochemistry;* University Science Books, **1991**.

(25)   Dexter, D. L. A Theory of Sensitized Luminescence in Solids. *J. Chem. Phys.* **1956**, *21*, 836-861.

(26)   Kim, T. G.; Castro, J. C.; Loudet, A.; Jiao, J. G.-S.; Hochstrasser, R. M.; Burgess, K.; Topp, M. R. Correlations of Structure and Rates of Energy Transfer for Through-Bond Energy-Transfer Cassettes. *J. Phys. Chem. A* **2006**, *110*, 20-27.

(27)   Acharya, J. R.; Zhang, H.; Xian, Li.; Nesterov, E. E. Chemically Controlled Amplified Ratiometric Fluorescence in Surface-Immobilized End-Capped Oligo(*p*-phenylene ethynylene)s. *J. Am. Chem. Soc.* **2009**, *131*, 880-881.

(28)   Nesterov, E. E.; Zhu, Z.; Swager, T. M. Conjugation Enhancement of Intramolecular Exciton Migration in Poly(p-phenylene ethynylene)s. *J. Am. Chem. Soc.* **2005,** *127*, 10083-10088.

CHAPTER 2 SURFACE-IMMOBILIZED MONOLAYERS OF CONJUGATED OLIGOMERS AS A PLATFORM FOR FLUORESCENT SENSOR DESIGN: THE EFFECT OF EXCITON DELOCALIZATION ON CHEMOSENSING PERFORMANCE[*,].**

2.1 Introduction

Densely packed films, such as a random spin-coated film of a conjugated polymer, exhibit rapid and facile migration of excited states to quenching or lower energy sites. The close intermolecular contact distances between polymer chains and the random distribution of electronic transition dipole moment vectors creates conditions that make it difficult to control exciton migration efficiency within the film. The use of conjugated polymers also creates another challenge in achieving control of the orientation of the molecules or chains themselves. Some examples of controlled molecular organization of conjugated polymers include Langmuir films[1] or liquid crystalline materials.[2] Despite some success in controlling polymer orientation and molecular organization, these methods still prove difficult in controlling exciton migration efficiency to design ratiometric sensors from these polymers. It is, however, much more convenient to control organization of small or medium-sized molecules.[3,4] Small molecule fluorescent sensors are easy to synthesize and purify, as well as enforce molecular organization by the formation of surface-immobilized monolayers. In fact, surface-immobilized monolayers of fluorescent molecules have been proven to be an effective method of fluorescent sensing for practical applications.[5-7] However, small molecule sensing, even sensing with more extensively delocalized fluorescent oligomers, suffers from a significant drawback.

Compared to conjugated polymers, small oligomers lack the efficient delocalization of excitons which is characteristic of conjugated fluorescent polymers. The consequence of poor exciton delocalization is a lack of signal amplification of analyte binding response. There are several obstacles that need to be overcome in order for a thin-film of molecularly organized oligomers to mimic the ideal sensing properties of a conjugated polymer. Uniform alignment of small π-conjugated fluorescent oligomers in a densely-packed monolayer should offer an excellent compromise to generate a useful intrinsically amplifying sensing platform. Dense packing ensures close intermolecular distances in order to offer efficient exciton "hopping" between oligomeric units. It was predicted that steric interactions within a monolayer would enforce parallel orientation of the rod-like rigid oligomer molecules thus offering ideal geometry for maximizing intermolecular energy transfer.

Recently, this concept of effective small oligomer monolayer fluorescent sensing has been utilized in the design of a ratiometric thin film sensor for cysteine.[8] It was observed that there was a high optical gain due to the efficient intermolecular energy transfer between rod-like end capped conjugated oligomers within the monolayer. This extended exciton delocalization resulted in photonic amplification in signal response in the ratiometric fluorescent sensor monolayers. The hypothesis was made that the optimal combination of dense packing and the enforced uniform molecular orientation in the monolayer rendered the small oligomers the ideal combination of factors to emulate the properties of a conjugated polymer sensor, with the added benefit of ratiometric fluorescent sensing behavior to yield a practically useful device. The concepts derived from this early work were applied to the conversion of a single-wavelength threshold sensor to a broad range, full-scale, ratiometric fluorescent sensor for pH.
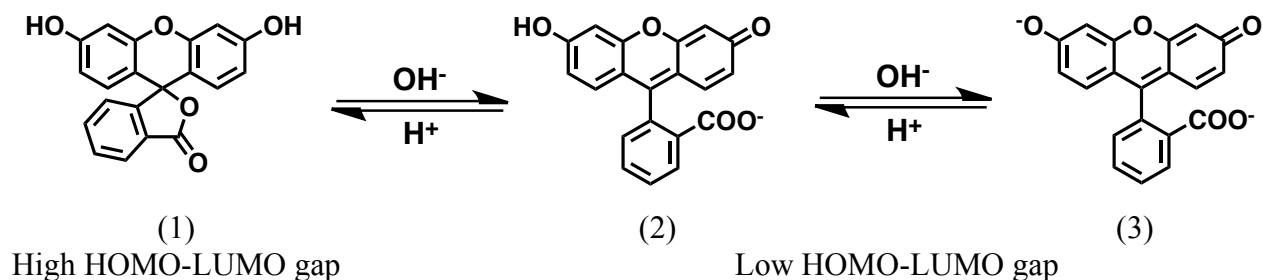
Figure 2.1. The three forms of fluorescein upon successive deprotonation of acidic hydrogens and the generation of a highly-emissive fluorophore.

Fluorescein is a well-known pH indicator.[9] It is a water-soluble dye that exists in three forms: a neutral lactone form (1, Figure 2.1); an anionic, ring opened form (2); and a dianionic form (3). Upon increasing pH, delocalization of the phenolate anion formed by deprotonation of the minimally fluorescent neutral lactone (1) resulted in a π-electron delocalized and highly fluorescent form (2) with the emission band maximum at approximately 525 nm. At even higher pH conditions, a doubly anionic form exists through the second deprotonation of the remaining phenolic oxygen (3). These spectroscopic properties of fluorescein make it a suitable and well-behaved acceptor of energy transfer from the photoexcited PE unit. The transition from a non-fluorescent compound to a fluorescent, bathochromically-shifted low energy gap form makes an ideal situation for increasing energy transfer to a fluorescein end cap with increasing pH.
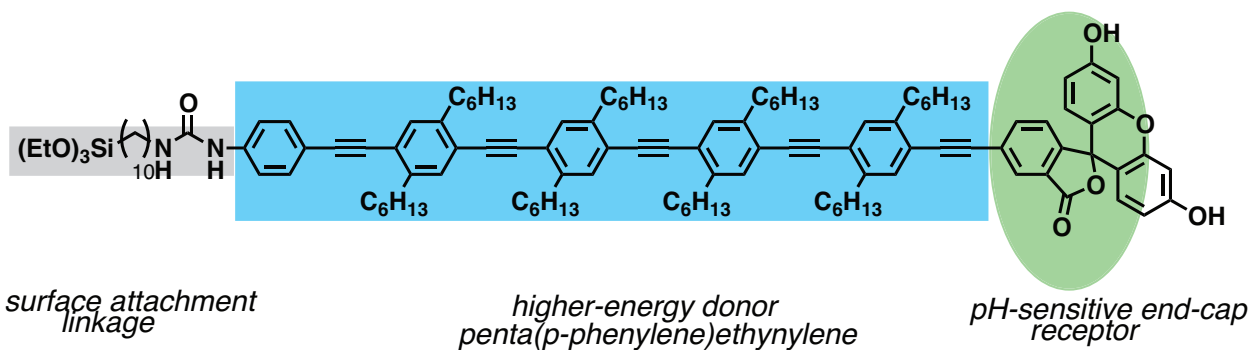
Figure 2.2. Structure of the ratiometric fluorescent pH sensor molecule used to generate surface-immobilized monolayers for pH sensing.

18

An energy transfer cassette consists of three fragments (Figure 2.2): The fluorescein end-cap, the PE donor group, and a triethoxysilyl-terminated surface attachment linkage that provides a convenient handle for assembly on a glass surface. Monolayers of this compound, once immobilized onto a glass surface constitute the ratiometric fluorescent pH sensing device described in this chapter.
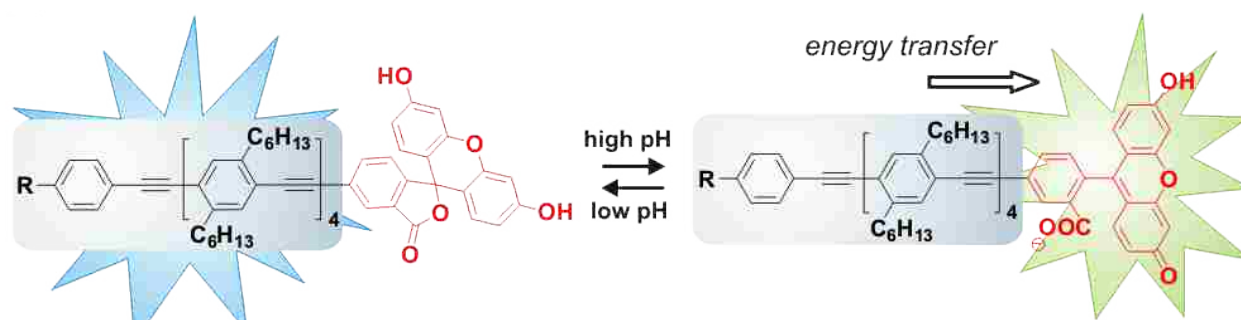
Figure 2.3. Origin of ratiometric response and general operating principle of the pH sensor described in this section.

Given the known properties of fluorescein as a pH dependent dye, at low pH the non-emissive fluorescein will be unable to accept excitons from the photoexcited PE donor unit. As the pH is adjusted incrementally towards more basic conditions, a larger percentage of the fluorescein groups exists in the highly delocalized and fluorescent anionic form and is therefore capable of accepting the excitons from the photoexcited PE donor unit (Figure 2.3). This results in increasing emission intensity of the fluorescein acceptor, with simultaneous decrease of the intensity of the higher-energy PE band. Overall, the relative ratio between the intensities of these two bands is controlled by the pH of the medium where the monolayer is exposed.

2.2 Results and Discussion

2.2.1 Synthesis

Scheme 2.1. Synthesis of pH sensor compound.
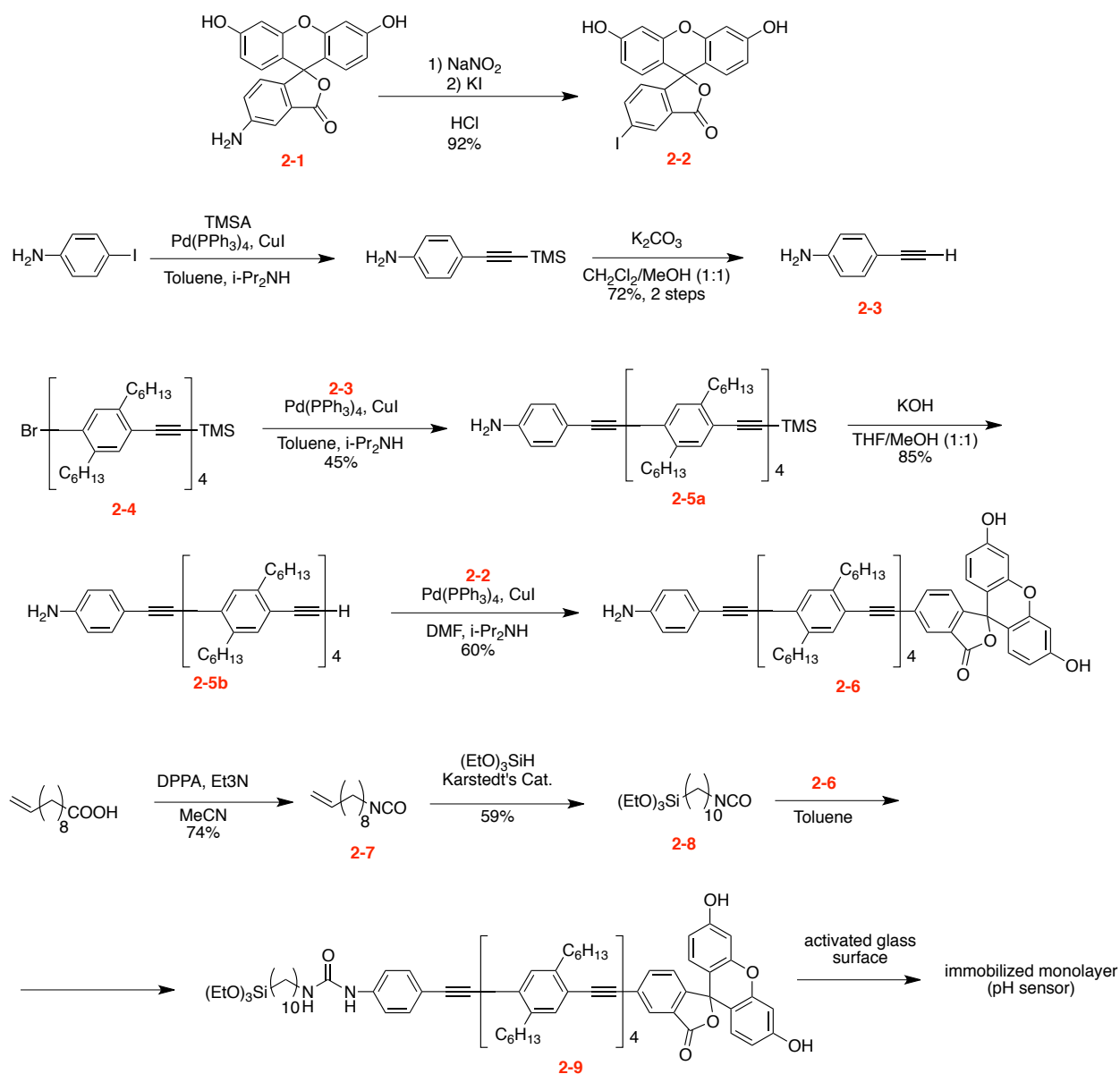
The pH sensor was assembled from its constituent parts in a convergent manner (Scheme 2.1). Synthesis of fluorescein with a synthetic handle for metal-catalyzed coupling reactions (halogen or pseudohalogen) is not possible through the classical Friedel-Crafts type condensation

reaction, which is the traditional method for the synthesis of fluorescein,[10] to obtain solely a single required regioisomer. A handle at the 5-position of the phenyl ring of fluorescein is desired for ideal molecular geometry when attached to the PE unit to orient the reactive portions of the receptor directly upwards into a sample solution. A classical route--Condensation of a halogenated phthalic anhydride with two equivalents of resorcinol will yield two regioisomers of halogenated fluorescein. Therefore, an alternate approach was needed, starting from 5-aminofluorescein (**2-1**) which was converted to the desired 5-iodofluorescein *via* diazotization and substiution with potassium iodide (Sandmeyer reaction) to form the receptor (**2-2**) with the desired handle for metal-catalyzed coupling reactions.[11]

The second component, the PE donor unit began with 4-iodoaniline, which was coupled using Sonogashira conditions with TMS-acetylene.[12] Subsequent base-mediated desilylation with potassium carbonate yielded the free acetylene (**2-3**). Compound **2-3** was coupled using the same Sonogashira conditions to previously synthesized tetramer **2**-4 to yield **2-5a** (generated by iterative Sonogashira coupling of dihexyl-substituted 4-halophenylacetylenes.[8] The final deprotection of the trimethylsilyl group under alkaline conditions completed the PE chromophore unit (**2-5b**). Compounds **2-5b** and 5-iodofluorescein (**2-2**) were coupled using yet another Sonogashira reaction, resulting in amino-terminated pH sensor (**2-6**). Unfortunately, the coupling of this compound was complicated by the partial catalytic reduction of fluorescein in the reaction conditions. Addition of a small amount of DDQ was found necessary to oxidize the end cap back to fluorescein.[†]

The surface attachment linker was synthesized through the Curtius rearrangement of ω-undecenoic acid using diphenylphosphoryl azide (DPPA) to form isocyanate (**2-7**).[13] Isocyanates are ideal for reactions with the amine on the terminus of the pH sensor **2-6** for two reasons: the isocyanate functional group is highly reactive towards nucleophiles and any such reactions result in high-yielding, robust urea coupling products requiring minimum purification. The terminal double bond of compound **2-7** was hydrosilylated with $(EtO)_3SiH$ using Karstedt's catalyst (see below)[14] to install the triethoxysilyl group, which is a handle for reaction with hydroxyl groups on activated glass, on compound **2-8**.

The decision to hydrosilylate at this step was advantageous due to the ability to purify the relatively volatile compound **2-8** by distillation (as opposed to column chromatography which would result in loss silylated of product due to its immobilization on silica gel). Distillation is a convenient purification method to remove the catalyst, which is a platinum species suspended in a matrix of vinyl-terminated poly(dimethyl)siloxane, and is non-volatile. There is a critical advantage in using this methodology (Method A, Scheme 2.2) as opposed to the previously developed approach[8] involving hydrosilylation of the terminal vinyl group in almost complete sensor molecule at the end of the synthesis (Method B, Scheme 2.2), due to the risk of hydrosilylation of the triple bonds, as well as the inability to adequately purify the final product. In the new approach, a solution of the isocyanate attachment linkage **2-8** and amine-terminated pH sensor **2-6** was simply heated gently overnight to form a robust urea linkage, resulting in the pH sensor ready for immobilization (**2-9**) on activated glass surfaces. Additional details on the synthesis and characterization of these compounds are available in the Experimental Section.

Scheme 2.2. Methods of surface attachment linkage installation.
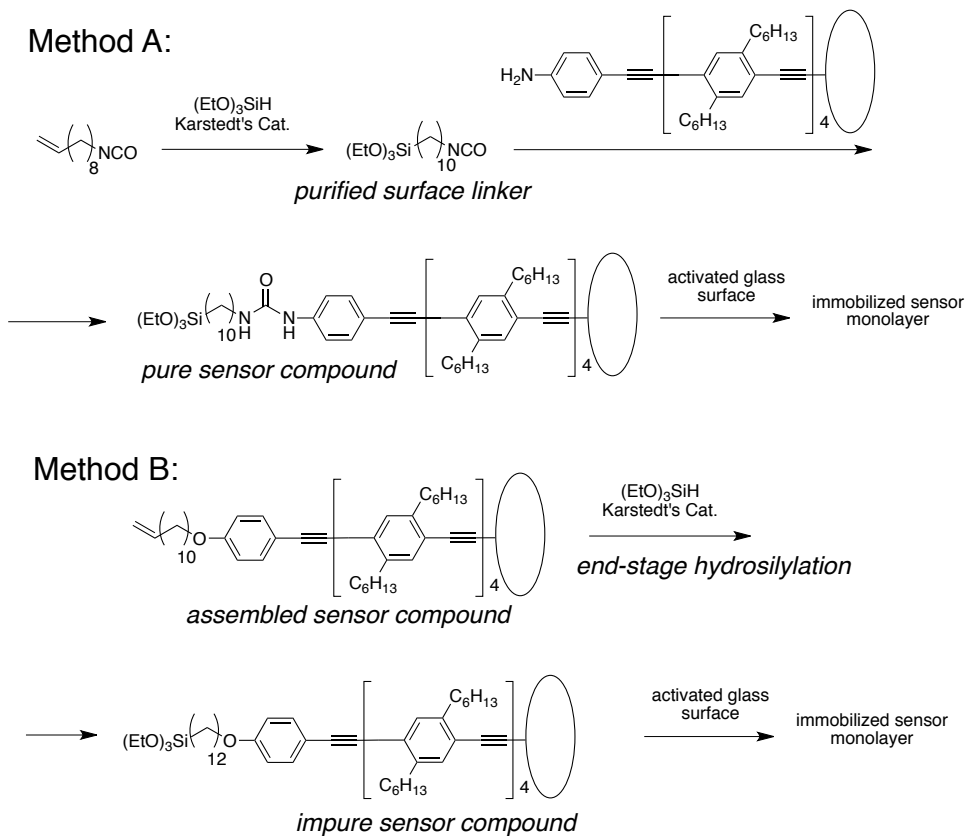
In the course of this project, an alternative method has been developed to generate pH sensing monolayers that simplifies synthetic efforts by the use of a silyl-protected fluorescein **2-A** (Scheme 2.3), utilized for a separate project described in Chapter 3 of this dissertation, that eliminated the need for oxidative workup and increased the overall product yields. The silyl-protected fluorescein was also readily soluble compared to 5-iodofluorescein, enabling the Sonogashira coupling reaction to occur in the toluene-diisopropylamine solvent mixture (yielding **2-B**) instead of a high-temperature reaction in a hard to remove solvent such as DMF. Coupling of **2-B** with isocyanate linker **2-8** yielded the silyl-protected sensor molecule **2-C** ready for surface immobilization to form monolayers (**2-D**). After immobilization to form monolayer, the silyl protecting groups on the monolayer surface were easily cleaved by exposure to aqueous pH 3 buffer to yield pH sensing monolayer **2-9A**.

Although preparation of the pH-sensing monolayer by this approach was practically more convenient (relative to the preparation of **2-9** and its subsequent surface immobilization), it had a disadvantage of producing a less densely packed monolayer, as could be seen from lower intensity of acceptor fluorophore emission in pH ratiometric response (vide infra). Thus, the actual choice of the approach to generate the monolayer should be decided by considering both advantages and disadvantages of these two methods.

Scheme 2.3. Modified synthetic route towards surface-immobilized pH sensors. (TIPS = triisopropylsilyl)
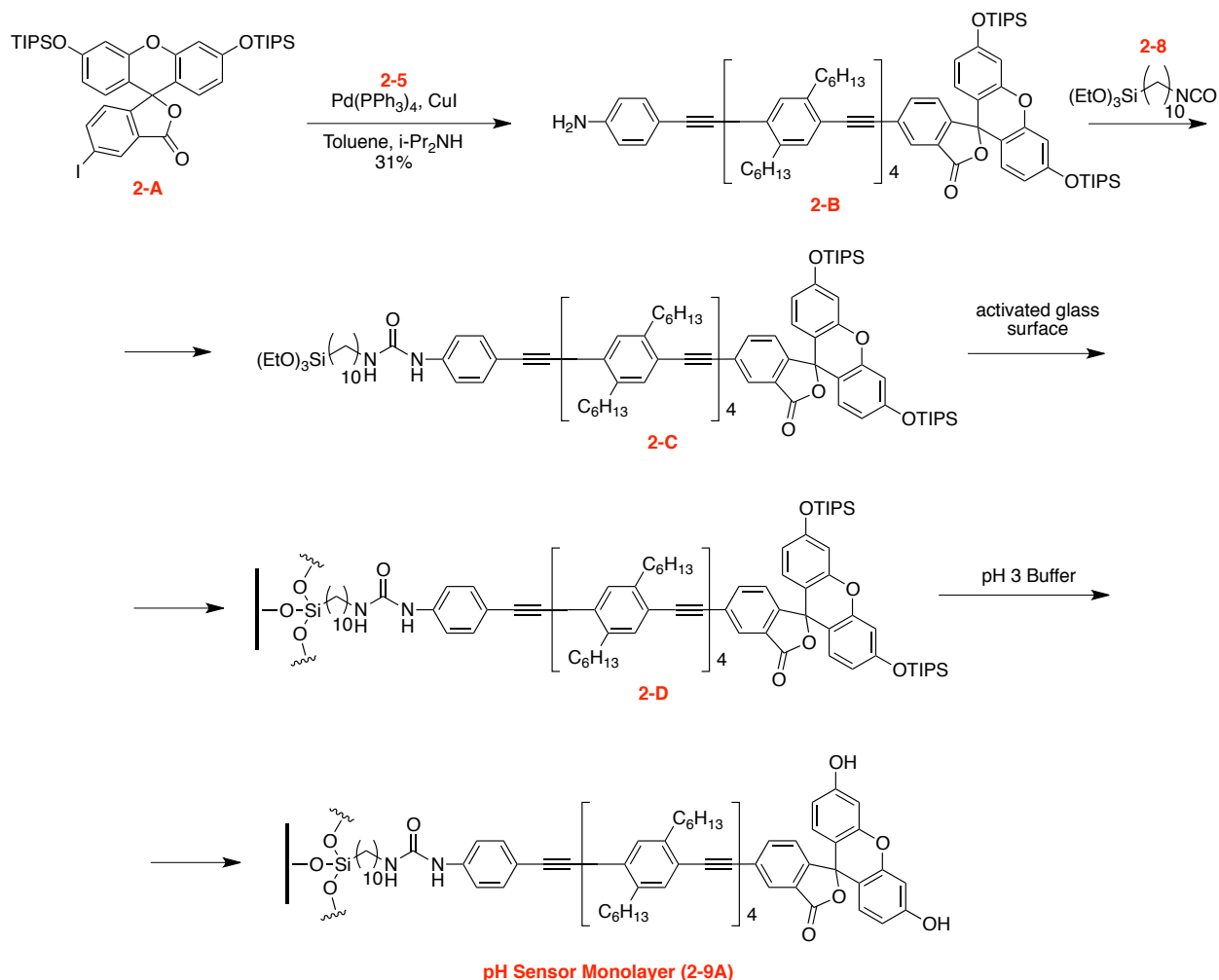
2.2.2 Preparation of Surface Immobilized Monolayers of pH Sensor

Glass cover slips (14mm x 25 mm) were activated using Piranha solution, then rinsed with ultrapure water. Piranha solution is a mixture of 98% sulfuric acid and 30% hydrogen peroxide, and at high temperatures generates a variety of reactive oxygen species that results in hydroxylation of the surface of glass. Hydroxyl-terminated glass (-OH) is very reactive towards siloxanes. The active glass surface, in the presence of compounds **2-9 or 2-C**, forms covalent bonds to the silyl anchor, hence covalently immobilizing the molecules by simply heating the glass slides in a dilute solution of either compound. For the immobilization of pH sensor **2-9**, the glass slides were heated in a dilute solution of the sensor in toluene. The glass slides were then washed and sonicated with organic solvent to remove unbound sensor, then subjected to a brief annealing at 80ºC in pH 9.5 buffer. The silyl protected pH sensor **2-C** was deposited in the same manner; however the annealing was carried out in pH 3 buffer in order to hydrolyze the silyl ether protecting groups. Due to the bulky triisopropyl protecting groups, monolayers of **2-C** were not as dense as monolayers generated from **2.9**, evidence of which will be provided later in this chapter. Additional details about surface immobilization are available in the Experimental Section.

2.2.3 Photophysical Properties

All spectroscopic data for this chapter were acquired on a Cary 50 UV/Vis spectrophotometer and a PTI QuantaMaster4/2006SE fluorimeter. The glass slides were cut and measured to fit along the diagonal of a 1 cm path length quartz fluorescence cuvette. Spectra were recorded with the slide inserted along the diagonal submerged in the aqueous buffer of choice. Solutions of pH 3-6 were phthalate buffers, pH 7-8 were phosphate buffers, and pH 9-11 were borate buffers. All solutions were prepared at an equivalent concentration of 0.05 M. A

single slide was used to acquire data for full pH ranges. Additional details about data acquisition are available in the Experimental Section.

2.2.4 pH-dependent Fluorescent Response

In solution, the pH receptor **2-2** behaves as a threshold fluorescent pH indicator (Figure 2.4). In the absorption spectrum, and at low pH, the major absorption band is centered at 440 nm and corresponds to the neutral fluorescein lactone form. As the pH is increased, conversion to the delocalized anionic form results in the appearance of a bathochromically-shifted absorbance band at 492 nm. However, above pH 4, there is no noticeable increase in this absorbance band. The same behavior is mirrored in its pH-dependent emission spectra with hardly any increase in fluorescent emission above pH 4.
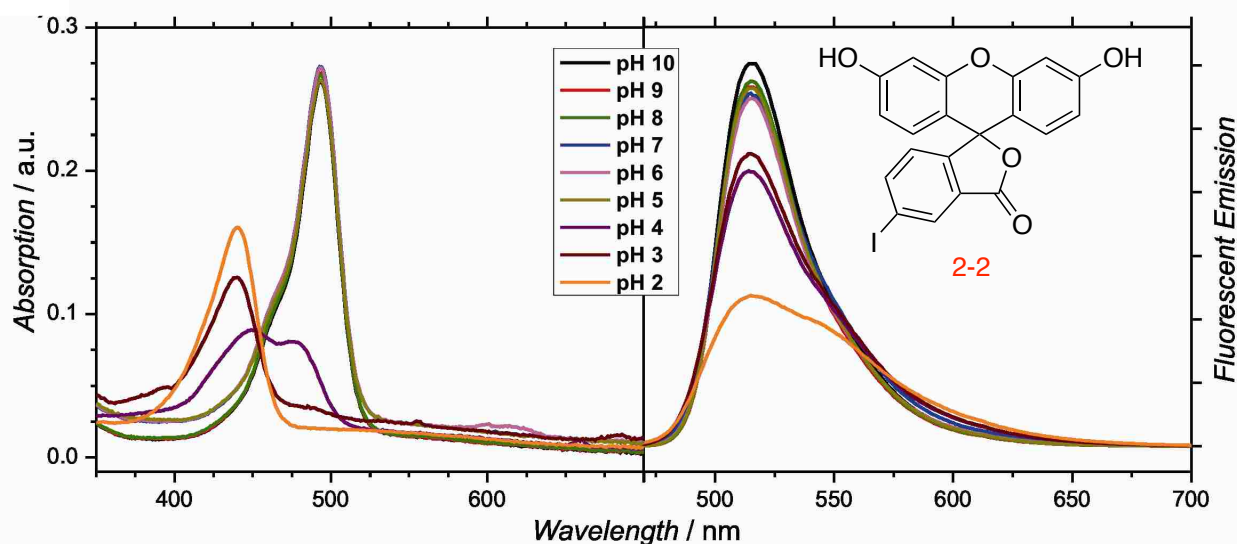
Figure 2.4. pH-Dependent absorption (left) and fluorescence (right) of a 0.04 mM solution of 5-iodofluorescein, **2-2**.

Immobilization of the receptor compound **2-10** altered the spectral properties of fluorescein and revealed new features (Figure 2.5). In addition to being slightly bathochromically shifted (22 nm for absorption, 10 nm for emission), the pH dependent spectral properties were altered. In the monolayer, the absorption band at 502 nm increased incrementally over a broader range of

pH (2 to 10) compared to the threshold behavior observed in solution. The broader pH-dependent absorption response in the monolayer could be due to the hindered formation of anionic species in a dense, surface-immobilized monolayer. The fluorescent response of monolayers of **2-10** was in a narrow range with only significant change in emission intensity in highly basic conditions, possibly due to intermolecular energy transfer to fewer lower-energy moieties present within the monolayer.[15]
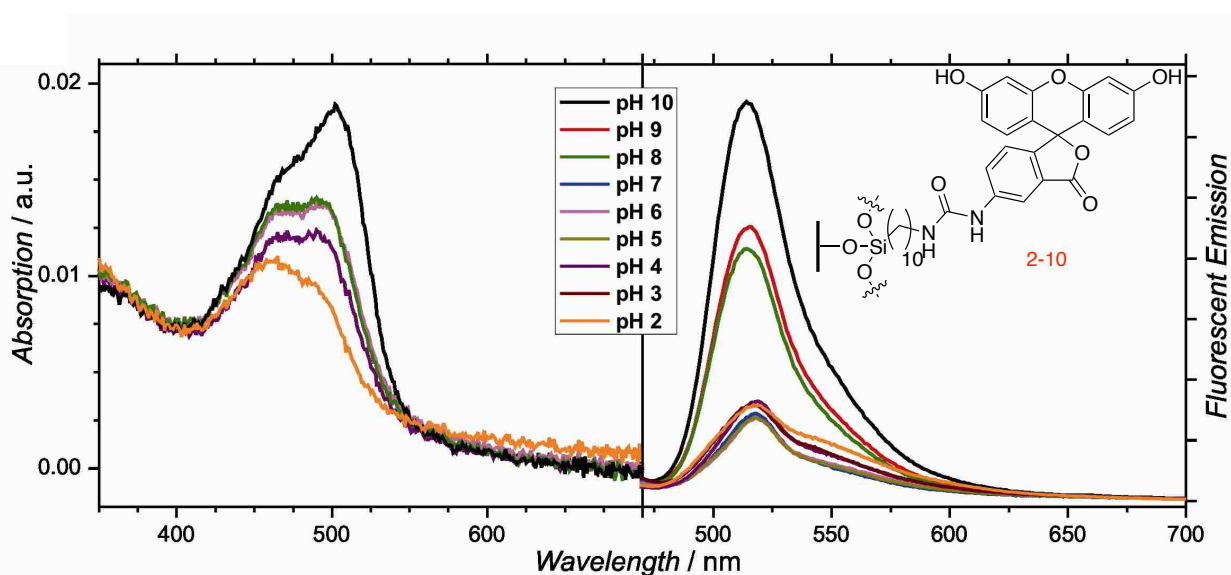
Figure 2.5. pH-Dependent absorption (left) and fluorescence (right) of a surface-immobilized monolayer of compound **2-10**.

In great contrast to the narrow range response of fluorescein in solution or in a monolayer, monolayers of the pH sensor **2-9** showed reversible, ratiometric pH dependent response over a broad pH range (2 to 10). At low pH, excitation of the PE chromophore produced a dominant emission at 415 nm corresponding to emission from the PE core. Gradual increase of pH resulted in an intensity decrease of the PE band with concomitant increase of the intensity of a new emission band at 525 nm corresponding to the fluorescein receptor. This transition was characterized by a well-defined isoemissive point at 505 nm (Figure 2.6). In the corresponding

UV/Vis spectra, the 370 nm absorbance band corresponding to the PE unit was unchanged and an incremental increase of fluorescein absorbance was observed upon increasing pH (analogous to the receptor only monolayer in Figure 2.5).
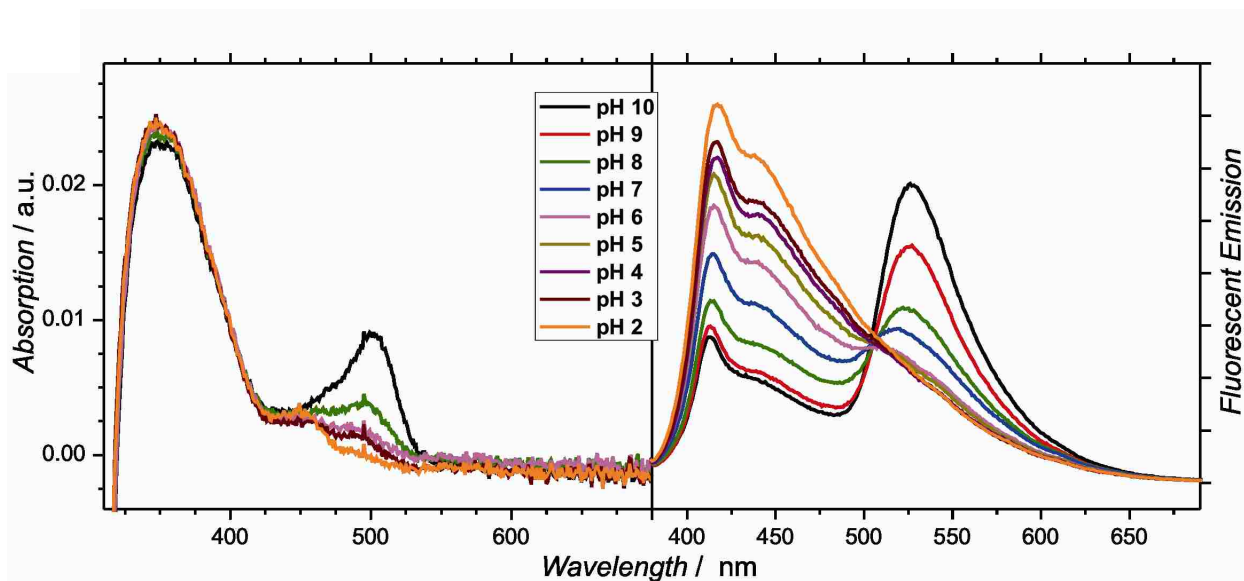
Figure 2.6. pH-Dependent absorption (left) and fluorescence (right) of a monolayer of compound **2-9**.

A well-defined isoemissive point confirms interconversion between two species. It is evident that a PE-fluorescein dyad is a useful ratiometric sensor with several intriguing properties. In the pH-dependent emission studies of **2-9**, the significant increase in emission of the fluorescein band at higher pH and accounting for the prior hypothesis that formation of anionic species in a surface-confined film could be hindered, a quantitative estimate of the energy transfer efficiency to the fluorescein receptor was carried out by superimposing the excitation spectrum of a monolayer of **2-9** at pH 10 normalized to the absorption band of fluorescein (500 nm) with the UV/Vis absorption spectrum of the same monolayer.
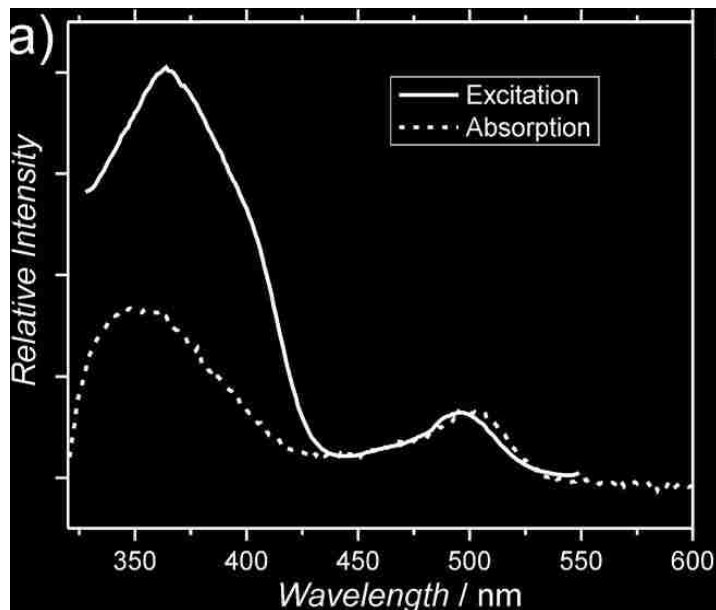
Figure 2.7. Absorption and corrected excitation spectra of a monolayer of **2-9** immobilized on a glass slide and immersed into a solution of pH 10 buffer (normalized at fluorescein region, ~500 nm).

The comparison of the PE absorption and excitation bands in the superimposed normalized spectra makes possible an estimation of the relative efficiency of energy transfer compared to direct excitation of the low energy fluorophore itself.[16] Comparison of the normalized spectra (Figure 2.7) revealed that the PE excitation band was approximately twice as intense as the same absorption band (370 nm). This ratio indicated that there would be an apparent energy transfer efficiency of 200% upon indirect excitation of fluorescein via energy transfer from the monolayer. Obviously, the efficiency of energy transfer cannot exceed 100%. The main assumption of this method is that emission quantum yield of the acceptor is independent of method of excitation.[17] Therefore, it needs to be recognized that experimental evidence in this case pointed that excitation of fluorescein receptors was more efficient when indirectly excited via energy transfer from the PE unit as compared to direct excitation. Indeed, similar results have been previously observed in the literature, namely in quantum dot-fluorescent dye

29

systems[18] and when conjugated polymers were used to excite small molecule fluorophores.[19] In our system, this observed result likely reflects the presence of signal amplification analogous to that which is present in spin-cast films of conjugated polymers. For comparison, a random spin-cast film (which was expected to behave like a film of long conjugated polymers) of **2-6** was prepared. It was found to exhibit broad fluorescent emission bands due to strong intermolecular aggregation. Ratiometric response was absent in this control system due to the multitude of intermolecular contacts, resulting in enhanced exciton migration to fluorescein units and therefore in poorly defined behavior of fluorescent emission intensity upon increasing pH (Figure 2.8).
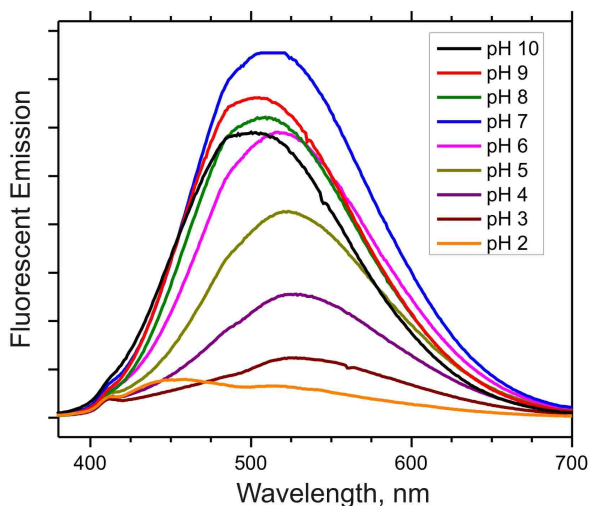
Figure 2.8 pH response of a spin-coated film of **2-6** featuring complete energy transfer to receptor fluorescein and absence of ratiometric response.[†]

Clearly, the covalently immobilized monolayers of the energy transfer cassettes **2-6** behaved differently than isotropic spin-coated samples. In a spin-coated sample, the molecules do not have the opportunity to organize into molecularly ordered assemblies resulting in random orientation of transition dipoles. Thus, excitation of the PE results in dominant fluorescein emission, even at pH 3. The first pKa of fluorescein is 4.31[20], and at pH 3, fluorescein exists only as 5% in the anionic fluorescent form (and is likely even lower in a surface-confined monolayer).

This observation reinforces the ability of these conjugated oligomers to funnel their excited state energy to the low energy sites in an isotropic film due to multitude of intermolecular contacts between oligomers. The unique ratiometric response observed in the molecularly organized monolayer leads to the conclusion that the uniform molecular organization (more direct evidence of which is presented later in this dissertation) enabled achieving an optimum balance between favorable parallel transition dipole orientation and reduction of intermolecular contacts to achieve such a response.

Thus, this platform of surface-immobilized monolayers has been shown to have the ability to convert narrow-range threshold fluorescent sensors into a controlled, reproducible, broad-range fluorescent ratiometric chemosensor. The response of these devices can be presented as a plot of the ratio of fluorescein intensity (I_{525}) to the sum of PE (I_{415}) and fluorescein intensity ($I_{525}/(I_{415}+I_{525})$). As expected, such a plot resembled a sigmoidal pH titration curve over the range of pH 2 to 10 (Figure 2.9) and such a curve can be used for a practical, field use pH determination using this monolayer sensor.
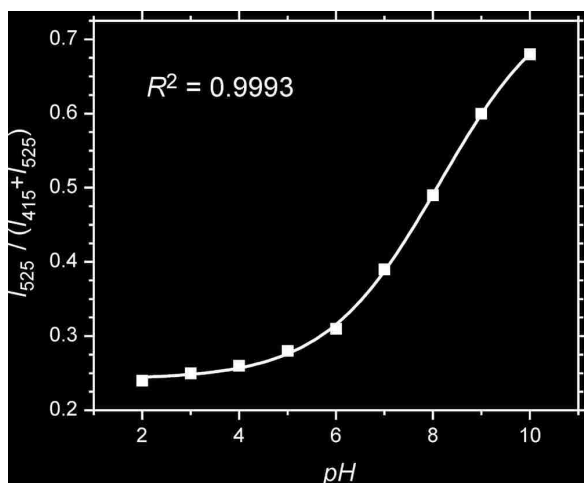
$$\frac{I_{525}}{I_{415} + I_{525}} = 0.7701 - \frac{0.5283}{1 + \exp\left[\dfrac{pH - 8.1336}{1.1757}\right]}$$

Figure 2.9. Sigmoidal fit of the ratiometric response ($I_{525}/(I_{415}+I_{525})$) as a function of pH, and corresponding exponential fitting function.

(EtO)$_3$Si — [10] — N — C(=O) — N — phenyl — ≡ — [C(C$_6$H$_{13}$)(C$_6$H$_{13}$) — ≡ — H]$_4$

2-11
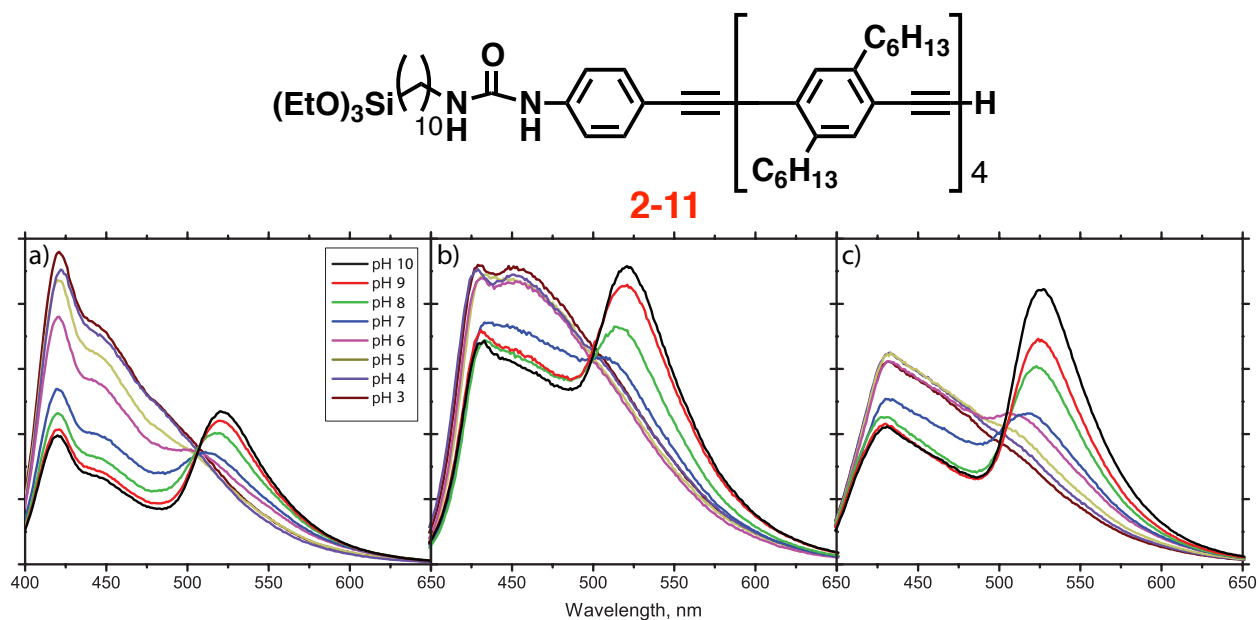
Figure 2.10. pH dependent ratiometric fluorescent response of monolayers consisting of only pH sensor **2-9A** (a), pH sensor **2-9A** co-immobilized with an equimolar amount of PE donor **2-11** (b), and pH sensor **2-9A** co-immobilized with three molar equivalents of PE **2-11** (c).

In order to ascertain the role of intermolecular exciton transfer within the monolayer, the stock solutions of the pH sensor were spiked with varying molar equivalents of a compound **2-11** containing solely the PE donor unit, which possess no fluorescein end-cap and thus can only show PE emission. These molecules, when co-deposited into monolayer with the pH sensor, can act as "antennae" or energy transmitters that will transfer their excited state energy to the pH sensor molecules containing low gap forms of fluorescein. Samples were generated from the 100% monolayer of the pH sensor (by silyl deprotection of **2-D**), as well as from the monolayers prepared by co-deposition from solutions of **2-9A** with varying amounts of **2-11**, and their ratiometric pH sensing properties were studied (Figure 2.10). A feature of pH sensing monolayers generated from the bulkier silyl-protected version (**2-D**) is a lower overall surface density, as evident by the smaller final Fluorescein:PE intensity ratio (I_{525}/I_{415}) at pH 10 compared to the monolayer of original sensor **2-9** at the same pH (Figures 2.9 and 2.6). An increasing amount of aggregation was found in films with large fraction of PE **2-11**, a seemingly

fundamental property of these molecules that lack an end cap receptor. However, ratiometric sensing properties still were present despite a less well-defined isoemissive point (as compared to monolayers of undiluted, 100% pH sensor). Upon increasing fraction of energy donor **2-11** the final $I_{525}/(I_{415}+I_{525})$ ratio at pH 10 was found to increase from approximately 1 to 1.3, to 2 (Figure 2.11).
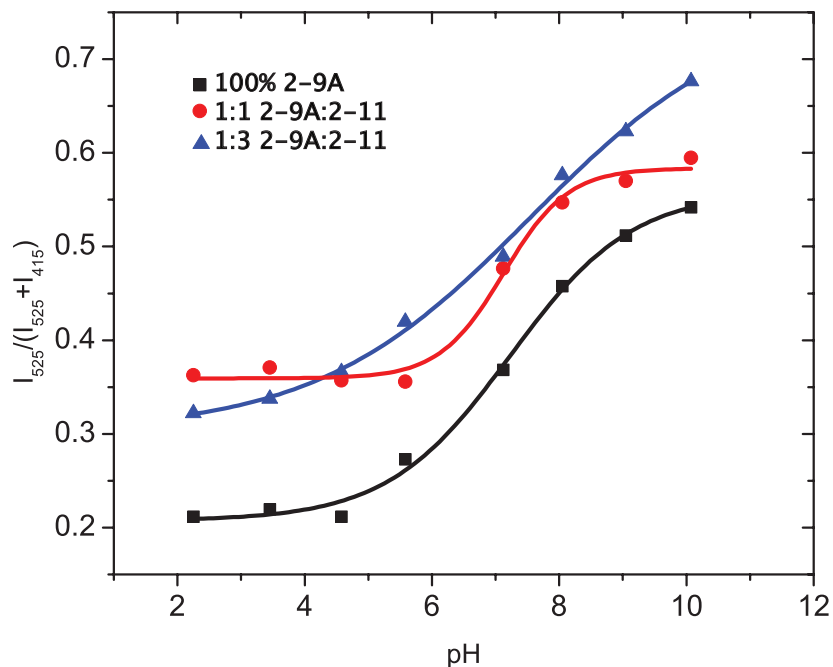
Figure 2.11. Ratiometric pH-dependent response curves for pH sensor monolayer diluted with varying fractions of PE unit **2-11**.

Despite the overall decreasing concentration of fluorescein groups in dilute monolayers, there was an increasing of the receptor emission. Applying similar approach to these "dilute" monolayers to estimate the relative efficiency of fluorescein excitation (via energy transfer) revealed that this efficiency decreased upon increasing fraction of **2-11**. This decreased efficiency of fluorescein excitation might be due to increasing exciton localization in the monolayer; however, the higher final ratio of fluorescein:PE emission indicated that there was possibly a greater amount of fully anionic fluoresceins due to the additional space between end cap groups. This additional space could relieve the repulsive effect between end cap groups,

allowing more anionic (and fluorescent) receptors to be formed. Earlier results have shown an apparent 200% efficiency of energy transfer to fluorescein acceptor in the 100% pH sensor monolayer (vide supra). An equimolar fraction of PE **2-11** in the monolayer decreased this apparent efficiency to approximately 100% (Figure 2.12). In this case, direct excitation of fluorescein vs. indirect excitation resulted in essentially equivalent outcome. Further dilution of the pH sensor **2-9A** with three equivalents of PE **2-11** resulted in further decrease to 50% of relative efficiency of energy transfer to fluorescein. Though the efficiency of receptor excitation through energy transfer was decreasing with higher concentrations of PE, it is possible that the smaller PE units were able to fill in the gaps resulting in a more dense monolayer, therefore resulting in greater fluorescein emission and a higher final fluorescein:PE ratio. Indeed, the pH detection range of the monolayer sensor with 1:1 ratio of **2-9A** to **2-11** was relatively narrow compared to the other two monolayers (Figure 2.11). The interplay between the two effects of a denser monolayer at the cost of reduced indirect fluorescein excitation efficiency (due to exciton localization) was seemingly responsible for the observed result.
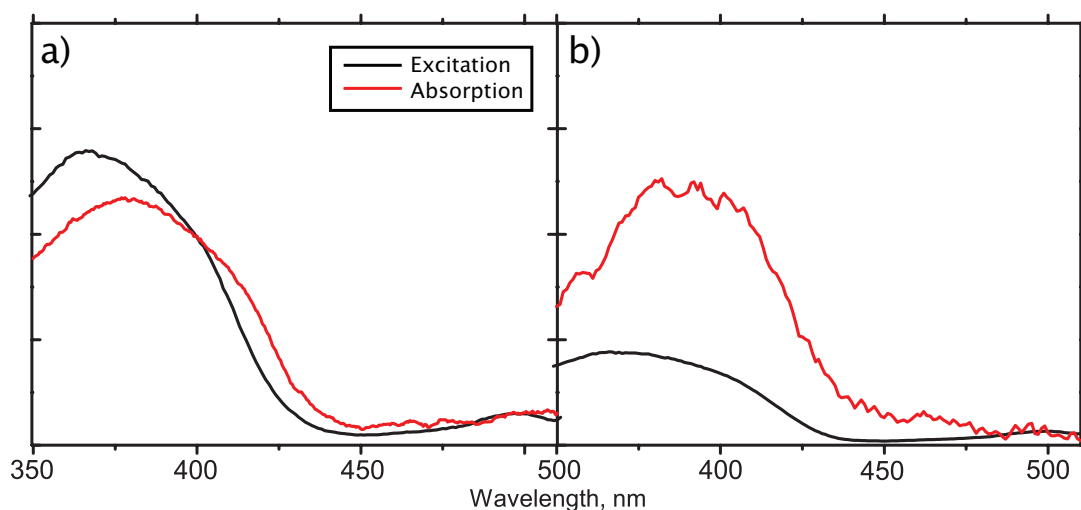
Figure 2.12. Absorption and corrected excitation spectra of a monolayer of **2-9** co-immobilized with 1 (a) and 3 (b) molar equivalents of **2-11** on a glass slide and immersed into a solution of pH 10 buffer (normalized at fluorescein region, ~500 nm).

2.3 Conclusion

In conclusion, monolayers of π-conjugated oligomers that show extensive two-dimensional exciton delocalization due to molecular organization have been prepared and have been proved to be useful ratiometric fluorescent sensors for pH due to signal amplification in the organized monolayer. The photonic amplification in this monolayer platform allowed for the conversion of a narrow range threshold pH indicator into a broad range, full scale pH ratiometric sensor. This strategy was found to be useful for conversion of single-wavelength threshold sensors into broad range sensors and offers advantages over small molecules or spin-cast films of conjugated polymers. Gaining deeper understanding of the origin of this photonic amplification requires additional studies (some of these studies are reported in the next chapter).

2.4 References

(1)   Kim, J.; Swager, T. M. Control of Conformational and Interpolymer Effects in Conjugated Polymers. *Nature*, **2001**, *411*, 1030-1034.

(2)   Grell, M.; Bradley, D. D. C.; Inbasekaran, M.; Woo, E. P. A Glass-Forming Conjugated Main-Chain Liquid Crystal Polymer for Polarized Electroluminescence Applications. *Adv. Mater.* **1997**, *9*, 798-802.

(3)   Iverson, I. K.; Casey, C. M.; Seo, W.; Tam-Chang, S.-W. Controlling Molecular Orientation in Solid Films via Self-Organization in the Liquid Crystalline Phase. *Langmuir*, **2002**, *18*, 3510-3516.

(4)   Tsukanova, V.; Harata, A.; Ogawa, T. Orientation Arrangement of Long-Chain Fluorescein Molecules Within the Monolayer at the Air/Water Interface Studied by the SHG Technique. *Langmuir*, **2000**, *16*, 1167-1171.

(5)   Basabe-Desmonts, L.; Beld, J.; Zimmerman, R. S.; Hernando, J.; Mela, P.; Garcia Parajo, M. F.; van Hulst, N. F.; van den Berg, A.; Reinhoudt, D. N.; Crego-Calama, M. A Simple Approach to Sensor Discovery and Fabrication on Self-Assembled Monolayers on Glass. *J. Am. Chem Soc.,* **2004**, *126*, 7293-7299.

(6)   Flink, S.; van Veggel, F. C. J. M.; Reinhoudt, D. N. Sensor Functionalities in Self-Assembled Monolayers. *Adv. Mater.* **2000**, *12*, 1315-1328.

(7)   Ding, L.; Fang, Y. Chemically Assembled Monolayers of Fluorophores as Chemical Sensing Materials. *Chem. Soc. Rev.* **2010**, *39*, 4258-4273.

(8)   Acharya, J. R.; Zhang, H.; Xian, Li.; Nesterov, E. E. Chemically Controlled Amplified Ratiometric Fluorescence in Surface-Immobilized End-Capped Oligo(*p*-phenylene ethynylene)s. *J. Am. Chem. Soc.* **2009**, *131*, 880-881.

(9)   Martin, M. M.; Lindqvist, L. The pH Dependence of Fluorescein Fluorescence. *J. Lumin.* **1975**, *10*, 381-390.

(10)   Baeyer, A. Ueber eine neue Klasse von Farbstoffen. *Ber. Dtsch. Chem. Ges.* **1871**, *4*, 555-558.

(11)   Jiao, G.-S.; Han, J. W.; Burgess, K. B. Syntheses of Regioisomerically Pure 5- or 6-Halogenated Fluoresceins. *J. Org. Chem.* **2003**, *68*, 8264-8267.

(12)   Lahti, P. M.; Serwinski, P. R. Limit of Delocalization in Through-Conjugated Dinitrenes: Aromatization or Bond Formation?. *Org. Lett.* **2003**, *5*, 2099-2102.

(13)   Kushner, A. M.; Gabuchian, V.; Johnson, E. G.; Guan, Z. Biomimetic Design of Reverisbly Unfolding Cross-Linker to Enhance Mechanical Properties of 3D Network Polymers. *J. Am. Chem. Soc.* **2007**, *129*, 14110-14111.

(14)   Chernyshev, E. A.; Belyakova, Z. V.; Knyazev, S. P.; Turkel'taub, G. N.; Parshina, E. V.; Serova, I. V.; Storozhenko, P. A. Hydrosilylation of Ethylene. *Russ. J. Gen. Chem.* **2006**, *76*, 225-228.

(15)   Schwartz, B. J. Conjugated Polymers as Molecular Materials: How Chain Conformation and Film Morphology Influence Energy Transfer and Interchain Interactions. *Ann. Rev. Phys. Chem.* **2003**, *54*, 141-172.

(16)   Gust, D.; Moore, T. A.; Moore, A. L.; Devadoss, C.; Lidell, P. A.; Hermant, R.; Nieman, R. A.; Demanche, L. J.; DeGraziano, J. M.; Gouni, I. Triplet and Singlet Energy Transfer in Carotene-Porphyrin Dyads: Role of the Linkage Bonds. *J. Am. Chem. Soc.* **1992**, *114*, 3590-3603.

(17)   Devadoss, C.; Bharathi, P.; Moore, J. S. Energy Transfer in Dendridic Molecules: Molecular Size Effects and the Role of an Energy Gradient. *J. Am. Chem. Soc.* **1996**, *118*, 9635-9644.

(18)   Medintz, I. L.; Clapp, A. R.; Mattoussi, H.; Goldman, E. R.; Fisher, B.; Mauro, J. M. Quantum Dot Bioconjugates for Imaging, Labelling, and Sensing. *Nat. Mater.* **2003**, *2*, 630-638.

(19) Levine, M.; Song, I.; Andrew, T. L.; Kooi, S. E.; Swager, T. M. Photoluminescent Energy Transfer from poly(Phenyleneethynylene)s to Near-Infrared Emitting Fluorophores. *J. Polym. Sci., Part A: Polym. Chem.* **2010**, *48*, 3382-3391.

(20) Niazi, A.; Yazdanipour, A.; Ghasemi, J.; Amini, A.; Bozorgzad, S.; Kubista, M. Spectrophotometric Investigation of the Acidity Constants of Fluorescein in Various Water-Organic Solvent Media. *Chem. Eng. Comm.* **2008**, *195*, 1257-1268.

CHAPTER 3. TUNING SIGNAL AMPLIFICATION IN THIN-FILM RATIOMETRIC FLUORESCENT CHEMOSENSORS

3.1 Introduction

Systems that possess extended π-conjugation benefit from extensive delocalization of excited states. This exciton delocalization can easily be harnessed for use in chemosensory devices, especially those which utilize energy gap differences in donor-acceptor dyads.[1] Prior results described earlier in this dissertation have shown that densely-packed immobilized monolayers of conjugated oligomers offer substantial optical gain in chemosensory applications.[2] Monolayers of surface-immobilized penta(*p*-phenylene ethynylene)-receptor dyads have been postulated in this early work to possess high levels of molecular organization within the monolayer that is responsible for the ratiometric sensing behavior of this system.[3] Since the efficiency of energy transfer depends heavily on the distance between donor and acceptor, the sensitivity of the devices is increased due to the close packing of molecules in monolayers of PE-receptor dyads. Conversely, increasing spatial separation of molecules is expected to diminish energy transfer efficiency.

According to the Förster theory of energy transfer, the efficiency is dependent on the spatial separation of the donor and acceptor moieties in an inverse-sixth relationship. Thus, the attenuation of energy transfer can be accomplished by increasing the spatial separation. Spatial separation can be effected through increasing the length of a connecting linker between two fluorophores[4], or an inert spacer polymer (e.g., PMMA) intermixed with a conjugated polymer.[5] Chains of conjugated polymers can be further separated through the use of bulkier solubilizing groups.[6] These modifications can be employed to attenuate the efficiency of energy transfer and thus, the signal amplification, in order to employ amplifying conjugated polymers for ratiometric fluorescent chemosensing. Unfortunately, these methods do not provide a simple and

reproducible means to fine tune energy transfer efficiency that is required for the control of ratiometric sensor performance. In contrast, a convenient and universal method of tuning signal amplification can be developed using our general strategy of surface-immobilized amplifying ratiometric fluorescent sensors. Remarkably, this method avoids additional synthetic efforts and can be applied on demand to a particular sensor should the need arise.

The parallel orientation and dense packing of molecules in the fluorescent sensor monolayers based on conjugated oligomers offers significant exciton delocalization and confers high sensitivity. The experiments described in the previous section have concluded that only a very small number of energy acceptors need to be present in the monolayer to elicit substantial energy transfer to these sites. Therefore, there is significant evidence that the excitons "funnel" to these acceptor sites through the two-dimensional π-electron network within the monolayer. Reactions with relatively low equilibrium constants yielding only small amounts of product can be used as a basis for chemosensing with this platform. However, for sensors harnessing quantitative chemical transformations, rapid saturation of the ratiometric response will be achieved due to efficient energy transfer operating even at low analyte concentrations. For practical applications, sensors must have an analyte detection range that is applicable for use in field tests and must cover ranges needed for particular applications as well as dictated by authorities such as regulatory agencies (EPA, OSHA, etc.). Therefore, there is a need to adjust the analyte detection range of the devices to a level that is useful for sensing of the particular analyte.

To expand the versatility of the monolayers as a general platform for ratiometric solid-state fluorescent sensing, the addition of a "diluting" moiety within the monolayer should slow down exciton migration due to increasing effective separation of sensor molecules within the monolayer (Figure 3.1).
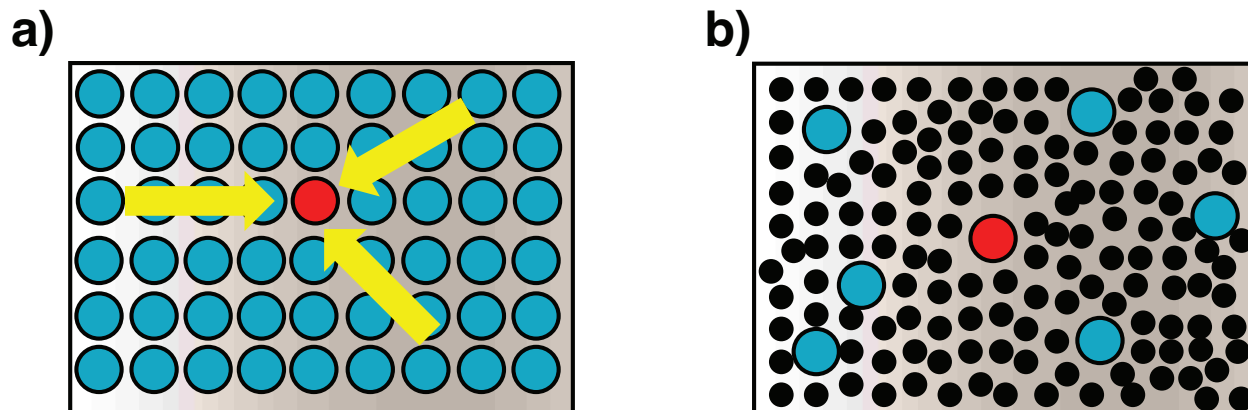
Figure 3.1. Cartoon illustrating efficient exciton migration in a monolayer of densely packed ratiometric fluorescent sensors (a, blue dots) and hindered energy transfer in a monolayer co-immobilized with inert alkyl siloxane dilutant (b).

When aliphatic alkylsilanes (e.g. octadecyldiethoxymethylsilane (ODMS)) are co-immobilized with active sensor molecules, they are expected to act as "spacers" that increase the distance between the sensor molecules thereby reducing the efficiency of intermolecular energy transfer. In general, by varying the ratio between "active" sensor compound and inert "diluter," one can achieve an effective attenuation of photonic amplification in the monolayer sensor.

To test this concept, a prototype sensor for fluoride was developed based on the special reactivity of fluoride towards silyl functionalities. Silyl ethers are a common alcohol-functionality protecting group ubiquitous in organic synthesis.[7] The deprotection of a silyl-protected alcohol is generally accomplished using a fluoride species, either an alkali metal fluoride, or the organic- soluble tetrabutylammonium fluoride (TBAF). The driving force for this reaction is the formation of a strong silicon-fluoride bond with bond dissociation energy of 576 kJ/mol.[8]

Functionalization of fluorescein with silyl protecting groups resulted in a non-fluorescent (and colorless) compound whose emission could be restored upon fluoride-mediated cleavage (Figure 3.2).[9] Thus, the protected (masked) form of fluorescein was unable to act as the acceptor of the

energy from a photoexcited PE donor unit (Figure 3.3). Upon deprotection, the formed fluorescein molecules became efficient energy transfer acceptors. Therefore, cassettes obtained by coupling protected fluorescein to an energy donor yield a convenient ratiometric fluorescent sensor for fluoride ion.
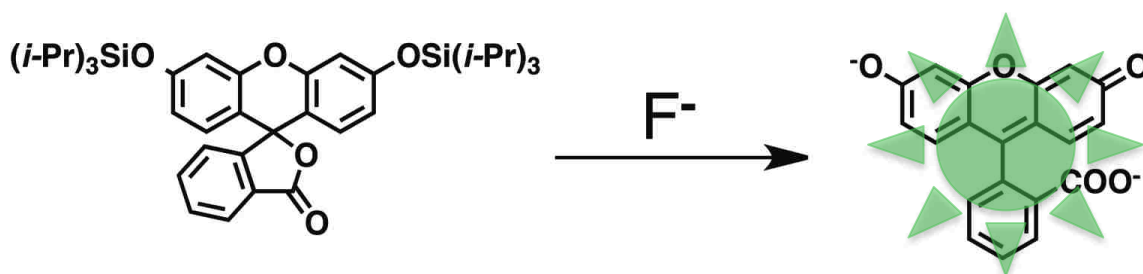
Figure 3.2. Release of a fluorophore upon fluoride-mediated silyl-ether cleavage of a protected fluorescein.
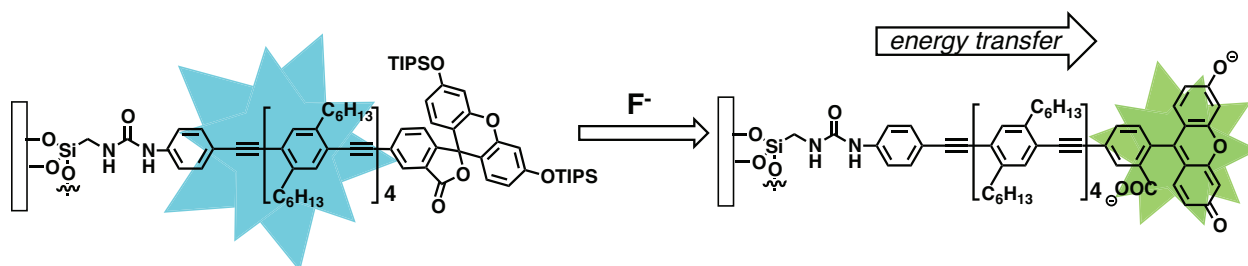
Figure 3.3. General operating principle and origin of ratiometric response in covalently immobilized ratiometric fluoride sensors utilizing silyl deprotection by fluoride ion.

The silyl-protected fluorescein acts as a high HOMO-LUMO gap group due to the lack of extended electronic conjugation. Exposure to fluoride yields a compound with a dramatically lower HOMO-LUMO gap (fluorescein), thus resulting in ratiometric response when incorporated into an energy transfer cassette.

3.2 Results and Discussion

3.2.1 Synthesis

Scheme 3.1. Synthesis of fluoride sensor compound.

The synthesis started with 5-iodofluorescein which was reacted with triisopropylsilyl (TIPS) chloride under standard silylation conditions (Scheme 3.1).[10] Sonogashira coupling of protected fluorescein with the PE unit† (**2-5**) proceeded smoothly without the need for additional oxidative workup (described in Chapter 2) to yield **2-B**. Surface anchor attachment was effected by

42

reaction with the isocyanate **2-8** to yield the fluoride sensor **2-C** that was immobilized on glass substrate to form monolayers **2-D**. Required reference compound **3-2**, containing only the receptor unit was synthesized in a similar manner (Scheme 3.2). Commercial 5-aminofluorescein was reacted with TIPS chloride yielding bis-TIPS compound **3-1** in which the linker was attached in a similar manner, resulting in the receptor-only reference compound **3-2**. Details regarding the synthesis of these compounds can be found in the Experimental Section.

Scheme 3.2. Synthesis of the fluoride receptor control compound.
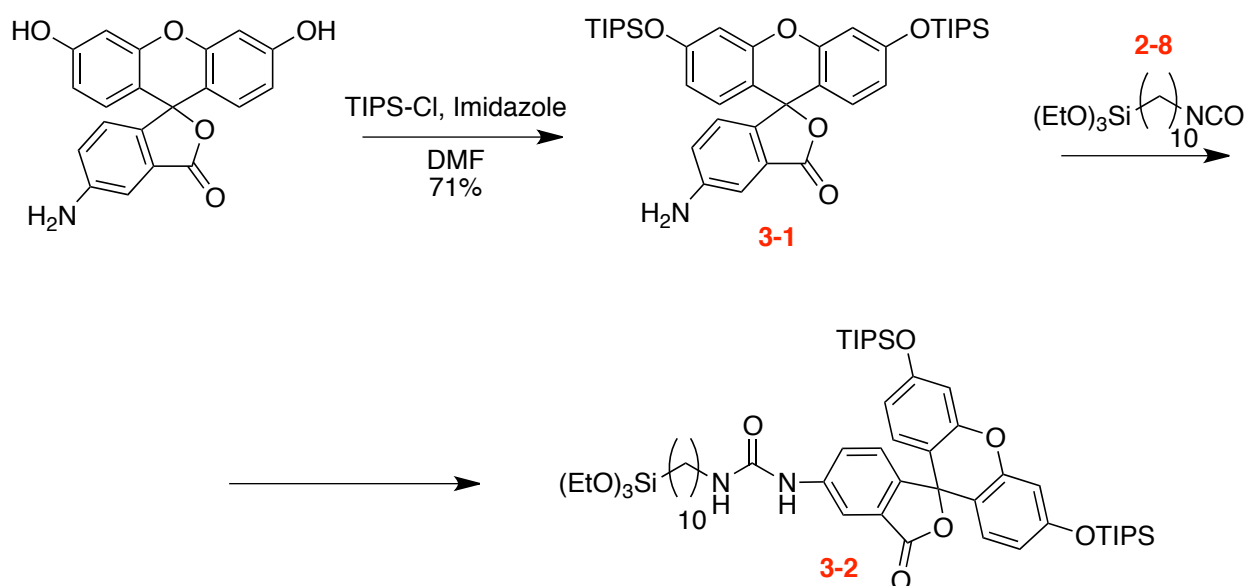
3.2.2 Preparation of Surface Immobilized Monolayers and Sensor Dilution

A solution of compound **2-C** or solutions of **2-C** with varying amount of inert "diluter" (ODMS) were used for immobilization on glass cover slips. The immobilization was carried out by immersing the substrate in these solutions with moderate heating. Monolayers were used fresh after a brief conditioning period in Bu$_4$NPF$_6$ in THF to effect surfactant-like surface reorganization. The solutions of sensor with ODMS were prepared by taking individual aliquots of a solution of compound **3-3** and mixing with 4 molar equivalents and 8 molar equivalents of

ODMS and maintaining a constant concentration of sensor. Additional details regarding monolayer preparation and sensor dilution can be found in the Experimental Section.

Electrochemical surface density measurements of the fluoride sensor **2-C** (immobilized in the conditions similar to those used for immobilization on glass) on indium-tin oxide (ITO) estimated a dense coverage with one molecule per 3 nm^2 (an estimate was obtained assuming one-electron oxidation for a redox peak at ~0.9 V) (Figure 3.4). A theoretical estimate of actual molecular area is 2 nm^2. This indicated a relatively dense packing of the molecules of **2-C** in the monolayer.
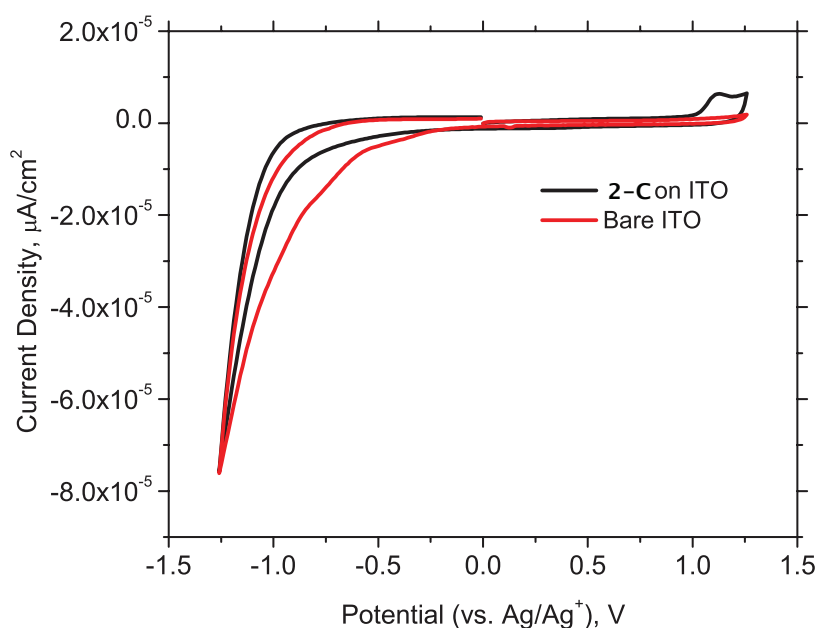
Figure 3.4. Cyclic voltammogram of a monolayer of fluoride sensor compound **2-C** immobilized on ITO/Glass, in 0.1 M Bu$_4$NPF$_6$ in dichloromethane. Sweep rate: 0.1 V/s.

3.3.1 Fluoride Exposure Studies

The stability of the monolayers of **2-C** was confirmed by the presence of an isoemissive point at 510 nm during a time-dependent fluoride exposure study (Figure 3.5). Indeed, fluoride-effected monolayer cleavage would result in gradual overall reduction in fluorescence intensity and loss of isoemissive point.
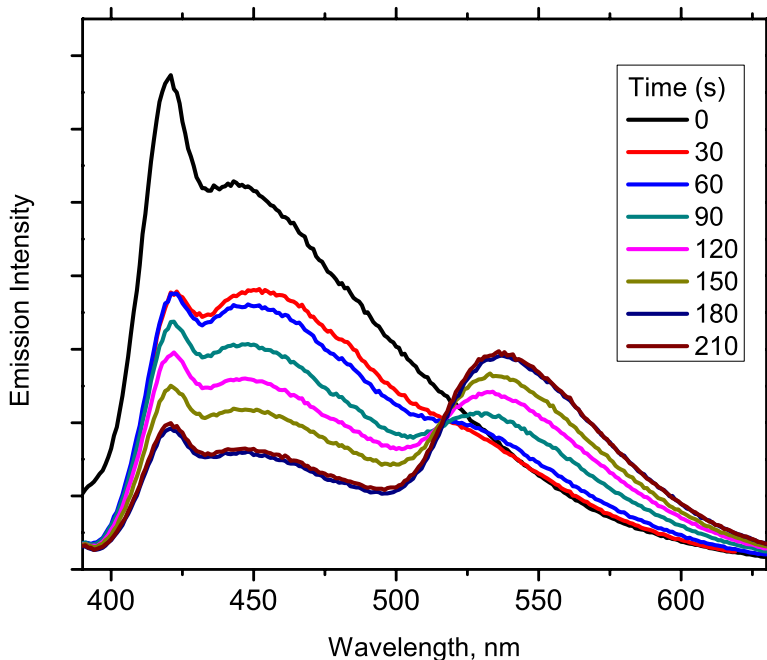
Figure 3.5. Time-dependent ratiometric emission of a monolayer of **2-C** immersed in 6.5 μM TBAF in THF.

   More reliable proof of monolayer integrity was obtained by examining the optical absorbance density over the period of exposure (Figure 3.6b). After exposure to TBAF in THF for three minutes, the PE absorbance band (370 nm) of the monolayer of the sensor compound **2-C** slightly increased. Also apparent was an increase of a bathochromically-shifted absorbance at 475 nm corresponding to fluorescein. These effects on the absorption spectrum of the fluoride sensor monolayers were mirrored in the exposure of a solution of precursor **2-B** to TBAF in THF (Figure 3.6a). In addition, an immobilized monolayer of compound **2-11** containing only the PE unit was found to be unaffected by the presence of fluoride over the duration of exposure based upon consistent emission spectra before and after immersion (Figure 3.7).
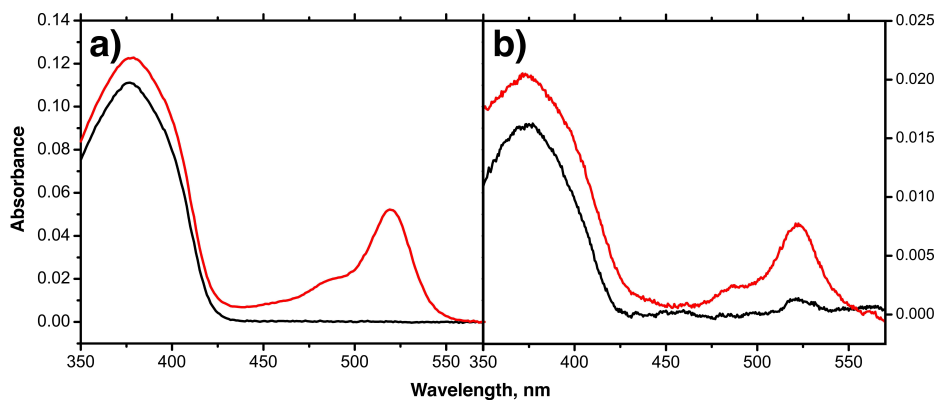
Figure 3.6. a) UV/vis absorption spectra of the 0.015 mM solution of **2-B** in THF before *(black trace)* and after *(red trace)* addition of 2 equivalents of Bu$_4$NF. b) UV/vis absorption spectra of the monolayer of **2-C** on glass before *(black trace)* and after *(red trace)* 3 min exposure to 9.0 μM solution of Bu$_4$NF in THF.
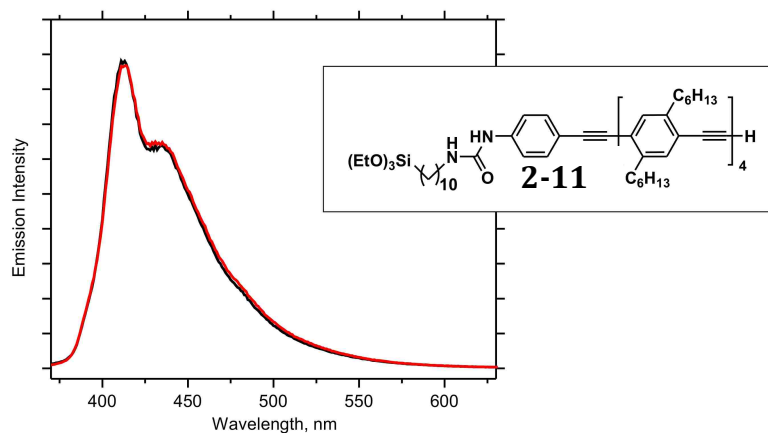
Figure 3.7. Emission spectra of the glass-immobilized monolayer of PE-only reference compound **2-11** before *(black trace)* and after *(red trace)* exposure to 9.0 μM solution of Bu$_4$NF in THF for 3 min. The absence of change in the spectra demonstrates integrity of the monolayer upon exposure to fluoride solution.

The pristine monolayers of **2-C** before exposure to fluoride (TBAF in THF) were characterized by a sharp emission at 420 nm (Figure 3.5). Due to the special reactivity of fluoride to Si-O bonds and the irreversibility of the desilylation reaction, these monolayers were used as dosimeters. Dosimeters differ from chemosensors because they are single use, meaning that they are exposed a single time and then disposed of. Thus, every experimental concentration point required a separate slide. Measurements of multiple spectra with a single slide were found

to be unreliable due to eventual fluoride cleavage of the siloxane linker. The 100% monolayer of **2-C** reached equilibrium in three minutes upon exposure to micromolar amounts of TBAF in THF (Figure 3.5).

Fluoride exposure of the 100% sensor monolayer showed a gradual increase in the fluorescein emission peak at 540 nm with concomitant decrease in the PE emission band at 420 nm. The ratio of fluorescein:OPE intensities gradually increased with increasing fluoride concentration (Figure 3.8). Ultimately, the concentration of fluoride became significant enough to cause monolayer cleavage and degradation and the ratio began to decrease after reaching a maximum value.
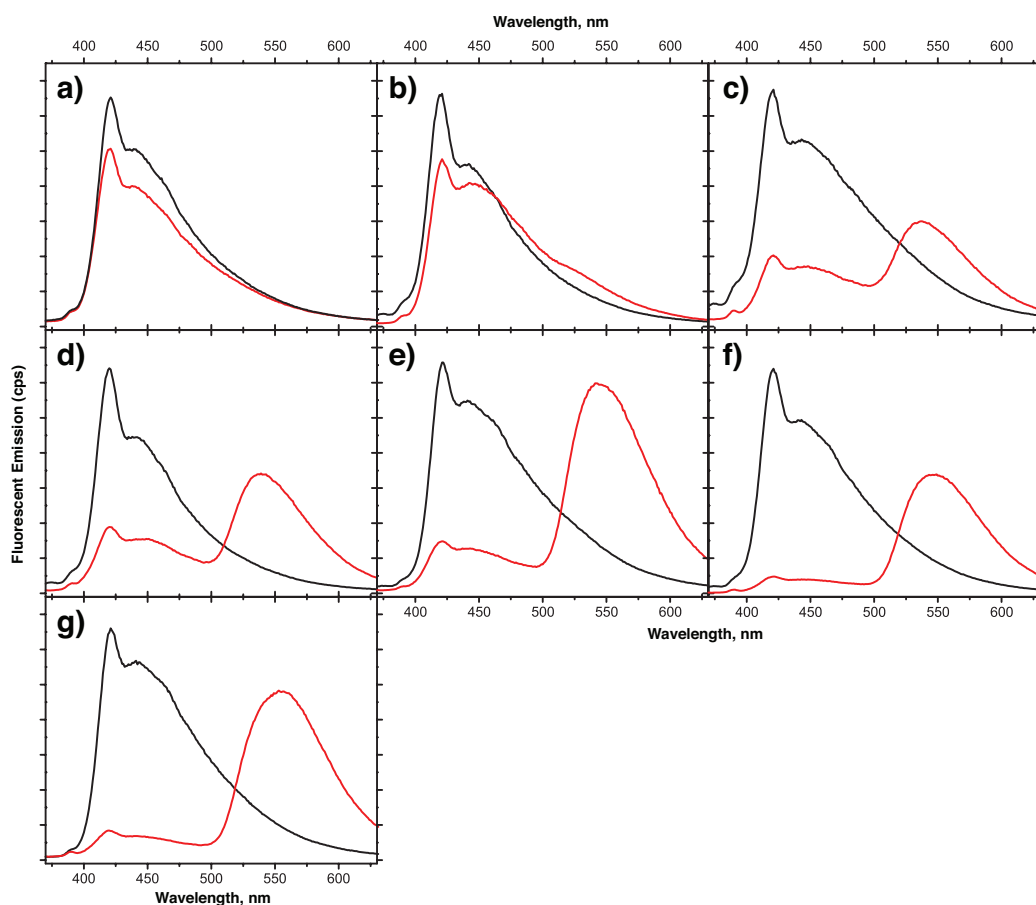
Figure 3.8. Fluorescence spectra of glass-immobilized monolayer of **2-C** prior to exposure to fluoride (*black traces*) and after exposure to Bu₄NF solutions in THF *(red traces)* with the following fluoride concentrations: 5.0 μM (a), 6.0 μM (b), 6.5 μM (c), and 7.0 μM (d), 7.5 μM (e), 9.0 μM (f), and 10.0 μM (g). Spectra were acquired at 350 nm irradiation.
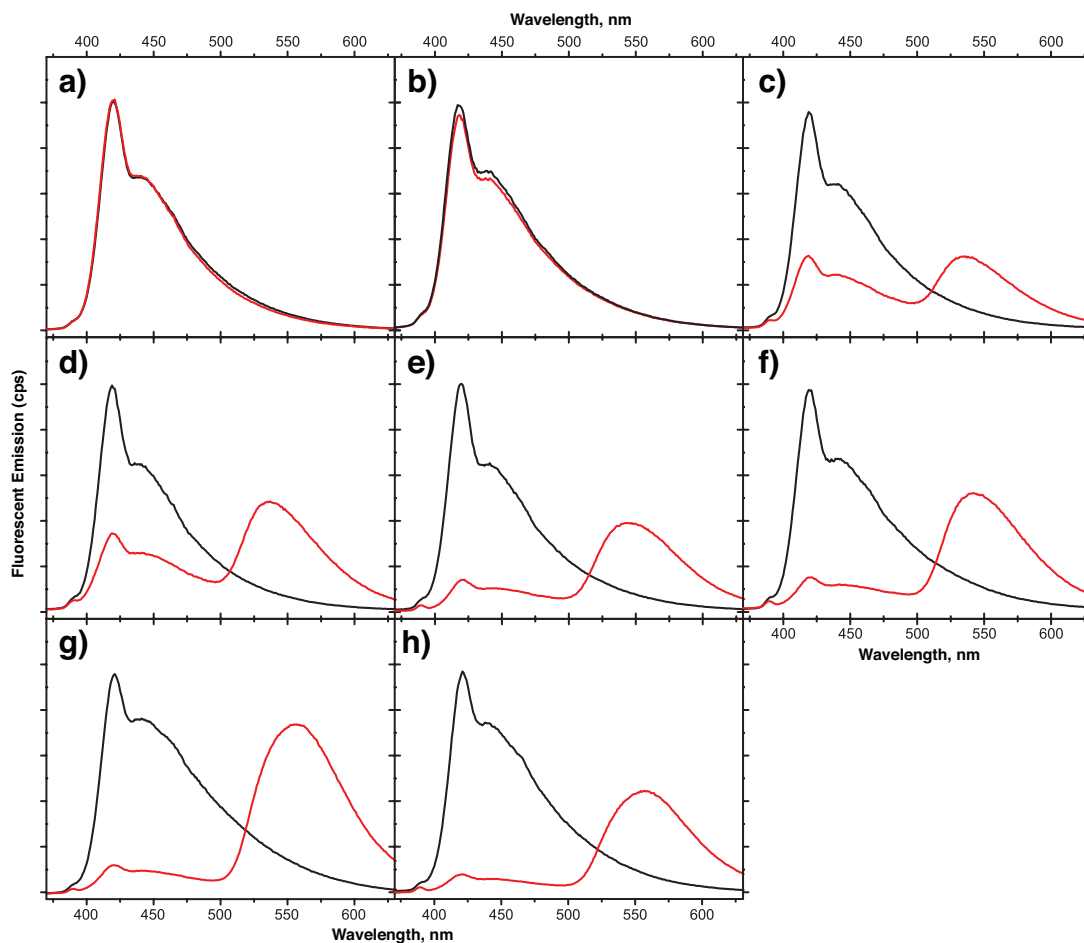
Figure 3.9. Fluorescence spectra of glass-immobilized monolayer of **2-C** prepared by co-deposition from solution of **2-C** and ODMS in 1:4 ratio prior to exposure to fluoride (*black traces*) and after exposure to Bu$_4$NF solutions in THF *(red traces)* with the following fluoride concentrations: 4.0 μM (a), 5.0 μM (b), 6.0 μM (c), and 7.0 μM (d), 9 μM (e), 10.0 μM (f), 12.0 μM (g), and 14.0 μM. Spectra were acquired at 350 nm irradiation.

Surface immobilization using a solution of four molar equivalents of ODMS and one equivalent of **2-C** (20% active sensor) produced monolayers which behave in a similar manner when exposed to fluoride (Figure 3.9) as the monolayers generated with 100% fluoride sensor. As expected, in the "dilute" monolayers, the aggregation-induced shoulder on the PE emission band was less severe compared to the 100% sensor monolayers due to diminished intermolecular contacts between **2-C** in the monolayer.
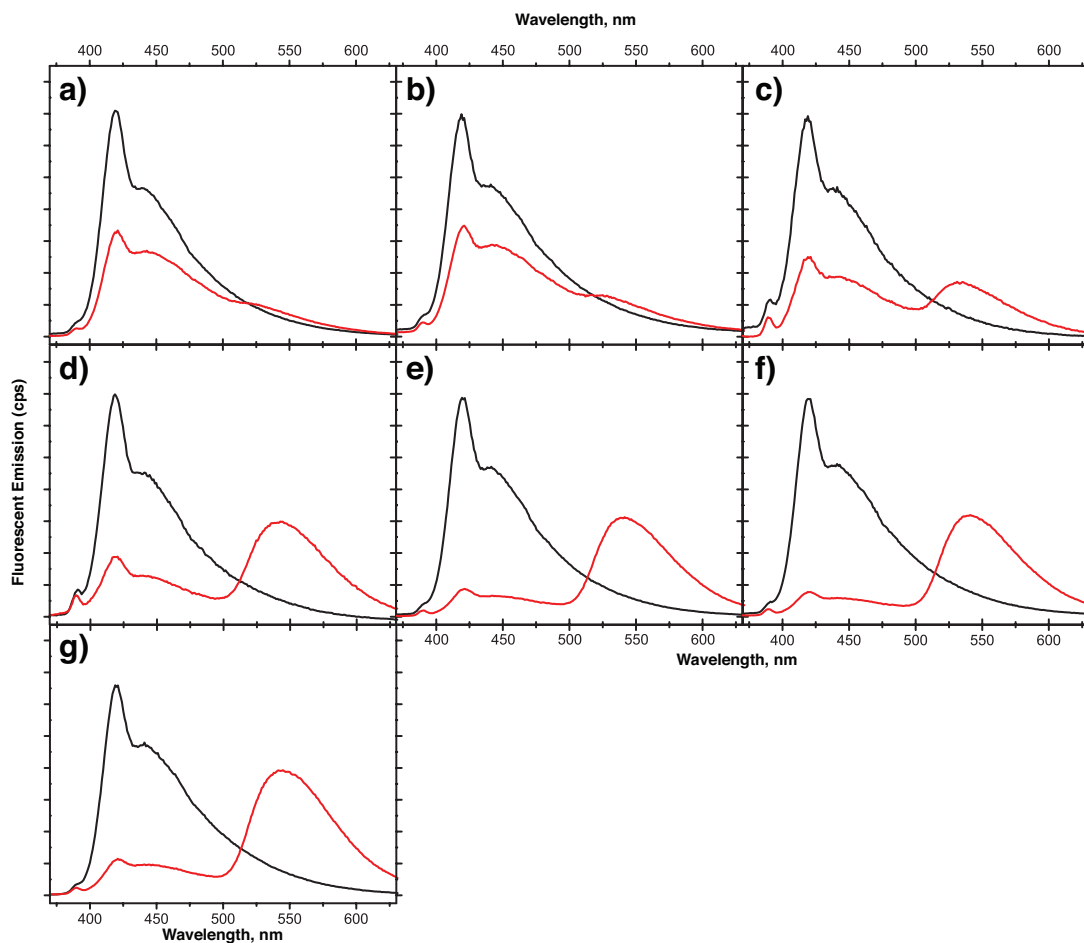
Figure 3.10. Fluorescence spectra of glass-immobilized monolayer of **2-C** prepared by co-deposition from solution of **2-C** and ODMS in 1:8 ratio prior to exposure to fluoride (*black traces*) and after exposure to Bu$_4$NF solutions in THF *(red traces)* with the following fluoride concentrations: 4.0 μM (a), 5.0 μM (b), 7 μM (c), and 11.0 μM (d), 15 μM (e), 16.0 μM (f), and 17.0 μM (g). Spectra were acquired at 350 nm irradiation.

Using further dilution of the deposition solution with a total of eight molar equivalents of ODMS (11% active sensor) yielded monolayers that were far less aggregated than the films with higher fractions of **2-C**. Upon exposure to fluoride, a fluorescein band with a maximum at 540 nm became apparent at lower fluoride concentrations due to the overall narrower bandwidth of the PE emission due to lower aggregation (Figure 3.10).

The ratiometric response of the sensor monolayers can be treated similarly to a Stern-Volmer plot (Figure 3.11) as the relationship between fluoride concentration and the ratio of intensities at 540 nm and 420 nm (I_{540}/I_{420}), which results in a sigmoidal response curve. Therefore, the true

effective sensing range was defined as the linear portion between the lower and upper limits of the distribution. The slope of this linear portion was defined as the detection sensitivity analogous to the Stern-Volmer quenching constant (K_{SV}). Indeed, the steep slope of the 100% monolayers of **2-C** was typical for a system with signal amplification due to enhanced energy transfer efficiency.
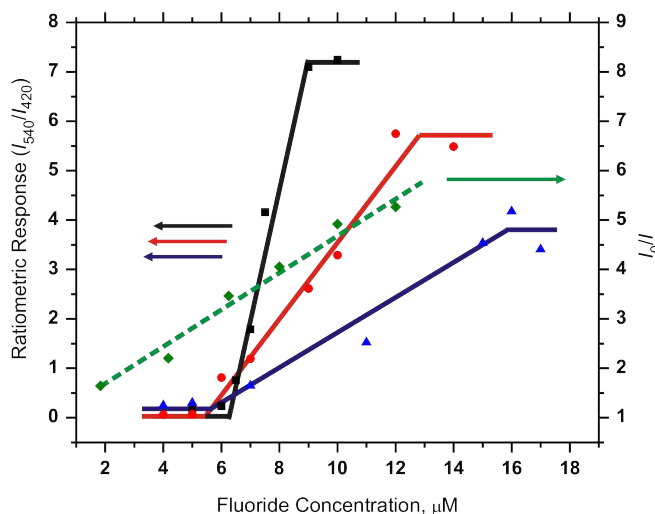
Figure 3.11. Ratiometric responses to fluoride (as ratio of intensities at 540 nm to 420 nm, I_{540}/I_{420}) of the densely packed monolayer of **2-C** *(squares, black trace)* and monolayers prepared by co-deposition of **2-C** and ODMS in ratio 1:4 *(circles, red trace)* and 1:8 *(triangles, blue trace)*. These three plots use the left ordinate axis. The slopes of the linear portions of the response curves: 2.42 *(black)*, 0.77 *(red)*, and 0.35 *(blue)*. Also shown is the turn-on fluorescent response (as Stern-Volmer I_0/I ratio at 540 nm) of the monolayer of the control compound **3-2** *(diamonds, dash green trace,* uses right ordinate axis), slope of the trace 0.38.

The effect of the dilution of the active sensor in the monolayers was dramatic. Upon addition of more equivalents of ODMS, the final detectable ratio of I_{540}/I_{420} became successively lower due to diminished energy transfer within the monolayer and thus lower photonic amplification. In addition, the sensitivity of detection became lower in correlation with degree of dilution in the monolayer (for the case of the 11% monolayer, the sensitivity dropped to 0.14 of the sensitivity of the 100% monolayer). It was also observed that the analyte detection range of the sensors was

broadened upon dilution. Dilution of the 100% film of **2-C** to 11% **2-C** (8 equivalents ODMS) tripled the overall fluoride sensing range of the films (The 100% fluoride sensor monolayer films showed a fluoride detection range from 6 to 9 µM, whereas the 20% films showed a range of 5 to 12 µM, and the 11% films were found to be useful from 5 to 15 µM.). Further surface dilution was found to have no effect of the ratiometric sensing behavior of the monolayers. Thus, it is likely that additional spatial separation beyond 8 molar equivalents of "dilutant" increased separation of the sensor molecules in the monolayer beyond the Förster radius for intermolecular energy transfer and therefore resulted in localization of excitons within individual molecules and shutting down the signal amplification mechanism. Therefore, the 11% monolayer of **2-C**, the molecules were behaving as isolated molecules that rely solely on intramolecular energy transfer to generate ratiometric response.

To support this conclusion, monolayers of compound **3-2** were generated containing only the receptor moiety. In this case, no energy transfer was possible upon irradiation at fluorescein absorption and a "turn-on" emission signal was generated (Figure 3.12), which is proportional to the extent of reaction on the surface. The detection sensitivity (K_{SV}) in this case was defined as the Stern-Volmer constant K_{SV}, i.e. the slope of the dependence of I_0/I on fluoride concentration (Figure 3.11, green trace). The experimentally derived K_{SV} value for monolayers of **3-2** (0.38) was found to be similar to that of the most "dilute" monolayer of **2-C** (11% monolayer, 0.35) which supported the conclusion of inhibited intermolecular energy transfer and vanishing signal amplification upon dilution of **2-C** in the monolayers. Overall, surface dilution enabled gradual tuning of the photonic amplification from a maximum of approximately 7 (in 100% sensor monolayer) to 1 (no amplification) in the 11% diluted monolayer.
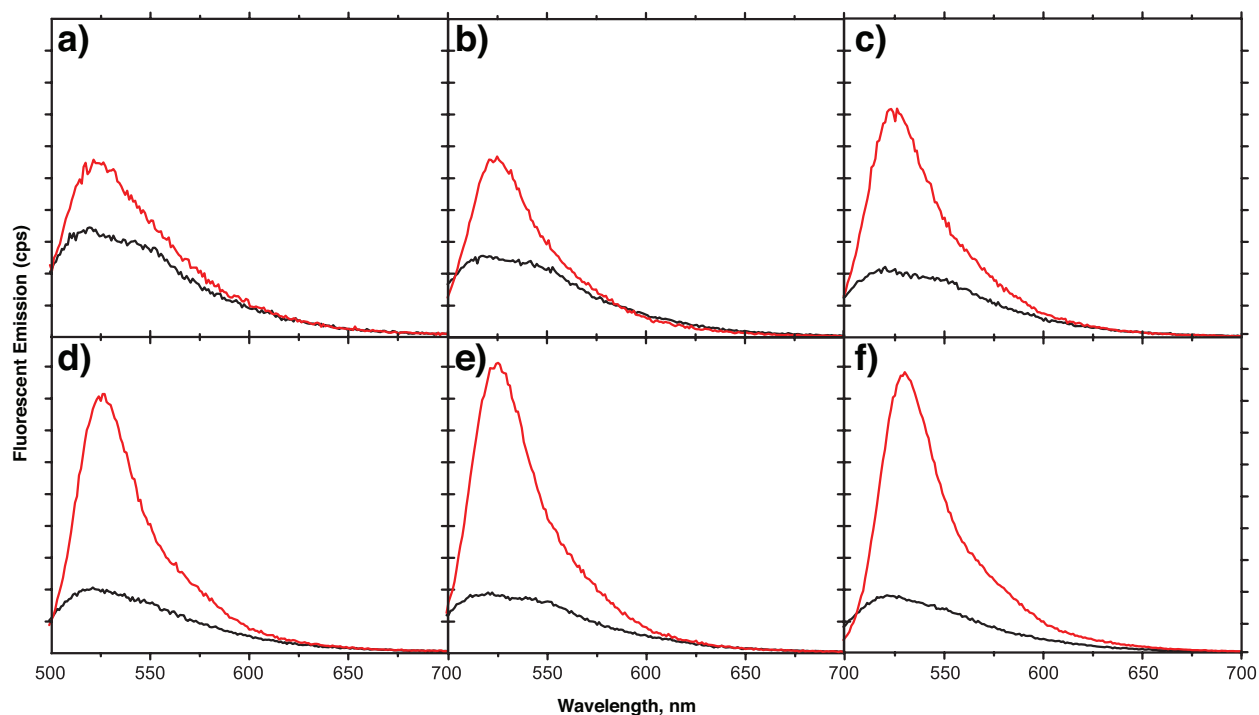
Figure 3.12. Fluorescence spectra of glass-immobilized monolayer of **3-2** prior to exposure to fluoride (*black traces*) and after exposure to Bu$_4$NF solutions in THF *(red traces)* with the following fluoride concentrations: 1.83 μM (a), 4.17 μM (b), 6.25 μM (c), 8.00 μM (d), 10.00 μM (e), and 12.0 μM (f). Spectra were acquired at 475 nm irradiation.

Further evidence for diminished energy transfer upon dilution of monolayers of **2-C** with ODMS could be gathered from the normalized excitation (at 510 nm) spectra corresponding to fluorescein emission (Figure 3.13). The band at 370 nm corresponded to excitation of fluorescein indirectly through energy transfer, where the band at 510 nm corresponded to direct fluorescein excitation. Upon decreasing concentration of active sensor **2-C** within the monolayer, the fluorescein direct excitation process became more significant (as evidenced by the higher intensity of the band at 510 nm) with respect to excitation resulting from the energy transfer. This is due to the increasing spatial separation between the active sensor molecules **2-C** within the monolayer making the energy transfer process (370 nm) less efficient.
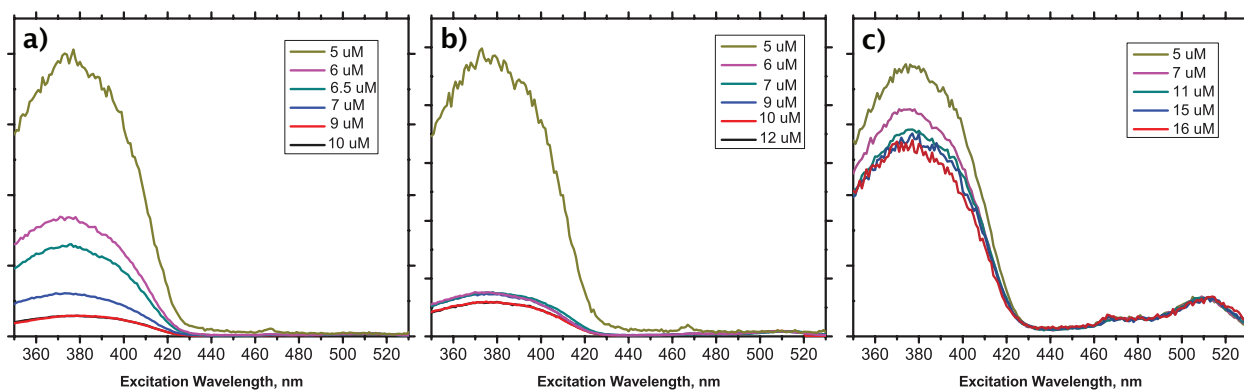
Figure 3.13. Normalized excitation spectra at the fluorescein absorption region (510 nm) for pure fluoride sensor monolayers (a), 20% monolayers (b), and 11% monolayers (c).

In order to rule out molecular realignment and other morphological changes upon increasing amounts of ODMS that might impact the rate of intermolecular energy transfer, optical anisotropy studies were carried out.[11] Variable angle optical anisotropy measurements on thin films of organic chromophores may provide information on the alignment of molecules in the film. UV-Visible absorption spectra of immobilized films of **2-C** with varying surface dilution were recorded with vertical and horizontal plane polarized light (to correct for anisotropy of the instrument detector) and then depolarized on the detector side of the sample (Figure 3.14). The angle of incident light was changed in 10º increments from 0º to 40º relative to substrate normal. An anisotropic film with uniform alignment of transition dipole moments will show a dependence of absorption on angle of plane-polarized light incidence with a maximum when the electric field component of the incident light is parallel to the transition dipole moment. While this is not the most accurate method to assess the molecular orientation, the experimental possibilities to do this are limited by the fact that the substrate is indeed a monolayer (thus weakly absorbing), and the optical anisotropy method at least lent some insight into the uniformity of molecular alignment of the sensor molecules at all dilution levels.
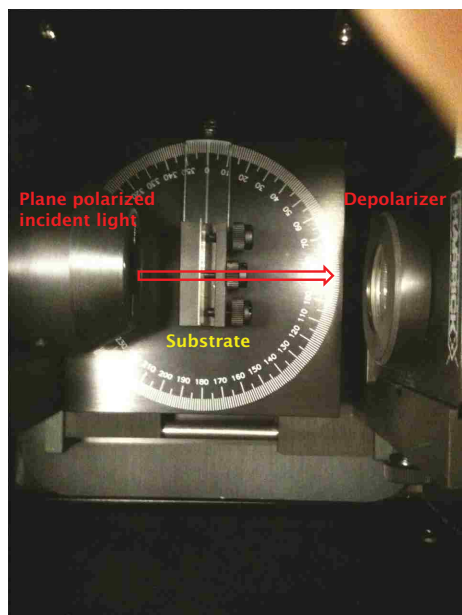
Figure 3.14. Experimental setup for determining anisotropy of thin films via variable-angle UV-Visible absorbance.

Once the spectra corresponding to vertical and horizontal polarization plane were collected at each incidence angle, they were converted to a plot of dichroic ratio (D_{HV}) versus wavelength (Figure 3.15a-c).

$$D_{HV} = \frac{A_H}{A_V} = 1 + \frac{2 - 3\sin^2\varphi}{\sin^2\varphi}\sin^2\delta \qquad (3.1)$$

In this method, the value of the dichroic ratio was extracted from a region of the spectrum with the least amount of noise (generally the maximum absorbance). A plot this ratio against angle of incidence that would result in a linear correlation is indicative of an anisotropic sample where the molecular binding angle (**φ**) relative to the surface normal can be obtained from Equation. 3.1. No linear correlation or high degree of scatter would be indicative of an isotropic sample.
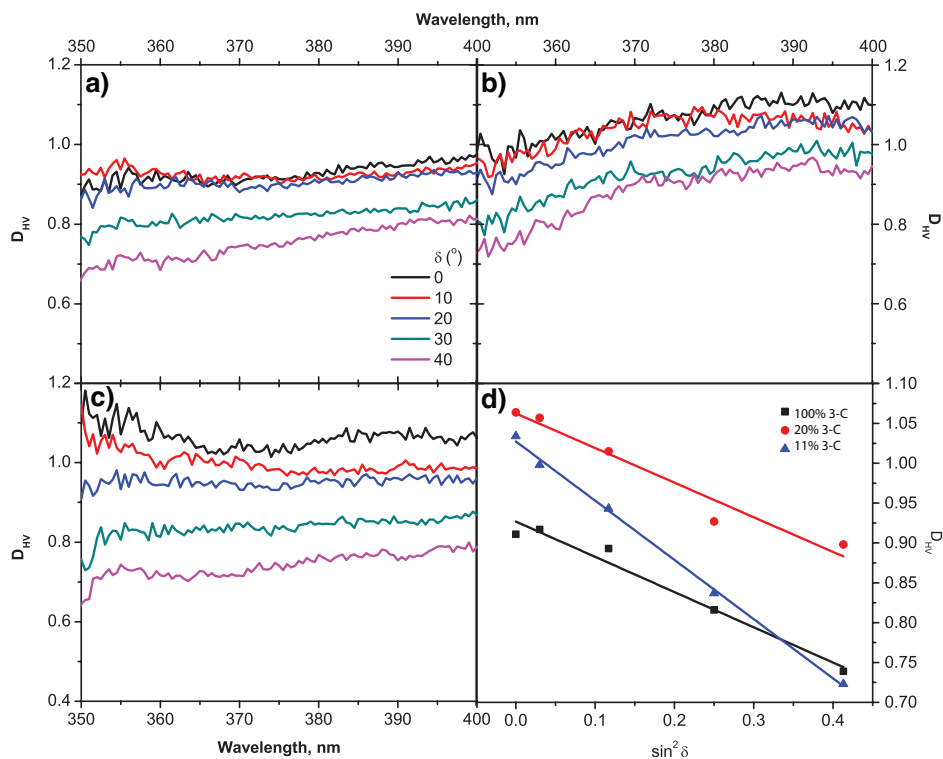
Figure 3.15. Wavelength dependence of the dichroic ratio D_{HV} at different twisting angles δ for "undiluted", 100% monolayer of **2-C** (a), and the monolayers prepared from solutions of **2-C** with ODMS "diluter" in molar ratio of 1:4 (b), and 1:8 (c). Linear relationship between D_{HV} at 370 nm and $\sin^2\delta$ for the monolayers in a-c (d).

Conversion of the absorption spectra to dichroic spectra and subsequent plotting vs. angle of incidence resulted in linear correlated functions (Figure 3.15d) for the monolayers with all levels of dilution. According to these results, all three dilution levels maintain anisotropy within the monolayer. Interestingly, the molecular angle with respect to the surface normal was apparently very similar (~60°); however, it must be stated that this method is not very accurate in determining the actual angles, especially with such low-absorbing samples. The sensor molecules apparently lay nearly flat within the monolayer in an arrangement very similar to roofing shingles, which would place one end cap fluorescein roughly directly on top of a PE of a neighboring molecule. Further understanding of the implication of such an organization with respect to intramolecular energy transfer efficiency requires additional studies.

3.3 Conclusion

In conclusion, a simple approach toward control of photonic amplification was developed and applied to a thin-film ratiometric sensor for fluoride based on surface immobilized conjugated oligomers. Using this approach, the signal amplification in these monolayers can be tuned by changing spatial separation of sensor molecules via co-deposition of an inert "diluter." This method also allows for the synthesis of fluorescent chemosensors with tunable sensitivity and detection range can be applied to future sensing materials and devices of this class. The end result is a practical device that can offer quantitative as well as qualitative data in the field using convenient handheld UV illumination. The devices transition from blue to green emissive after exposure to fluoride, a change that can be readily recognized by the human eye (Figure 3.16).
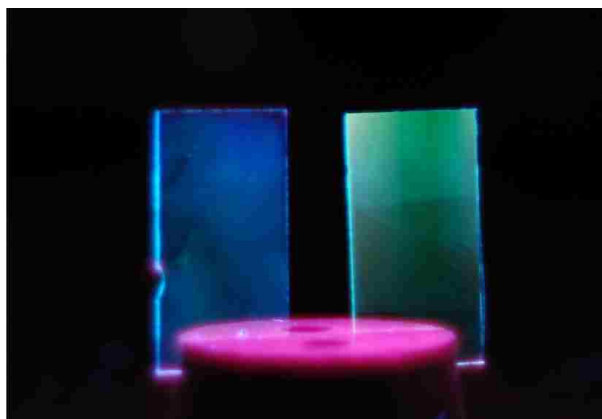
Figure 3.16. A slide of 100% monolayer **2-C** under handheld UV illumination before fluoride exposure (blue) and after fluoride exposure (green).

In addition, experiments that probed the morphological nature of this type of sensing film have been carried out which gave some insight into the effect of molecular organization on energy transfer efficiency in these materials. The fundamental properties determined in this chapter will be applied to further sensors of this class in order to generate more versatile thin-film ratiometric fluorescent sensor devices.

3.4 References

(1)   Thomas, S.W., III.; Joly, G. D.; Swager, T. M., Chemical Sensors Based On Amplifying Fluorescent Conjugated Polymers. *Chem. Rev.* **2007**, *107,* 1339-1386.

(2)   Acharya, J. R.; Zhang, H.; Xian, Li.; Nesterov, E. E. Chemically Controlled Amplified Ratiometric Fluorescence in Surface-Immobilized End-Capped Oligo(*p*-phenylene ethynylene)s. *J. Am. Chem. Soc.* **2009**, *131*, 880-881.

(3)   Imsick, B. G.; Acharya, J. R.; Nesterov, E. E. Surface-Immobilized Monolayers of Conjugated Oligomers as a Platform for Fluorescent Sensors Design: The Effect of Exciton Delocalization on Chemosensing Performance. *Adv. Mater.* **2013**, *25*, 120-124.

(4)   Guliyev, R.; Coskun, A.; Akkaya, E. U., Design Strategies for Ratiometric Chemosensors: Modulation of Excitation Energy Transfer at the Energy Donor Site. *J. Am. Chem. Soc.*, **2009**, *131*, 9007-9013.

(5)   Park, S.-J.; Gesquiere, A. J.; Yu, J.; Barbara, P. F., Charge Injection and Photooxidation of Single Conjugated Polymer Molecules. *J. Am. Chem. Soc.* **2004**, *126*, 4116-4117.

(6)   Kohn, P.; Ghazaryan, L.; Gupta, G.; Sommer, M.; Wicklein, A.; Thelakkat, M.; Thurn-Albrecht. T. Thermochromic Behavior, Packing, and Thin Film Structure of an Electron Accepting Side-Chain Polymer. *Macromolecules.* **2012**, *45*, 5676-5683.

(7)   Wuts, P. G. M.; Greene, T. W. *Greene's Protective Groups in Organic Synthesis*, Wiley, **2006.**

(8)   *Handbook of Chemistry and Physics 91st Edition*, CRC Press, **2010**.

(9)   Yang, X.-F.; Ye, S.-J.; Bai, Q.; Wang, X.-Q., A Fluorescein-based Fluorogenic Probe for Fluoride Ion Based on the Fluoride-induced Cleavage of *tert*-butyldimethylsilyl Ether. *J. Fluoresc.* **2007**, *17*, 81-87.

(10)   Ruecker, C., The Triisopropylsilyl Group in Organic Chemistry: Just a Protective Group, or More? *Chem. Rev.* **1995**, *95*, 1009–1064.

(11)   Martínez V. M.; Arbeloa, F. L.; Prieto, J. B.; Arbeloa, I. L., Orientation of Adsorbed Dyes in the Interlayer of Space of Clays. 1. Anisotropy of Rhodamine 6G in Laponite Films by Vis-Absorption with Polarized Light. *Chem. Mater.* **2005**, *17*, 4134-4141.

CHAPTER 4. A NOVEL SEMINAPTHOFLUORESCEIN DYE AS A BROAD ABSORPTION FLUORESCENT TAG

4.1 Introduction

Fluorescent dyes are popular luminescent tags for cellular assay studies and optical imaging of organelles in intracellular environments.[1] These tags are functionalized with synthetic "handles" that are stable in aqueous media, however reactive to nucleophilic sites *in vivo*. Functionalities include *N*-hydroxysuccinimidyl (NHS) esters, isothiocyanates, or phosphoramidites and are succeptible to nucleophilic residues (cysteine, histidine, or lysine) on proteins and render the biomolecules permanently labeled for imaging studies. Such labeled proteins are useful for the study of dynamic processes such as protein docking, folding, or other binding events through the use of fluorescence resonance energy transfer, or FRET, a homonym for the Förster energy transfer process.
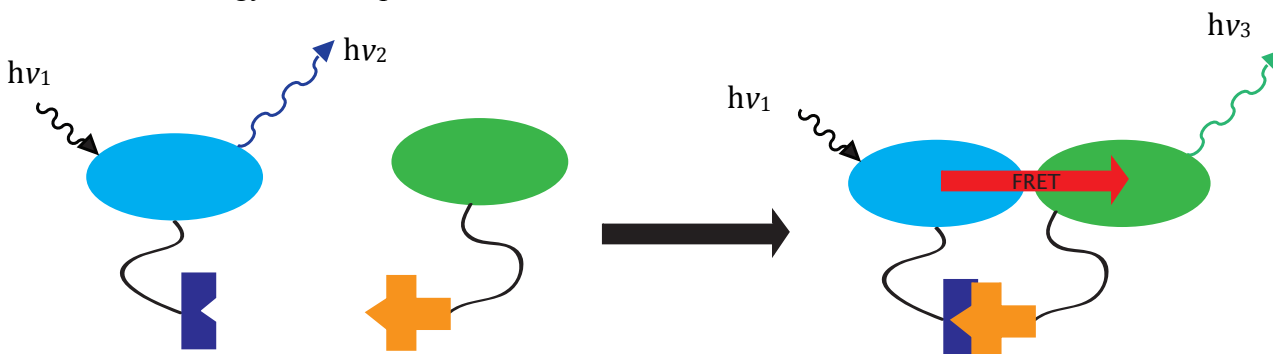
Figure 4.1. Cartoon representing FRET for biological imaging applications.

Biological FRET studies take advantage of the distance dependency of donor and acceptor fluorophores to reveal kinetic characteristics of the process in question. Also important is the overlap integral between donor emission and acceptor absorption, where a greater overlap results in a higher efficiency of the FRET process. A representative use of FRET (Figure 4.1) is where two separate proteins are labeled, one with a donor fluorophore and the other with an acceptor. In the absence of binding, excitation of the donor results in solely its own emission due to the

lack of FRET processes.   Upon binding, the donor and acceptor come in close proximity and

FRET becomes significant.[2] An alternative use is monitoring the organization of DNA, in that

two complimentary strands of nucleobases are individually labeled with a donor-acceptor pair.

Upon helix formation the two fluorescent dyes can undergo FRET due to the close proximity.
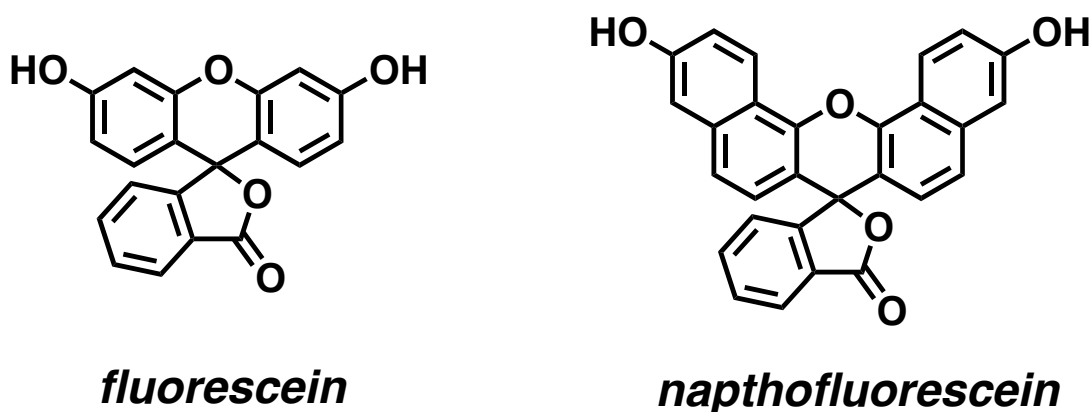
Figure 4.2. Common fluorescein derivatives: fluorescein and napthofluorescein.

   Fluorescein and its derivatives (Figure 4.2) are commonly used tags for cellular assay studies.

Fluorescein is not ideal for long duration FRET studies due to its susceptibility towards

photobleaching to form non-emissive species.   It also is characterized by a relatively narrow

absorption spectrum, rendering it a poor FRET acceptor.   Napthofluorescein is an improvement

upon fluorescein, but it is still characterized by a narrow absorption band despite exhibiting

significantly red-shifted emission while offering no additional stabilization towards

photobleaching.   Thus, both of these dyes are not optimal for applications in FRET studies.   In

addition, emission characteristics of fluorescein-type dyes show strong pH-dependence and these

dyes are poorly emissive at less-than-neutral pH due to a closed lactone disrupting electron

delocalization.
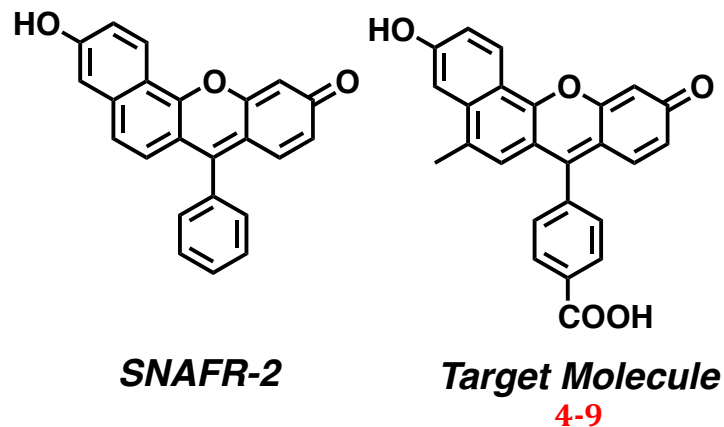
Figure 4.3. Previously synthesized minor regioisomer SNAFR-2 and the target molecule **4-9** of synthetic work in this chapter.

Ideally, a FRET donor should have significant emission over a broad range of wavelengths so that it can operate with a wide variety of FRET acceptors.[3] In addition, the donor fluorophore can be preferentially excited to avoid accidental direct excitation of the acceptor. Thus, fluorophores with very large Stokes shifts are very useful in FRET studies as they can be excited at lower wavelengths that red-shifted acceptors do not absorb. Broad absorption can enable a dye to be compatible with any other higher energy fluorophores or even used in combination with multiple dyes in order to develop more sophisticated multiplexing experiments. A group of semi-napthofluorescein compounds previously developed showed promising spectral properties for FRET applications.[4] Strongin et al. have previously developed a series of semi-napthofluorones that were shown to have significantly red-shifted and broad absorption, when compared to regular fluoresceins and napthofluoresceins, due to the absence of symmetry and extended conjugation. Another key feature is the absence of the *ortho*-carboxylate group that ensures higher delocalization (and thus, higher and bathochromically-shifted emission) in more acidic conditions. In Strongin's original synthesis, a minor product formed in this synthesis, SNAFR-2 (Figure 4.3), was found to comprise less than 1% of the hard-to-separate product mixture, but was found to have interesting properties that would warrant a direct, targeted synthesis (not

developed as of now).[5] Also desired would be to fit the dye with a reactive "handle" for future use in bio-conjugation. In this particular case, we planned to incorporate a carboxylic acid group that can be conveniently converted to an NHS ester when needed for bio-conjugation.

4.2 Results and Discussion

4.2.1 Synthesis

Scheme 4.1. Synthesis of target semi-napthofluorescein dye **4-9**.
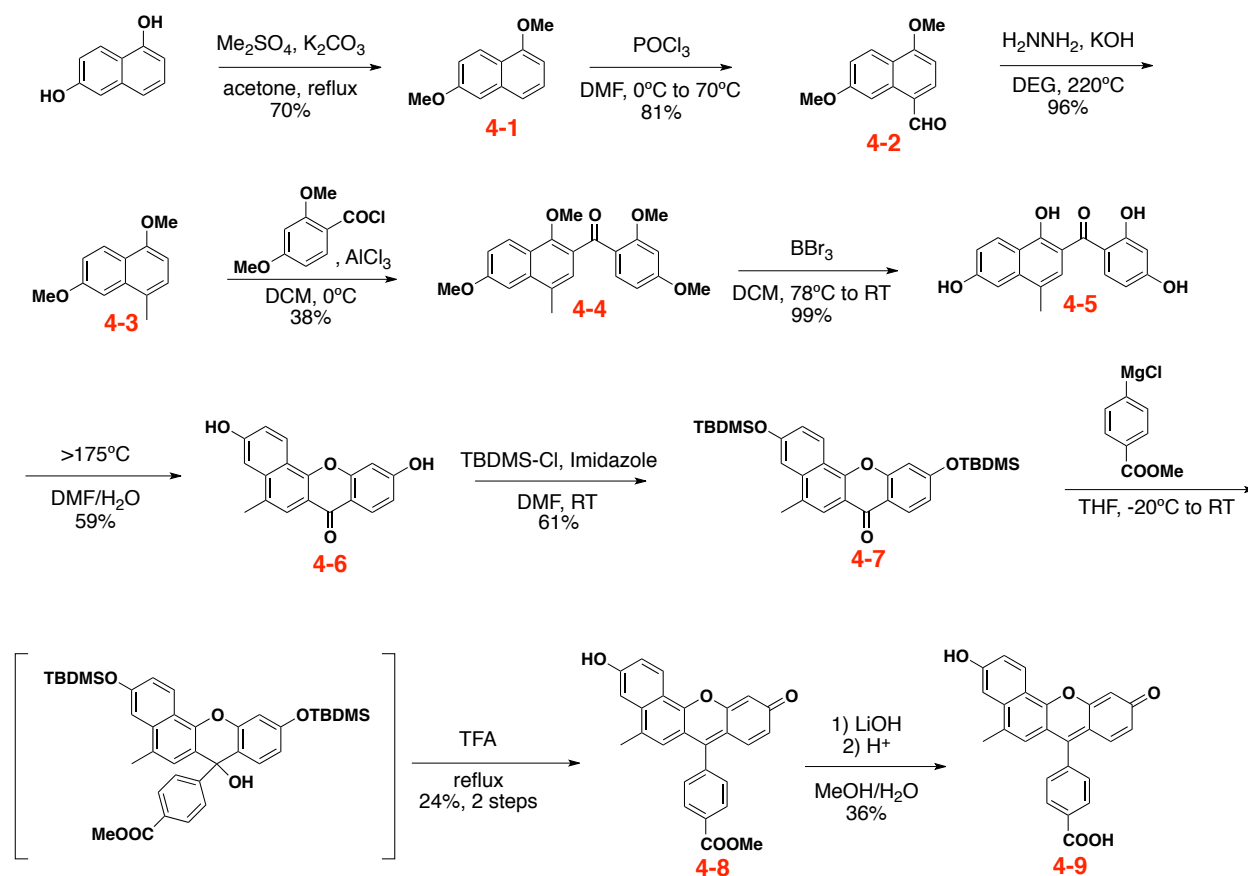
The synthesis to yield target dye **4-9** as a main product is outlined in Scheme 4.1. Starting from commercially available 1,6-dihydroxynapthalene, the synthesis began by converting OH groups using dimethylsulfate to generate 1,6-dimethoxynapthalene **4-1**.[6] A complicating issue was that any electrophilic substitution on the compound **4-1** would be directed to the 4-position of the naphthalene ring. Such substitution would then produce a wrong regioisomer of the dye.

Therefore, we decided to block the reactive 4-position by adding a methyl group there. This was done by the sequence of Vilsmeier-Haack formylation (**4-2**)[7] and Kishner-Wolff reduction[8] to yield **4-3**. Once the 4-position was blocked, the next electrophilic substitution was directed to the 2-position. The acid chloride for Friedel-Crafts acylation was simply generated by treatment of 2,4-dimethoxybenzoic acid with oxalyl chloride in dichloromethane with catalytic DMF. Using a stoichiometric amount of aluminum chloride and 2,4-dimethoxybenzoyl chloride, **4-3** was acylated predominantly at the 2 position, yielding **4-4** as was confirmed by X-ray crystallography (Figure 4.4).
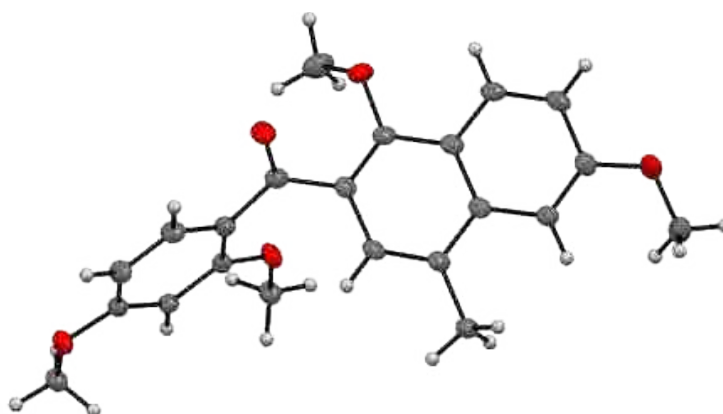
Figure 4.4. Structure of compound **4-4** as confirmed by single crystal X-ray diffraction.

All four methoxy groups in compound **4-4** were demethylated using excess BBr_3 to form **4-5**, when thermally cyclized/dehydrated in a mixture of DMF and water to form semi-napthoxanthone **4-6**. This transformation can also be effected using only water[9] and a Lewis acid catalyst (such as zinc acetate); however, higher temperatures (300ºC, sealed tube) were required and milder conditions were developed for safety reasons. Interestingly, crude **4-5** was found to result in higher yield than specially purified material, presumably due to residual

hydrogen bromide from quenching of the boron tribromide. Due to the poor solubility of **4-6**, it was used as obtained to convert into bis-silyl protected compound **4-7**. The compound **4-7** was surprisingly crystalline given the well-known (and experimentally observed, in this case) disordered nature of TBDMS groups. The structure of **4-7** was confirmed by single crystal X-ray analysis (Figure 4.5).
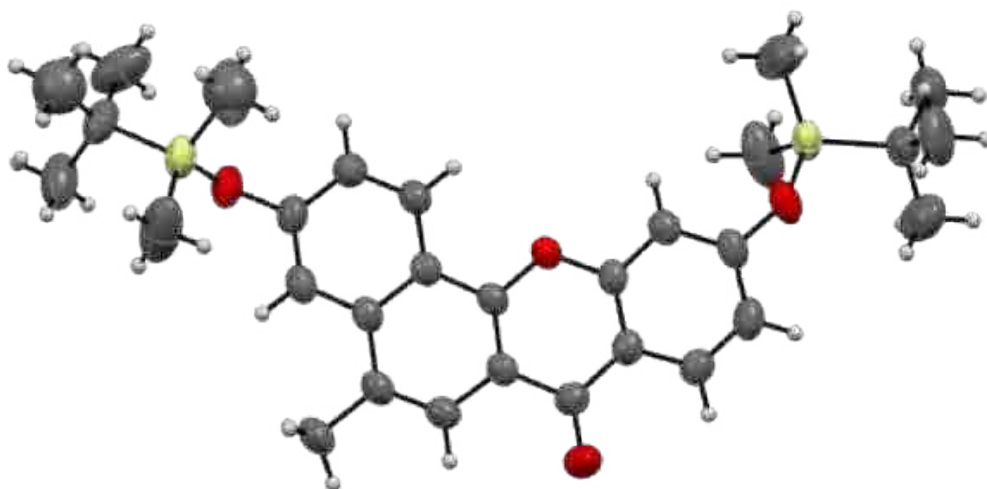
Figure 4.5. Structure of TBDMS-protected seminaphthoxanthone **4-7** as confirmed by single crystal X-ray diffraction.

With precise temperature control, a Grignard reagent could be generated from methyl 4-iodobenzoate that is unreactive to the methyl ester functionality using magnesium-halogen exchange with isopropylmagnesium chloride of precisely known concentration.[10] Addition of this Grignard reagent to **4-7** yielded an intermediate tertiary alcohol. In a one-pot reaction, the Grignard reagent was added to the protected seminapthoxanthone and the reaction mixture was refluxed with TFA to simultaneously cleave the protecting groups and cause the elimination of water in the alcohol forming an intensely colored fluorescent dye, **4-8**. The structure of the compound **4-8** was confirmed by single crystal X-ray diffraction (Figure 4.6). The synthesis was

completed with hydrolysis of the methyl ester with LiOH to form the final product **4-9** which

was purified through precipitation from basic aqueous solution. The overall yield of **4-9** based on

1,6-dihydroxynapthalene was approximately 5%.
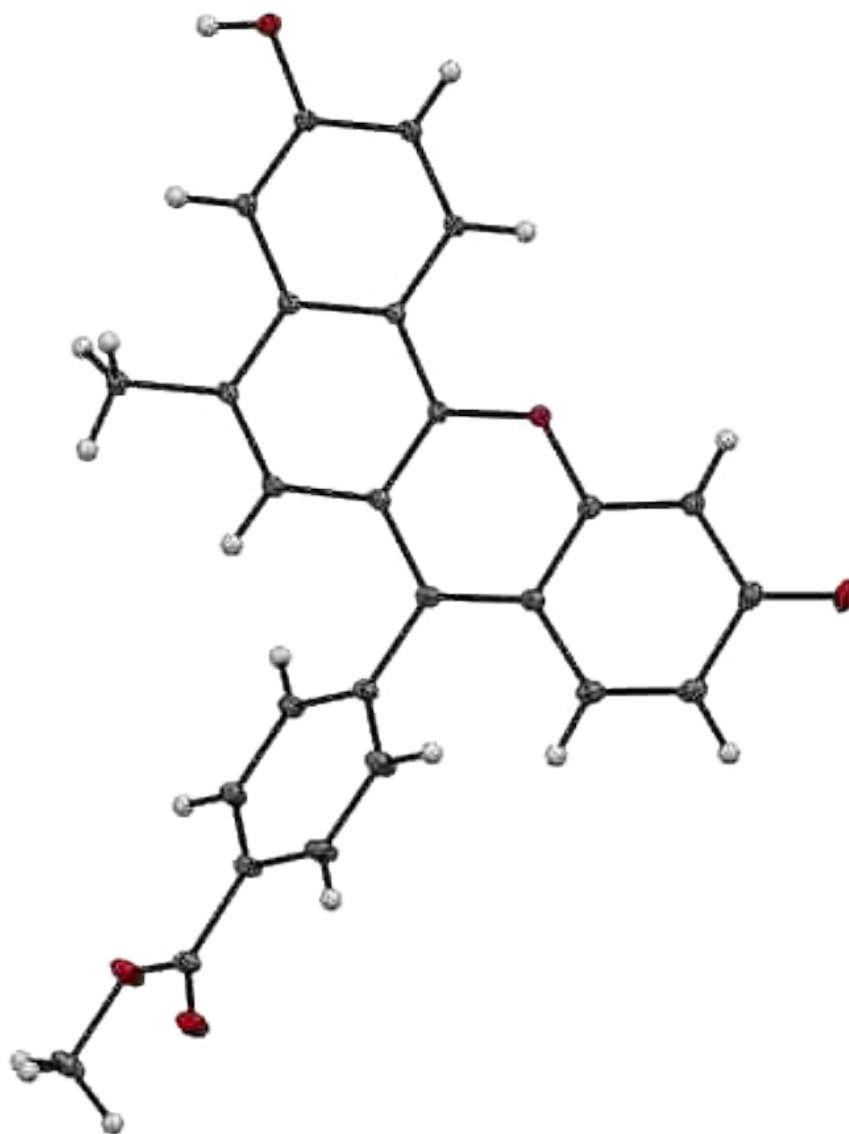
Figure 4.6. Structure of compound **4-8** as confirmed by single crystal X-ray diffraction.

4.2.2. Spectroscopic Properties

All spectroscopic measurements were carried out on a Cary 50 spectrophotometer and a PTI QuantaMaster4/2006SE fluorimeter. pH-dependent studies were carried out using buffer solutions (pH 3-6 (phthalate), pH 7-8 (phosphate), and pH 9-11 (borate)) at a concentration of 0.05 M. Quantum efficiencies were quantified using quinine sulfate in 1N H_2SO_4 as a standard. Additional details about data acquisition are available in the Experimental Section.

The newly synthesized fluorescent dye, **4-9**, when solubilized in DMSO and added to buffers of various pH values, exhibited intriguing absorption characteristics (Figure 4.7). In basic solutions, the intense absorption maximum was centered at 550 nm with gradual hypsochromic shift upon increasing acidity.
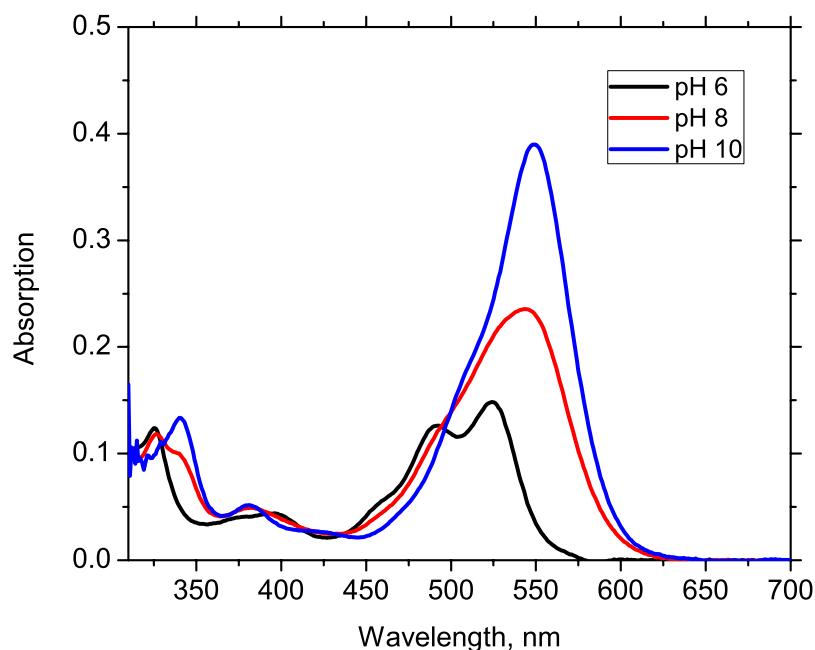
Figure 4.7. UV/Vis absorption spectra 13 μM solution of **4-9** at various pH values. Extinction coefficients at the band maxima: 30000 (pH 10); 18000 (pH 8); 11500 (pH 6).

Interestingly, the dye exhibited significant absorbance within the 310-450nm range at all pH values, and showed a peculiar absorption band around 325 nm that was probably characteristic of electronic transitions in an isolated naphthalene fragment.[5]
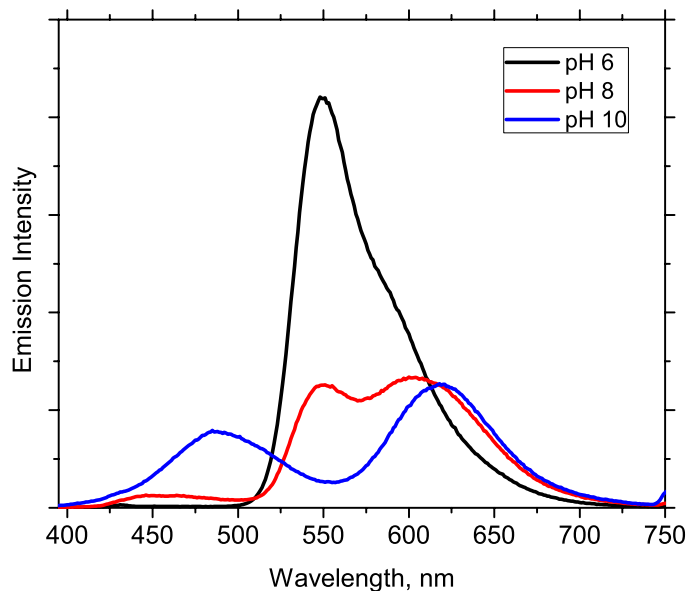
Figure 4.8. Emission spectra of compound **4-9** in 0.05 M pH 6, 8, and 10 buffers (acquired at 370 nm excitation).

Excitation into the maximum absorption band revealed two emission bands at higher pH (480 nm and 625 nm) and a single band under acidic conditions (550 nm). Quantum efficiencies were determined to be 0.29 at pH 6, 0.20 at pH 8, and 0.17 at pH 10 upon excitation at approximately 375 nm. Interestingly, the properties of this dye partially disagree with the conclusion of Urano et al.[11] In their studies of the roles of substituent groups on fluoresceins, they concluded that an *ortho* substituent on the isolated phenylene moiety was required in order to obtain high quantum yields of fluorescence by enforcing orthogonality of the benzene ring. However, the dye **4-9** synthesized in this chapter had reasonably high quantum yields, especially for an orange emitting dye. Excitation at the absorption range of 310-450nm range resulted in significantly

bathochromically shifted emission independent of wavelength of excitation, therefore resulting in a Stokes shifts of approximately 250 nm at pH 10, and approximately 175 nm at pH 6 (Figure 4.8). This large Stokes shift is advantageous for use of this dye as a "universal" FRET donor, as it can work with minimal interference with many of the more red-shifted acceptor dyes. The excitation spectrum (625 nm, pH 10) also showed similar features to the absorption spectrum at pH 10. (Figure 4.9).
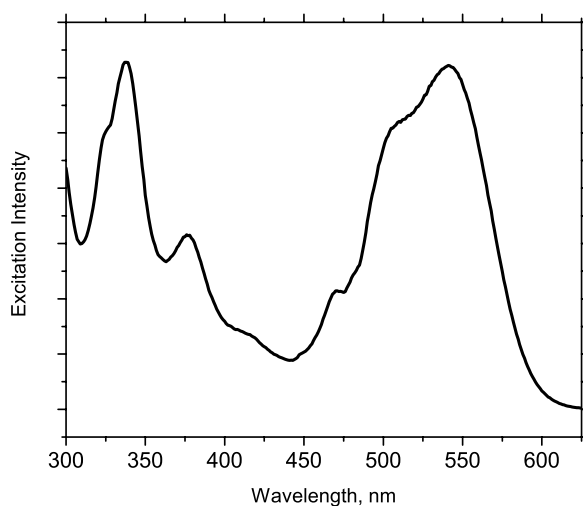
Figure 4.9. Excitation spectrum (625 nm) of compound **4-9** at pH 10.

4.3 Conclusion

In conclusion, a broad absorption dye with significantly red-shifted emission has been synthesized and characterized. Due to its large Stokes shift, it makes an ideal candidate for use as a universal FRET donor in biological studies. The large difference between excitation and emission is useful for pairing with FRET acceptors to avoid incidental direct excitation of acceptor fluorophores due to overlap of absorption spectra in classical FRET pairs. In addition, the high quantum efficiency of excitation is useful in obtaining high quality data. Future studies will utilize the carboxylic acid handle for bioconjugation.

4.4 References

(1)   Silvius, John R.; Nabi, Ivan Robert. Fluorescence-quenching and Resonance Energy Transfer Studies of Lipid Microdomains in Model and Biological Membranes. *Mol. Mem. Bio.* **2006**, *23*, 5–16.

(2)   Anslyn, A. V.; Dougherty, D. A. *Modern Physical Organic Chemistry*. University Science Books: Sausalito, 2006.

(3)   Takahusa, H.; Kikuchi, K.; Urano, Y.; Higuchi, T.; Nagano, T. Intramolecular Fluroescence Resonance Energy Transfer System with Coumarin Donor Included in β-Cyclodextrin. *Anal. Chem.* **2001**, *73*, 939-942.

(4)   Yong, Y.; Lowry, M.; Xu, X.; Escobedo, J. O.; Sibrian-Vazquez, M.; Wong, L.; Schowalter, C. M.; Jensen, T. J.; Fronczek, F. R.; Warner, I. M.; Strongin, R. M. Seminapthofluorones are a Family of Water-Soluble, Low Molecular Weight, NIR-Emitting Fluorophores. *Proc. Natl. Acad. Sci. USA* **2008**, *105*, 8829-8834.

(5)   Yang, Y.; Lowry, M.; Schowalter, C. M.; Fakayode, S. O.; Escobedo, J. O.; Xu, X.; Zhang, H.; Jensen, T. J.; Fronczek, F. R.; Warner, I. M.; Strongin, R. M. An Organic White Light-Emititng Fluorophore. *J. Am. Chem. Soc.* **2006,** *128*, 14081-14092.

(6)   Corrie, J. E. T.; Papageorgiou, G. Synthesis and Evaluation of Photolabile Sulfonamides as Potential Reagents for Rapid Photorelease of Neuroactive Amines. *J. Chem. Soc., Perkin Trans. 1.* **1996**, *13*, 1583-1592.

(7)   Doetz, K. H.; Popall, M. Carbene Ligands as Anthracyclinone Synthons, 6. - Metal Carbene Chelates as Key Reagents in Syntheses of the Daunomycinone Series: Regiospecific Annulation of Arylcarbene Ligands as a Strategy towards the Synthesis of Rings B and C. *Chem. Ber.* **1988**, *121*, 665-672

(8)   Buu-Hoi, N. P.; Lavit, D. Compounds with Potential Activity Against Lethal Radiations. V. Methyl Homologs of 1,5-Dihydroxynapthalene. *J. Org. Chem.* **1955**, *20*, 1191-1196.

(9)   Chen, C.-A.; Yeh, R.-H.; Lawrence, D. S. Design and Synthesis of a Fluroescent Reporter of Protein Kinase Activity. *J. Am. Chem. Soc.* **2002**, *124*, 3840-3841.

(10)   Mottram, L. F.; Boonyarattanakalin, S.; Kovel, R. E.; Peterson, B. R. The Pennsylvania Green Fluorophore: A Hybrid of Oregon Green and Tokyo Green for the Construction of Hydrophobic and pH-Insensitive Molecular Probes. *Org. Lett.* **2006**, *8*, 581-584.

(11)   Urano, Y.; Kamiya, M.; Kanda, K.; Ueno, T.; Hirose, K.; Nagano, T. Evolution of Fluorescein as a Platform for Finely Tunable Fluorescence Probes. *J. Am. Chem. Soc.* **2005**, *127*, 4888-4894.

CHAPTER 5. EXPERIMENTAL SECTION

5.1 General Considerations

All reactions were performed under an atmosphere of dry nitrogen, except those that required Schlenk techniques, which were performed under an atmosphere of ultrapure argon. Melting points were determined in open capillaries and are uncorrected. Chromatographic separations were carried out on silica gel (EMD, 60 Å, 40-63 μM, pH = 6.8-7.0) slurry packed into glass columns. Toluene, THF, dichloromethane, and hexane were dried by passing through columns of activated alumina and *N,N*-dimethylformamide (DMF) was dried though a column of molecular sieves both contained in a PS-400 Solvent Purification System from Innovative Technologies, Inc. The water content in the solvents was confirmed by coulometric titration on a Mettler Toledo DL 32 diaphragmless coulometric titrator. High purity $Pd(PPh_3)_4$ was obtained from Strem, while all other reagents were obtained from Sigma-Aldrich and Alfa Aesar and used as received. Indium tin oxide (ITO) coated glass with an 8-12 Ω/cm^2 surface resistivity was purchased from Delta Technologies, Ltd.. ^{1}H NMR spectra were recorded at 250 MHz unless otherwise indicated and are reported in parts per million downfield from tetramethylsilane. UV-Visible spectra were recorded on a Varian Cary 50 spectrophotometer. Optical anisotropy measurements were performed on a Agilent Cary 5000 spectrophotometer with photomultiplier tube detector. Fluorescence studies were carried out using a PTI QuantaMaster4/2006SE spectrofluorimeter. Quantum yields of monolayers were estimated in thin films by using a spin-coated film prepared using a 0.1 mM solution of 9,10-diphenylanthracene ($\Phi = 0.83$) in PMMA. Optical anisotropy experiments were performed on a Cary 5000 spectrophotometer with a sample mounted on a Brewster angle holder, optical polarizer before the sample, and a depolarizer placed after the substrate, and corrected with an isotropic spin-coated sample. High-

resolution mass spectra were obtained at the Mass Spectrometry Facility at Louisiana State University using an ESI-TOF or MALDI-TOF method with peak matching protocol to determine the mass and error range of the molecular ion. Electrochemical measurements were carried out on an Autolab PGSTAT 302 potentiostat from Eco Chemie.

5.2 Substrate Cleaning and Activation

Microscope cover slips (25x25mm) were cut using a ceramic cutting tile to fit diagonally in a 1 cm cuvette with minimal movement. The glass pieces were then washed with acetone, chloroform, methanol, and then water for 30 minutes each under sonication. The slides were then thoroughly dried under a flow of nitrogen. The cleaned slides were placed in 20 mL scintillation vials and filled with freshly prepared piranha solution (7:3 H_2SO_4:30% H_2O_2) until the cover slip was submerged. (**DANGER!!!** Piranha solutions are extremely corrosive and oxidizing. It must be prepared carefully due to exothermic mixing. Ensure that all contact surfaces are clean and free of any solvents from previous washings or other organic contaminants or else explosive conditions can be generated.) The vials were placed in a heating block at 75°C for 1 h, then were allowed to cool to room temperature and the slide removed and rinsed with copious amounts of Millipore-filtered water. The rinsed slides were then dried under a flow of nitrogen and protected from dust and other particulates overnight and were then ready for immobilzation. ITO was activated using "basic piranha" (NH_4OH:H_2O_2:Water, 1:1:5) and prewashed using the same procedure as the glass slides.

5.3 Monolayer Preparation Procedure

   Preparation of pH Sensor (2-9) Monolayers. The freshly activated glass slides were immersed into 0.2 mM solutions of one of the compounds **2-9**, **2-11** (in toluene), or **2-10** (in DMF) and kept at 80 °C for 2 h. After cooling to room temperature, the slides were rinsed with

copious amount of chloroform upon ultrasonication. After drying, the monolayer-modified slides were annealed by heating to 80 °C in aqueous buffered solution (pH 9.5) for 2 h. The annealed slides were washed with water and dried under the flow of nitrogen.

Preparation of Fluoride Sensor (2-C) Monolayers and Diluted Monolayers. A 0.1 mM stock solution of **2-C** was prepared in dry toluene. For monolayer "dilution" studies, three stock solutions of octadecyl(triethoxy)methylsilane (ODMS) were prepared with concentrations 0.8 mM, 1.6 mM, and 2.4 mM. Scintillation vials were filled with 8 ml of the stock solution of **2-C** and 4 ml of each of the three ODMS stock solutions were added to end up with 1:4, 1:8, and 1:12 molar ratio of **2-C** to ODMS. For slides with un-dilute monolayer of **2-C**, 4 ml of toluene was added to 8 ml of the stock solution of **2-C**. Thus, all series of deposition solutions maintained a uniform sensor **2-C** concentration of 0.06 mM. Two freshly activated slides were carefully placed in each scintillation vial with deposition solutions in such a way that they did not fall on top of each other, and the vials were kept at 70 °C for 1 h. The slides were then removed and rinsed with copious toluene, and sonicated for 30 min in toluene, followed by a second copious toluene rinse and drying under nitrogen.

5.4 pH Sensor Experiments

pH Sensor monolayers of compound **2-9** were inserted diagonally into a cuvette and the cuvette was filled carefully with the buffer of the desired pH and the absorbance and emission spectrum recorded. The pH value was changed by carefully removing the current buffer solution from the cuvette with a glass pipette and replacing with a new one, without disturbing the position of the glass slide. For the modified method of generating pH sensor monolayers (Scheme 2.3), using the silicon-protected monolayer of precursor **2-C** was first hydrolyzed for 5 minutes at pH 3, after that it was ready for ratiometric pH studies. Both routes to pH sensing

monolayers were exposed to the buffer solutions from low pH to high. Various pH buffer solutions were prepared from 0.1 M stock solutions of potassium hydrogen phthalate (pH 3-5), potassium dihydrogen phosphate (pH 6-8), or sodium tetraborate (pH 9-10), then carefully adjusted with 0.1 M HCl or 0.1 M NaOH to exact pH values, and finally diluted to a final concentration of 0.05 M.

5.5 Fluoride Sensor Exposure Conditions

Freshly prepared slides were immersed in 0.4 mM Bu_4NPF_6 in THF for 30 seconds, and then placed in a spectrofluorimeter cuvette along the diagonal. The cuvette was filled with THF and the emission spectrum of the pristine film was measured. The solvent was carefully removed with a pipette and replaced with Bu_4NF solution of required concentration and allowed to remain in the cuvette for 3 minutes, after which the emission and excitation spectrum was recorded. The slide was then removed and the cuvette thoroughly washed for the next experiment. Each slide was used to measure response on only one concentration of fluoride.

5.6 Evaluation of Monolayer Density of 3-C.
Cyclic voltammetry measurements were performed using an Autolab PGSTAT 302 potentiostat. The measurements were carried out using a three-electrode system with monolayer-modified ITO/glass working electrode (electrode area ~1.13 cm^2), $Ag/AgNO_3$ non-aqueous reference electrode, and a Pt gauze counter electrode in 0.1 M Bu_4NPF_6 solution in CH_2Cl_2 as supporting electrolyte. The reference electrode was checked against ferrocene standard every time before and after the experiments were performed, and the measured potentials were corrected based on the Fc/Fc^+ redox potential value.

The surface coverage density was estimated based on the measured area of the redox peak corresponding to irreversible oxidation of fluorescein group at ~0.9 V (Figure 3-14). The value

was corrected by the corresponding data for the bare ITO electrode. Assuming the reduction

being a one-electron process, the surface density Γ was estimated using the formula:

$$\Gamma = \frac{Q}{F}$$

where Q is the redox peak area (C cm^{-2}), and F is Faraday constant (96500 C mol^{-1}). For the

current case ($Q = 4.98 \times 10^{-6}$ C cm^{-2} after correcting for bare ITO electrode), the surface density Γ

was estimated as 5.17×10^{-11} mol cm^{-2}, which translates to 3.2 nm^2 per molecule of **3-C**.

5.7 Synthetic Details

5-Iodofluorescein (2-2) was prepared following the procedure by Burgess et al.[1] Reaction of

1.0 g of 5-aminofluorescein yielded 1.2 g (92%) of **2-2** as an orange solid, mp 334-336 °C (lit.

mp[1] 323-325 °C). ^{1}H NMR (δ, DMSO-$d6$): 10.12 (broad s, 2H), 8.28 (s, 1H), 8.07 (d, $J = 8.0$

Hz, 1H), 7.06 (d, $J = 8.0$ Hz, 1H), 6.70-6.40 (m, 6H).

4-Aminophenylacetylene (2-3) was prepared in two steps from 4-iodoaniline. First, a

mixture of 8.70 g (39.7 mmol) of 4-iodoaniline, 3.19 g (4.59 ml, 43.7 mmol) of TMS-acetylene,

0.55 g (0.78 mmol) of Pd(PPh$_3$)$_2$Cl$_2$ and 0.28 g (1.43 mmol) of CuI in 75 ml of THF – i-Pr$_2$NH

(7:3) mixture was stirred in a sealed Air-free flask at 40 °C for 12 h. After allowing to cool to

room temperature, the reaction mixture was poured into water and extracted with ether three

times. Combined organic fractions were washed with brine and dried over anhydrous Na$_2$SO$_4$.

After concentration in vacuo, the brown oil product was redissolved in CH$_2$Cl$_2$, filtered through a

short plug of silica gel and concentrated in vacuo to afford a yellow solid. This solid was

dissolved in 60 ml of methanol and vigorously stirred with 13.52 g (97.8 mmol) of K$_2$CO$_3$ at

room temperature for 12 h. The reaction mixture was poured into a saturated aqueous solution of

NH$_4$Cl and extracted with ethyl acetate. The organic fraction was washed with brine, and dried

over anhydrous Na_2SO_4. After concentration in vacuo, the crude product was redissolved in a small volume of ethyl acetate and filtered through a short plug of silica gel to afford 3.35 g (72%) of **2-3** as a brown solid, mp 99-100 °C(lit.[2] mp 104-105 °C). ^{1}H NMR (250 MHz, CDCl$_3$) d 7.29 (d, J = 8.7 Hz, 2H), 6.59 (d, J = 8.7 Hz, 2H), 3. 81 (broad s, 2H), 2.95 (s, 1H).

Compound 2-4 was prepared following the literature procedure.[3]

Compound 2-5a. A mixture of 0.29 g (0.23 mmol) of the iodide **2-4**, 32 mg (0.28 mmol) of 4-aminophenylacetylene **2-3**, 23 mg (0.02 mmol) of Pd(PPh$_3$)$_4$, and 1 grain of CuI in 8 ml of toluene – i-Pr$_2$NH (7:3) mixture was stirred in a sealed Air-free flask at 55 °C for 36 h. After cooling down to room temperature, the reaction mixture was concentrated in vacuo, and the crude product was purified by column chromatography on silica gel (eluent hexanes-CHCl$_3$ 1:1). A fraction with R_f 0.6 afforded 0.13 g (45%) of **2-5a** as yellow sticky solid, mp 130-134 °C. ^{1}H NMR (250 MHz, CDCl$_3$) d 7.45-7.25 (m, 10H), 6.65 (d, J = 8.5 Hz, 2H), 3.82 (s, 2H), 2.92-2.60 (m, 16H), 1.85-1.50 (m, 16H), 1.50-1.20 (m, 48H), 0.98-0.80 (m, 24H), 0.26 (s, 9H).

Compound 2-5b. A solution of 100 mg (0.08 mmol) of **2-5a** in 20 ml of THF was added to a stirred solution of 13 mg (0.24 mmol) of KOH in 10 ml of methanol at room temperature. After stirring for 1 h at room temperature, the reaction mixture was poured into water, extracted with CH$_2$Cl$_2$, washed with water and brine, and dried over anhydrous Na_2SO_4. After concentration in vacuo, the crude product was purified by column chromatography on silica gel (eluent hexanes-CHCl$_3$ 1:1). A fraction with R_f 0.54 afforded 80 mg (85%) of **2-5b** as a yellow solid, mp 118-121 °C. ^{1}H NMR (250 MHz, CDCl$_3$), d 7.45-7.24 (m, 10H), 6.67 (d, 2H, J = 8.5 Hz,) 3.84 (s, 2H), 3.32 (s, 1H), 2.92-2.70 (m, 16H), 1.68-1.55 (m, 16H), 1.50-1.25 (m, 48H), 1.00-0.84 (m, 24H).

Compound 2-6. A mixture of 110 mg (0.092 mmol) of **2-5b**, 63.0 mg (0.14 mmol) of 5-iodofluorescein **2-2**, 11 mg (9.5 mmol) of Pd(PPh$_3$)$_4$, and 1 small grain of CuI in 6 ml of

anhydrous DMF and 4 ml of *i*-Pr$_2$NH was stirred in a sealed Air-free flask for 36 h at 60 °C. The reaction mixture was allowed to cool down to room temperature and passed through a short plug of silica gel using chloroform as an eluent. The solution was concentrated in vacuo and the crude product was purified by column chromatography on silica gel (eluent methanol – CH$_2$Cl$_2$ 1:9). A fraction with R_f 0.42 afforded 86 mg (60%) of **2-6** as a reddish-brown solid, mp 248-254 °C. ^{1}H NMR (250 MHz, CDCl$_3$) d 8.23 (br. s, 1H), 7.85-7.30 (m, 19H), 6.98 (br. s, 1H), 6.66 (d, 4H, *J* = 8.4 Hz), 3.05-2.70 (m, 16H), 1.91-1.62 (m, 16H), 1.50-1.20 (m, 48H), 0.98-0.80 (m, 24H).

11-Isocyanoatodec-1-ene (2-7) was prepared following the modified literature procedure.[4] Diphenylphosphoryl azide (15.0 g, 11.75 ml, 54.4 mmol) was added dropwise to the mixture of 10.03 g (54.4 mmol) of ω-undecenoic acid, and 5.44 g (7.5 ml, 53.8 mmol) of triethylamine in 50 ml of acetonitrile and the reaction mixture was stirred at 50 °C for 2 h. After concentration in vacuo, the crude product was dissolved in 50 ml of CH$_2$Cl$_2$, diluted under nitrogen to a 2 l volume with hexanes, and allowed to settle until thick oil formed at the bottom of the solution. The hexane solution was decanted off and concentrated and the residue was subjected to Kugelrohr distillation (95 °C, 0.01 mm Hg), resulting in 7.32 g (74 %) of 11-isocyanoatodec-1-ene **2-7** as a colorless oil. The ^{1}H NMR data were in agreement with the previously published spectrum.[4]

Triethoxy-11-isocyanatodecylsilane (2-8) was prepared following the modified literature procedure.[5] A solution of 3.93 g (21.7 mmol) of 11-isocyanoatodec-1-ene and 1.0 ml of a 0.1 M Karstedt's catalyst solution in vinyl-terminated poly(dimethylsiloxane) was stirred at room temperature for 10 min, followed by dropwise addition of 5.74 g (6.45 ml, 43.4 mmol) of triethoxysilane. The resulting solution was stirred for 12 h under inert atmosphere. After concentration in vacuo, the oily residue was subjected to Kugelrohr distillation (80 °C, 0.01 mm

Hg) to yield 4.42 g (59%) of **2-8** as a colorless oil. The ^{1}H NMR data were in agreement with the previously published spectrum.[5]

pH Sensor compound 2-9. Triethoxy-11-isocyanatodecylsilane **2-8** (17 ml of a 0.406 M stock solution in toluene, 6.9 mmol) was added to a solution of 10 mg (6.6 mmol) of compound **2-6** in 0.5 ml of toluene, and the resulting mixture was stirred at 50 °C overnight. After concentration in vacuo, the crude product was purified by column chromatography on silica gel (eluent CH$_2$Cl$_2$) to yield quantitatively compound **2-9** as a reddish-brown solid. ^{1}H NMR (250 MHz, CDCl$_3$) d 8.13 (s, 1H), 7.85-7.00 (m, 20H), 6.90-6.75 (m, 2H), 5.09 (br. s, 1H), 4.10 (br. S, 1H), 3.83 (q, J = 7.5 Hz, 6H), 3.35-3.15 (m, 2H), 3.00-2.72 (m, 16H), 1.90-1.60 (m, 16H), 1.60-1.15 (m, 73H), 0.98-0.80 (m, 24H), 0.75-0.55 (m, 2H). MS (MALDI-TOF) m/e 1866.59 (calcd for C$_{125}$H$_{164}$N$_2$O$_9$Si 1865.22).

Compound 2-10. In a non-optimized procedure, triethoxy-11-isocyanatodecylsilane **2-8** (160 ml of a 0.406 M stock solution in toluene, 0.06 mmol) was added a solution of 22 mg (0.06 mmol) of 5-aminofluorescein in 0.4 ml of DMF and the reaction mixture was stirred at 50 °C for 6 h. The resulting solution of **2-10** was concentrated in vacuo, redissolved in EtOAc and subjected to flash chromatography on silica gel (eluent EtOAc) to yield 12 mg (27%) of **2** as a red oil. ^{1}H NMR (250 MHz, CDCl$_3$) d 7.15 (s, 1H), 7.06 (s, 1H), 6.82 (d, J = 8.5 Hz, 1H), 6.78-6.71 (m, 2H), 6.70-6.60 (m, 2H), 6.57 (d, J = 2 Hz, 1H), 6.46 (d, J = 8.5 Hz, 1H), 5.25-5.15 (m, 1H), 4.07 (br. s, 1H), 3.81 (q, J = 7.5 Hz, 6H), 3.35-3.20 (m, 2H), 1.80-1.50 (m, 4H), 1.50-1.10 (m, 21H), 0.70-0.60 (m, 2H). HRMS m/e 693.3202 [M+H]$^+$ (calcd for C$_{37}$H$_{49}$N$_2$O$_9$Si 693.3202).

Compound 2-11. Triethoxy-11-isocyanatodecylsilane **2-8** (73 ml of a 0.406 M stock solution in toluene, 0.03 mmol) was added to a solution of 36 mg (0.03 mmol) of compound **2-5b** in 0.5 ml of toluene, and the reaction mixture was stirred overnight at 50 °C, and then concentrated in

vacuo. The crude product was further purified by flash chromatography on silica gel (eluent CH$_2$Cl$_2$) which resulted in a quantitative yield of the title compound **2-11** as a yellow sticky solid. ^{1}H NMR (250 MHz, CDCl$_3$) 7.46 (d, J = 8.5 Hz, 1H), 7.42-7.30 (m, 8H), 6.67 (d, J = 8.5 Hz, 2H), 4.98-4.86 (m, 1H), 4.10 (br. s, 1H), 3.83 (q, J = 7.0 Hz, 6H), 3.34-3.20 (m, 3H), 2.96-2.70 (m, 16H), 1.85-1.55 (m, 16H), 1.50-1.20 (m, 73H), 0.98-0.80 (m, 24H), 0.70-0.55 (m, 2H). MS (MALDI-TOF) m/e 1535.42 (calcd for C$_{105}$H$_{154}$N$_2$O$_4$Si 1535.17).

Bis(triisopropylsilyl)-5-iodofluorescein (2-A). To a solution of 0.34 g (0.74 mmol) of **2-2** and 0.36 g (5.30 mmol) of imidazole in 5 ml of anhydrous DMF, 0.50 g (0.55 ml, 2.60 mmol) of neat triisopropylsilyl chloride (TIPS-Cl) was added dropwise at room temperature. The reaction mixture was stirred at room temperature for 24 h, then poured into CH$_2$Cl$_2$ and washed successively with water, brine, and dried over MgSO$_4$. After concentration in vacuo, the crude product was purified by column chromatography on silica gel (eluent hexanes − EtOAc 9:1) yielding 0.46 g (59%) of **2-A** as a colorless oil, R_f 0.35. ^{1}H NMR (CDCl$_3$) δ 8.34 (d, J = 1.5 Hz, 1H); 7.95 (dd, , J_1 = 8.0, J_2 = 1.5 Hz, 1H); 6.93 (d, , J = 8.0 Hz, 1H); 6.75 (d, J = 2.0 Hz, 2H); 6.65-6.50 (m, 4H); 1.28 (septet, J = 7.5 Hz, 6H); 1.08 (d, J = 7.5 Hz, 36H). HRMS (ESI-TOF) m/e 771.2385 M$^+$ (calcd. for C$_{38}$H$_{52}$IO$_5$Si$_2$ 771.2392).

Compound 2-B. A mixture of 0.48 g (0.45 mmol) of alkyne **2-5b** (prepared following the literature procedure[1]), 0.38 g (0.49 mmol) of iodide **2-A**, 2 mg (2 μmol) of Pd(PPh$_3$)$_4$ and one grain of CuI in 3 ml of toluene-diisopropylamine (7:3) was stirred in a sealed Schlenk flask at 45 °C for 24 h. After allowing to cool to room temperature, the reaction mixture was poured into CH$_2$Cl$_2$ and washed successively with saturated NaHCO$_3$, water, and brine. After concentration in vacuo, the crude product was further purified by column chromatography on silica gel (eluent CH$_2$Cl$_2$ − hexanes 1:1) to yield 0.26 g (31%) of **2-B** as a yellow oil, R_f 0.40. ^{1}H NMR (CDCl$_3$) δ

8.16 (s, 1H); 7.79 (d, J = 8.5 Hz, 1H); 7.71 (broad s, 1H); 7.50-7.30 (m, 10H); 7.18 (d, J = 7.8 Hz, 2H); 6.78 (s, 2H); 6.70-6.50 (m, 4H); 3.87 (broad s, 2H); 2.92-2.72 (m, 16H); 1.80-1.65 (m, 16H); 1.55-1.20 (m, 50H); 1.20-1.05 (m, 36H); 1.00-0.80 (m, 24H).

Fluoride sensor compound 2-C. A solution of 76 mg (41 μmol) of compound **2-B** and 14 mg (41 μmol) of triethoxy-(10-isocyanatodecyl)silane **2-8** (prepared following the literature procedure[5]) in 1 ml of toluene was stirred at 50 °C for 24 h. After concentration in vacuo, the crude product as brown oil was purified by column chromatography on silica gel (eluent CH_2Cl_2 – hexanes 1:2) to yield **1** in quantitative yield as a brown oil, R_f 0.50. ^{1}H NMR ($CDCl_3$) δ 8.12 (s, 1H); 7.85-7.75 (m, 2H); 7.50-7.30 (m, 10H); 7.15 (d, J = 2.5 Hz, 2H); 6.75 (d, J =2.4 Hz, 2H); 6.66 (d, J = 8.8 Hz, 2H); 6.57 (dd, J_1 = 8.8, J_2 = 2.4 Hz, 2H); 6.24 (s, 1H); 4.60-4.50 (m, 1H); 3.81 (q, J = 7.0 Hz, 6H); 3.30-3.20 (m, 2H); 2.90-2.70 (m, 16H); 1.82-1.62 (m, 16H); 1.50-1.20 (m, 79H); 1.10 (d, J = 5 Hz, 36H); 0.90-0.80 (m, 24H); 0.70-0.60 (m, 2H). MS (MALDI-TOF) m/e M$^+$ 2177.49 (calcd. for $C_{143}H_{204}N_2O_9Si_3$ 2178.54).

Bis(triisopropylsilyl)-5-aminofluorescein (3-1). Triisopropylsilylchloride (0.27 g, 0.3 ml, 1.44 mmol) was added dropwise to a solution of 100 mg (0.29 mmol) of 5-aminofluorescein and 100 mg (1.47 mmol) of imidazole in 0.5 ml of anhydrous DMF, and the reaction mixture was stirred for 12 h at room temperature. Hexane (30 ml) and ethyl acetate (15 ml) were added to the reaction mixture followed by washing with water (3×15 ml), brine (15 ml), and drying over Na_2SO_4. After concentration in vacuo, the crude white solid was purified by washing with cold hexane and drying under vacuum, yielding 135 mg (71%) of **3-1** as a pale yellow solid, mp. 279-280 °C (decomp.). ^{1}H NMR ($CDCl_3$) δ 7.18 (s, 1H), 6.93 (s, 2H), 6.80-6.60 (m, 4H), 6.55 (d, J = 7.5 Hz, 2H), 1.45-1.10 (m, 6H), 1.06 (d, J = 8.3 Hz, 36H). HRMS (ESI-TOF) m/e M$^+$ 660.3534 (calcd. for $C_{38}H_{54}NO_5Si_2$ 660.3535).

Reference compound 3-2. A solution of 54 mg (82 µmol) of **3-1** and 28 mg (81 µmol) of isocyanate **2-8** in 1 ml of toluene was stirred at 50 °C for 24 h, and then was diluted with 135 ml of toluene to make a ~0.6 mM stock solution of **3-2** required for its immobilization on glass. A small portion of the reaction mixture was concentrated in vacuo for NMR characterization. ^{1}H NMR (CDCl$_3$) δ 8.33 (d, J = 7.0 Hz, 1H), 8.18 (s, 1H), 7.79 (s, 1H), 7.10 (d, J = 7.0 Hz, 1H), 6.80-6.50 (m, 6H), 5.45 (broad s, 1H), 3.81 (q, J = 7.0 Hz, 6H), 3.20-3.00 (m, 2H), 1.50-1.00 (m, 67H); 0.70-0.60 (m, 2H).

1,6-Dimethoxynaphthalene 4-1. Dimethyl sulfate (19 mL, 200 mmol) was added dropwise to a mixture of 10.43g (65.13 mmol) 1,6-dihydroxynaphthalene and 32.53 g (235.37 mmol) potassium carbonate in 80 mL of anhydrous acetone and was heated at reflux for 5 h. The reaction mixture was allowed to cool then poured into water and extracted with hexanes. The combined organic fractions were washed with brine and dried over sodium sulfate and then concentrated *in vacuo*. The crude product was recrystallized from hexanes yielding 8.58 g (70%) of **4-1** brown crystals, mp 53-55 °C(lit.[6] mp 54-57 °C). ^{1}H NMR (acetone-*d6*) δ 8.11 (d, J = 9.2 Hz, 1H), 7.34 (d, J = 4.5 Hz, 2H), 7.22 (s, 1H), 7.10 (dd, J_1 = 9.2, J_2 = 2.3 Hz, 1H), 6.78 (t, J = 4.5 Hz, 1H), 3.97 (s, 3H), 3.89 (s, 3H).

4-Formyl-1,6-dimethoxynaphthalene 4-2. Phosphorus (V) oxychloride (102 g, 0.67 mol) was added dropwise *slowly* to 120 mL of anhydrous DMF at 0°C and allowed to stir at this temperature for 1 h. The reaction vessel was then immersed into an oil bath and the temperature raised to 70°C. A solution of 25.11 g (0.13 mmol) of compound **4-1** in 60 mL of anhydrous DMF was added dropwise and allowed to stir for 2 h and then allowed to cool to room temperature. The reaction mixture was poured onto an ice/2 M NaOH mixture and allowed to stir for 1 h, after which the product was filtered off on a sintered glass funnel to yield 23.40 g (81%) of **4-2** as a

bright yellow solid that required no further purification, mp 75-77 °C(lit.[7] mp 78-79 °C). ^{1}H

NMR (acetone-*d6*) δ 10.14 (s, 1H), 8.82 (s, 1H), 8.19 (d, *J* = 5.7 Hz), 8.00 (d, *J* = 5.0 Hz), 7.20

(d, *J* = 5.7 Hz), 7.00 (d, *J* = 5.0 Hz), 4.10 (s, 3H), 3.94 (s, 3H).

4-Methyl-1,6-dimethoxynaphthalene 4-3. Hydrazine hydrate (11 mL, 0.36 mmol) was

added dropwise to a mixture of 23.40 g (0.11 mmol) of compound **4-2** and 18.28 g (0.36 mmol)

potassium hydroxide in 240 mL diethylene glycol at 150°C and stirred for two hours, and then to

200°C for an additional two hours. The reaction mixture was cooled, poured onto a solution of 2

M HCl and extracted with ether. The combined ethereal extracts were washed with brine and

dried over Na$_2$SO$_4$ and finally concentrated *in vacuo* yielding 20.98 g (96%) of **4-3** as a brown

solid that required no further purification, mp 56-57°C. ^{1}H NMR (acetone-*d6*) δ 8.16 (d, *J* = 5.7

Hz, 1H), 7.25 (s, 1H), 7.20 (d, *J* = 4.8 Hz, 1H), 7.15 (d, *J* = 5.7 Hz), 6.87 (d, *J* = 4.8 Hz), 3.95 (s,

3H), 3.92 (s, 3H), 2.54 (s, 3H).

2,4-Dimethoxybenzoyl chloride. Oxalyl chloride (35.52 g, 24 mL, 0.28 mmol) was added

dropwise to a solution of 10.13 g (55.66 mmol) 2,4-dimethoxybenzoic acid in 100 mL dry

dichloromethane with a drop of DMF. The reaction mixture was allowed to stir for 6 h at room

temperature. The reaction mixture was then concentrated *in vacuo* and the resulting faint yellow

solid was used without further purification.

Compound 4-4. A solution of 10.50 g (52.35 mmol) 2,4-dimethoxybenzoyl chloride in 40

mL anhydrous CH$_2$Cl$_2$ was added dropwise to a mixture of 9.51 g (47.01 mmol) of compound **4-3** and 7.32 g (54.87 mmol) of aluminum chloride in 100 mL anhydrous CH$_2$Cl$_2$ at 0°C and

allowed to stir for 5 h. After the reaction was complete, the reaction mixture was poured into 3

mL of concentrated HCl in 40 mL of water, then diluted with dichloromethane and washed with

2 M NaOH solution. The combined organic fractions were combined, washed with brine and

dried over magnesium sulfate and concentrated yielding a brown oil. The resulting oil

recrystallized from EtOH yielding 6.67 g (38%) of **4-4** as tan crystals, mp 133-135 ºC(lit.[8] mp

135-136 ºC). ^{1}H NMR (acetone-*d6*) δ 8.12 (d, *J* = 9.2 Hz, 1H), 7.54 (d, *J* = 8.9 Hz, 1H), 7.31

(broad s, 2H), 7.20 (dd, *J$_1$* = 9.1, *J$_2$* = 2.4 Hz, 1H), 6.5-6.7 (m, 2H), 3.97 (s, 3H), 3.88 (s, 3H),

3.68 (s, 3H), 3.58 (s, 3H), 2.58 (s, 3H).

Compound 4-5. Boron tribromide (31 mL, 0.33 mol) was added neat dropwise to a solution

of 6.02 g (16.43 mmol) of compound **4-4** in 800 mL anhydrous CH_2Cl_2 at -78ºC. The reaction

mixture was allowed to rise to room temperature while stirring overnight, then was quenched

with plenty of water. The reaction mixture was extracted with ethyl acetate and the combined

organic extracts were washed with plenty of water, brine, dried over sodium sulfate and

concentrated *in vacuo* resulting in a quantitative yield of **4-5** as a fluffy yellow-orange solid, mp

>300ºC (decomp.). ^{1}H NMR (acetone-*d6*) δ 8.34 (d, *J* = 5.6 Hz, 1H), 7.57 (d, *J* = 5.4 Hz, 1H),

7.39 (s, 1H), 7.20-7.27 (m, 2H), 6.40-6.57 (m, 2H), 2.46 (s, 3H).

Semi-naphtho[c]xanthone 4-6. Compound **4-5** (223 mg, 0.75 mmol) and zinc acetate (25

mg) were placed into a thick-walled pressure flask and flushed with argon. Degassed water (24

mL) was added to the flask then sealed with a PTFE screw cap and the vessel was heated to 200-

230ºC for 5 h. The flask was allowed to cool to room temperature and the crude precipitate

filtered, and recrystallized from EtOH, yielding 108 mg (49%) of **4-6** as pale yellow crystals, mp

>300ºC (decomp.). ^{1}H NMR (DMSO-*d6*) δ 10.86 (broad s, 1H), 10.42 (broad s, 1H), 8.52 (d, *J* =

8.7 Hz, 1H), 8.03 (d, *J* = 8.2 Hz, 1H), 7.82 (s, 1H), 7.29 (broad s, 2H), 7.05 (s, 1H), 6.91 (d, *J* =

8.2 Hz, 1H), 2.55 (s, 3H).

Alternate Procedure for Preparation of 4-6. Compound **4-5** (1.82 g, 5.86 mmol) was

dissolved in 15 mL DMF and 15 mL water in a sealed tube that was purged with argon for 30

minutes. In a sand bath, the reaction mixture was heated to 175ºC overnight. When the reaction was complete, it was allowed to cool to room temperature and was poured into water. The crude product was filtered and 1.00 g (59%) of **4-6** was obtained as pale yellow crystals. ^{1}H NMR corresponded to prior results for compound **4-6** obtained in the previous method.

Compound 4-7. *Tert*-butyldimethylsilyl chloride (801 mg, 5.31 mmol) was added as a solid to a mixture of 618 mg (2.11 mmol) of compound **4-6** and 906 mg (13.31 mmol) of imidazole in 5 mL dry DMF and was allowed to stir overnight at room temperature. When the reaction was complete, the reaction mixture was poured into water and extracted with dichloromethane. The organic fraction was washed with brine and dried over $MgSO_4$. Concentration *in vacuo* resulted in a crude oil that was further purified by column chromatography on silica gel (eluent - hexanes:ethyl acetate, 5:1, R_f = 0.4) to yield 672 mg (61%) of compound **4-7** as a tan solid, mp 145-156ºC (decomp.). ^{1}H NMR ($CDCl_3$) δ 8.66 (d, J = 7.5 Hz, 1H), 8.11 (d, J = 7.5 Hz, 1H), 7.87 (s, 1H), 7.40-7.20 (m, 3H), 7.01 (d, J = 7.5 Hz, 1H), 2.47 (s, 3H), 0.98 (s, 18H), 0.30 (s, 12H).

Seminapthofluorescein methyl ester 4-8. 4-iodomethylbenzoate (544 mg, 2.07 mmol) was dissolved in 20 mL dry THF, to which 1.25 mL of 1.5M isopropyl magnesium chloride in hexanes was added dropwise. The reaction mixture was allowed to stir for 15 minutes at -20ºC, then a solution of 720 mg (1.38 mmol) TBDMS-protected xanthone **4-7** in 5 mL THF was added dropwise and the reaction mixture was warmed to room temperature and stirred overnight. When the reaction was complete, 1 mL of trifluoroacetic acid was added slowly and the reaction mixture was stirred for 30 minutes. The reaction mixture was then poured into ethyl acetate, washed with water, brine, and finally dried over Na_2SO_4. Concentration *in vacuo* gave the crude product which was further purified by column chromatography (eluent $CHCl_3$:MeOH 90:10 →

CHCl$_3$:MeOH:AcOH 80:19:1) to yield 127 mg (24%) of the compound **4-8** as a red solid, mp 137-138 ºC (decomp.). ^{1}H NMR (DMSO-*d6*) δ 8.49 (d, *J* = 9 Hz, 1H), 8.20 (d, *J* = 7.5 Hz, 2H), 7.64 (d, *J* = 7.5 Hz, 2H), 7.25 (d, *J* = 9 Hz, 1H), 7.16 (s, 1H), 6.97 (d, *J* = 10 Hz, 1H), 6.76 (s, 1H), 6.50-6.40 (m, 2H), 3.92 (s, 3H), 2.36 (s, 3H).

Seminapthofluorescein carboxylic acid 4-9. A 1M solution of lithium hydroxide (5 mL, 5 mmol) was added dropwise to 100 mg (0.26 mmol) seminapthofluorescein methyl ester **4-8** in 15 mL of methanol and 10 mL of water. The reaction was allowed to stir for 1 h at room temperature. When the reaction was complete, the methanol was removed *in vacuo* and the solution was acidified slowly with 2M HCl. The resulting precipitate was filtered and further purified by repeated reprecipitation with 2M HCl, yielding 35 mg (36%) of the title compound as a pink solid, mp 156-157ºC (decomp.). ^{1}H NMR (DMSO-*d6*) δ 9.01 (d, *J* = 9 Hz, 1H), 8.28 (d, *J* = 8 Hz, 2H), 7.83 (s, 1H), 7.73 (d, *J* = 8 Hz, 2H), 7.68 (d, *J* = 9 Hz, 1H), 7.53 (d, *J* = 9 Hz, 1H), 7.50 (s, 1H), 7.42 (d, *J* = 9 Hz, 1H), 7.21 (s, 1H), 2.51 (s, 3H). HRMS (ESI-TOF) *m*/e [M+H]$^+$ 397.1060 calcd. for C$_{25}$H$_{17}$O$_5$ 397.1071.

5.8 References

(1)   Jiao, G.-S.; Han, J. W.; Burgess, K. B. Syntheses of Regioisomerically Pure 5- or 6-Halogenated Fluoresceins. *J. Org. Chem.* **2003**, *68*, 8264-8267.

(2)   Takahashi, S.; Kuryoyama, Y.; Sonogashira, K.; Haginara, N. A Convenient Synthesis of Ethynylarenes and Diethynylarenes. *Synthesis* **1980**, 627-630.

(3)   Acharya, J. R.; Zhang, H.; Xian, Li.; Nesterov, E. E. Chemically Controlled Amplified Ratiometric Fluorescence in Surface-Immobilized End-Capped Oligo(*p*-phenylene ethynylene)s. *J. Am. Chem. Soc.* **2009**, *131*, 880-881.

(4)   A. M. Kushner, V. Gabuchian, E. G. Johnson, Z. Guan. Biomimetic Design of Reversibly Unfolding Cross-Linker to Enhance Mechanical Properties of 3D Network Polymers. *J. Am. Chem. Soc.* **2007**, *129*, 14110-14111.

(5)   P. Joly, N. Ardès-Guisot, S. Kar, M. Granier, J.-O. Durand, O. Melnyk. *Eur. J. Org. Chem.* **2005**, 2473-2480.

(6)   Soriano, A.; Casado, V.; Corte, A.; Lluis, C.; Franco, R.; Venture, R.; Molero, A.; Royo, M.; Fanelli, F.; Albericio, F. Adenosine A_{2A} Receptor-Antagonist/Dopamine D_2 Receptor-Agonist Bivalent Ligands as Pharmacological Tools to Detect A_{2A}-D_2 Receptor Heteromers. *J. Med. Chem.* **2009**, *52,* 5590-5602.

(7)   Basu, B.; Mukherjee, D. Reductive Methylation of Naphthoic Esters *Chem. Commun.* **1984**, *2*, 105-106.

(8)   Kim, S. H.; Gunther, J. R.; Katzenellenbogen, J. A. Nonclassical SNAPFL Analogue as a Cy5 Resnance Energy Transfer Partner. *Org. Lett.* **2008**, *10*, 4931-4934.

APPENDIX A: PERMISSIONS

JOHN WILEY AND SONS LICENSE
TERMS AND CONDITIONS

Apr 18, 2013

This is a License Agreement between Brian G Imsick ("You") and John Wiley and Sons ("John Wiley and Sons") provided by Copyright Clearance Center ("CCC"). The license consists of your order details, the terms and conditions provided by John Wiley and Sons, and the payment terms and conditions.

All payments must be made in full to CCC. For payment instructions, please see information listed at the bottom of this form.

License Number	3132050484899
License date	Apr 18, 2013
Licensed content publisher	John Wiley and Sons
Licensed content publication	Angewandte Chemie International Edition
Licensed content title	A Fluorescent Self-Amplifying Wavelength-Responsive Sensory Polymer for Fluoride Ions
Licensed copyright line	Copyright © 2003 WILEY-VCH Verlag GmbH & Co. KGaA, Weinheim
Licensed content author	Tae-Hyun Kim,Timothy M. Swager
Licensed content date	Sep 23, 2003
Start page	4803
End page	4806
Type of use	Dissertation/Thesis
Requestor type	University/Academic
Format	Print and electronic
Portion	Figure/table
Number of figures/tables	1
Original Wiley figure/table number(s)	Figure 2
Will you be translating?	No
Total	0.00 USD
Terms and Conditions	

TERMS AND CONDITIONS

This copyrighted material is owned by or exclusively licensed to John Wiley & Sons, Inc. or one of its group companies (each a "Wiley Company") or a society for whom a Wiley

Copyright Clearance Center

RightsLink®

Home   Account Info   Help

ACS Publications
High quality. High impact.

Title: Chemosensory Performance of Molecularly Imprinted Fluorescent Conjugated Polymer Materials

Author: Jiahui Li,Claire E. Kendig, and, and Evgueni E. Nesterov*

Publication: Journal of the American Chemical Society

Publisher: American Chemical Society

Date: Dec 1, 2007

Copyright © 2007, American Chemical Society

Logged in as:
Brian Imsick
Account #:
3000645288

LOGOUT

BACK   CLOSE WINDOW

Copyright Clearance Center RightsLink®

Home   Account Info   Help

ACS Publications
High quality. High impact.

Title: Chemically Controlled Amplified Ratiometric Fluorescence in Surface-Immobilized End-Capped Oligo(p-phenylene ethynylene)s

Author: Jiba Raj Acharya, Huating Zhang, Xian Li, and Evgueni E. Nesterov

Publication: Journal of the American Chemical Society

Publisher: American Chemical Society

Date: Jan 1, 2009

Copyright © 2009, American Chemical Society

Logged in as:
Brian Imsick
Account #:
3000645288

LOGOUT

PERMISSION/LICENSE IS GRANTED FOR YOUR ORDER AT NO CHARGE

This type of permission/license, instead of the standard Terms & Conditions, is sent to you because no fee is being charged for your order. Please note the following:

- Permission is granted for your request in both print and electronic formats, and translations.
- If figures and/or tables were requested, they may be adapted or used in part.
- Please print this page for your records and send a copy of it to your publisher/graduate school.
- Appropriate credit for the requested material should be given as follows: "Reprinted (adapted) with permission from (COMPLETE REFERENCE CITATION). Copyright (YEAR) American Chemical Society." Insert appropriate information in place of the capitalized words.
- One-time permission is granted only for the use specified in your request. No additional uses are granted (such as derivative works or other editions). For any other uses, please submit a new request.

If credit is given to another source for the material you requested, permission must be obtained from that source.

BACK   CLOSE WINDOW

Title: Signal Ratio Amplification via Modulation of Resonance Energy Transfer: Proof of Principle in an Emission Ratiometric Hg(II) Sensor

Author: Ali Coskun and and Engin U. Akkaya*

Publication: Journal of the American Chemical Society

Publisher: American Chemical Society

Date: Nov 1, 2006

Copyright © 2006, American Chemical Society

PERMISSION/LICENSE IS GRANTED FOR YOUR ORDER AT NO CHARGE

This type of permission/license, instead of the standard Terms & Conditions, is sent to you because no fee is being charged for your order. Please note the following:

- Permission is granted for your request in both print and electronic formats, and translations.
- If figures and/or tables were requested, they may be adapted or used in part.
- Please print this page for your records and send a copy of it to your publisher/graduate school.
- Appropriate credit for the requested material should be given as follows: "Reprinted (adapted) with permission from (COMPLETE REFERENCE CITATION). Copyright (YEAR) American Chemical Society." Insert appropriate information in place of the capitalized words.
- One-time permission is granted only for the use specified in your request. No additional uses are granted (such as derivative works or other editions). For any other uses, please submit a new request.

If credit is given to another source for the material you requested, permission must be obtained from that source.

BACK   CLOSE WINDOW

JOHN WILEY AND SONS LICENSE
TERMS AND CONDITIONS

Apr 11, 2013

This is a License Agreement between Brian G Imsick ("You") and John Wiley and Sons
("John Wiley and Sons") provided by Copyright Clearance Center ("CCC"). The license
consists of your order details, the terms and conditions provided by John Wiley and Sons,
and the payment terms and conditions.

**All payments must be made in full to CCC. For payment instructions, please see
information listed at the bottom of this form.**

License Number	3126140820094
License date	Apr 11, 2013
Licensed content publisher	John Wiley and Sons
Licensed content publication	Advanced Materials
Licensed content title	Surface-Immobilized Monolayers of Conjugated Oligomers as a Platform for Fluorescent Sensors Design: The Effect of Exciton Delocalization on Chemosensing Performance
Licensed copyright line	Copyright © 2013 WILEY-VCH Verlag GmbH & Co. KGaA, Weinheim
Licensed content author	Brian G. Imsick,Jiba Raj Acharya,Evgueni E. Nesterov
Licensed content date	Oct 16, 2012
Start page	120
End page	124
Type of use	Dissertation/Thesis
Requestor type	Author of this Wiley article
Format	Print
Portion	Full article
Will you be translating?	No
Total	0.00 USD
Terms and Conditions	

TERMS AND CONDITIONS

This copyrighted material is owned by or exclusively licensed to John Wiley & Sons, Inc. or
one of its group companies (each a "Wiley Company") or a society for whom a Wiley
Company has exclusive publishing rights in relation to a particular journal (collectively
�WILEY�). By clicking "accept" in connection with completing this licensing transaction,

Print This Page

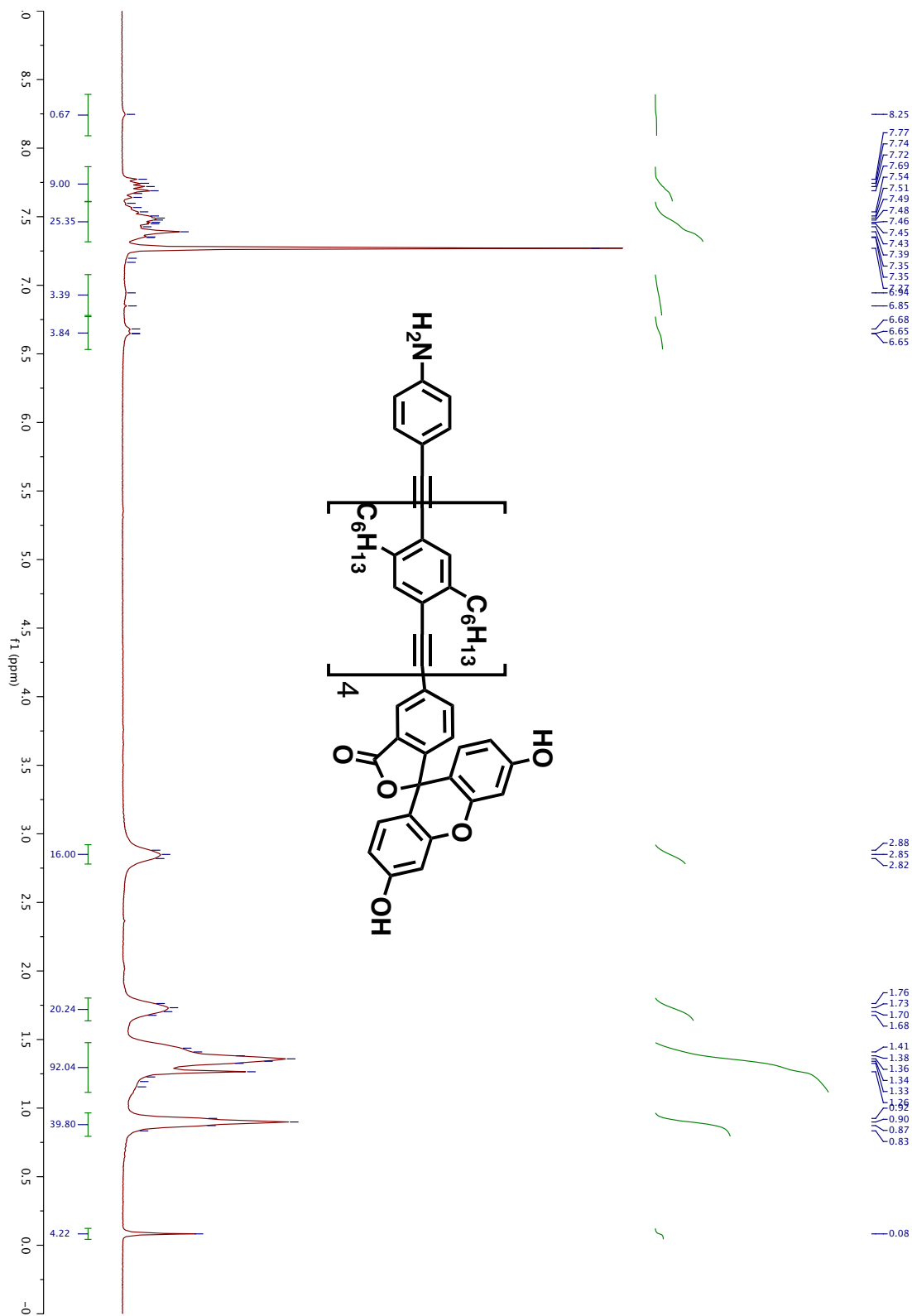# APPENDIX B: NUCLEAR MAGNETIC RESONANCE DATA
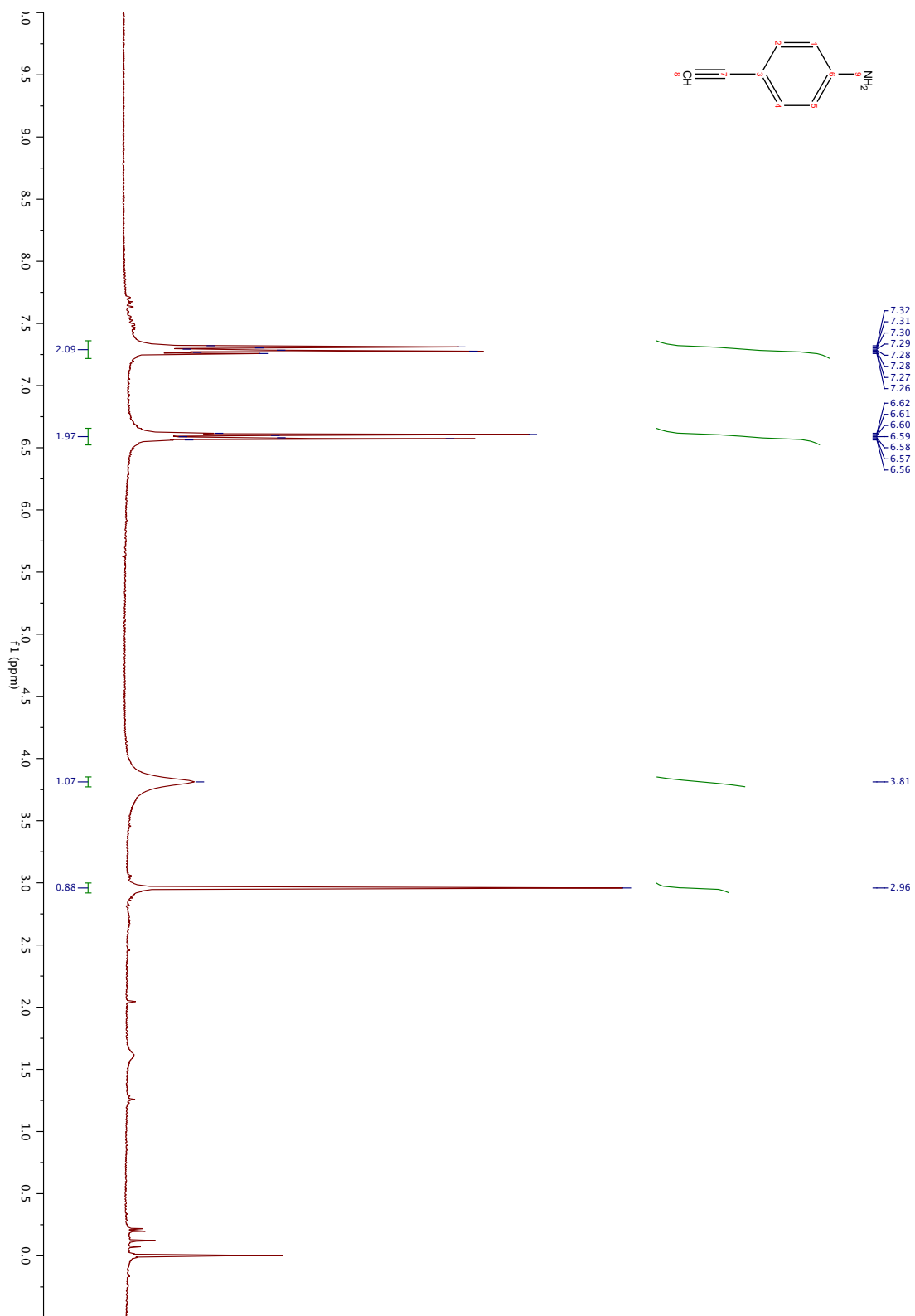
Compound **2-3** (250 MHz, CDCl$_3$)
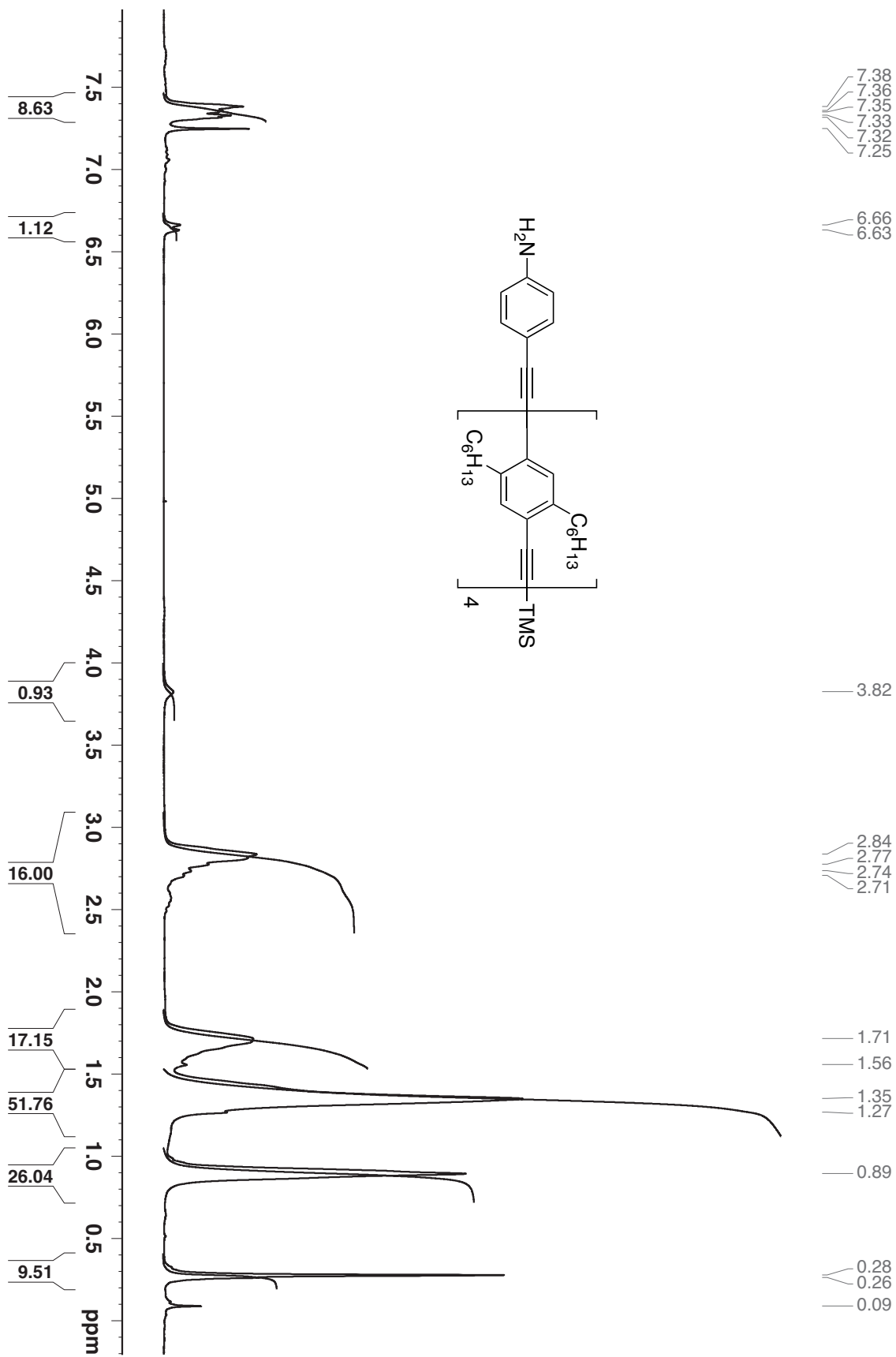
Compound **2-5a** (250 MHz, CDCl$_3$)

91
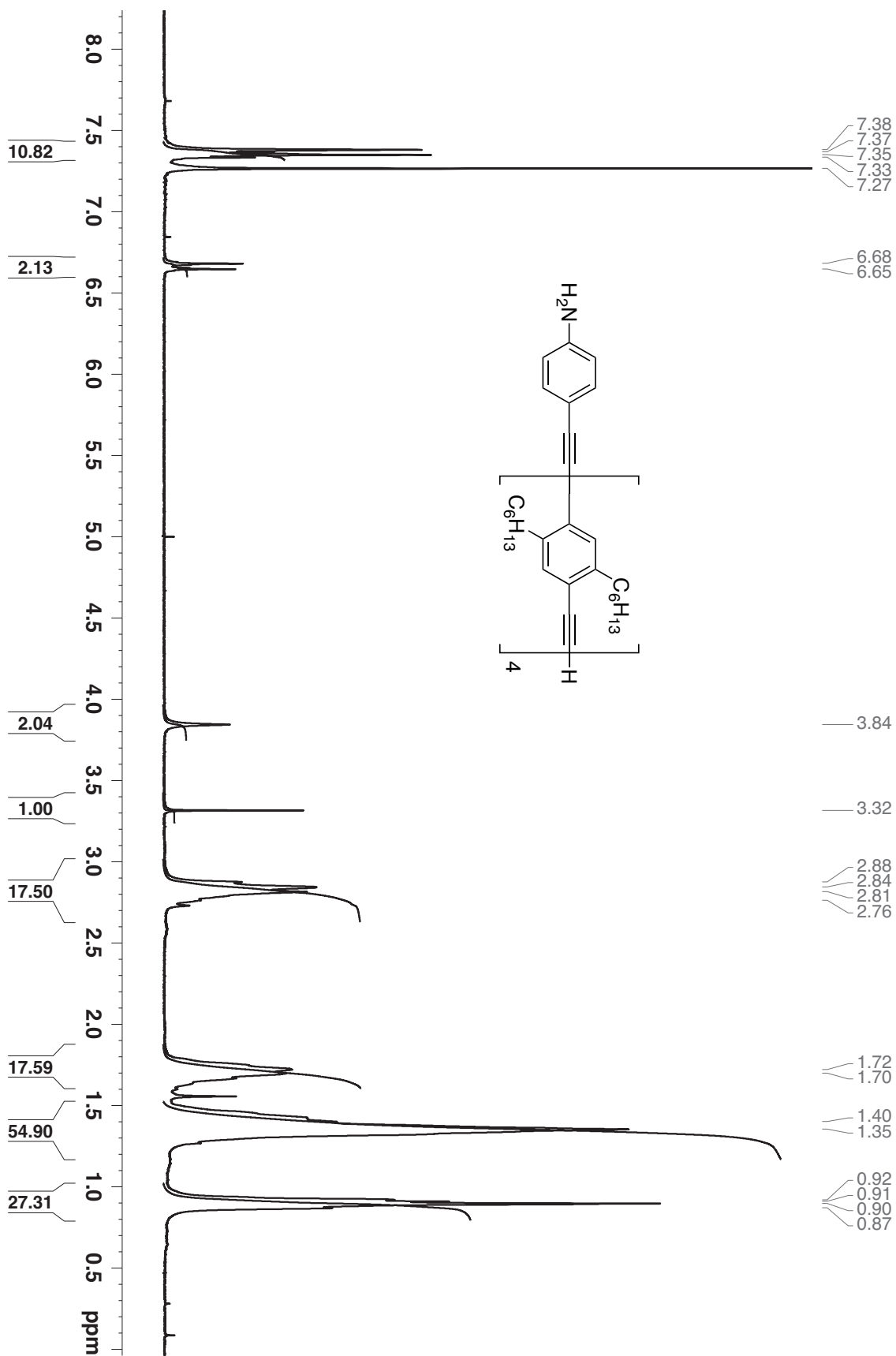
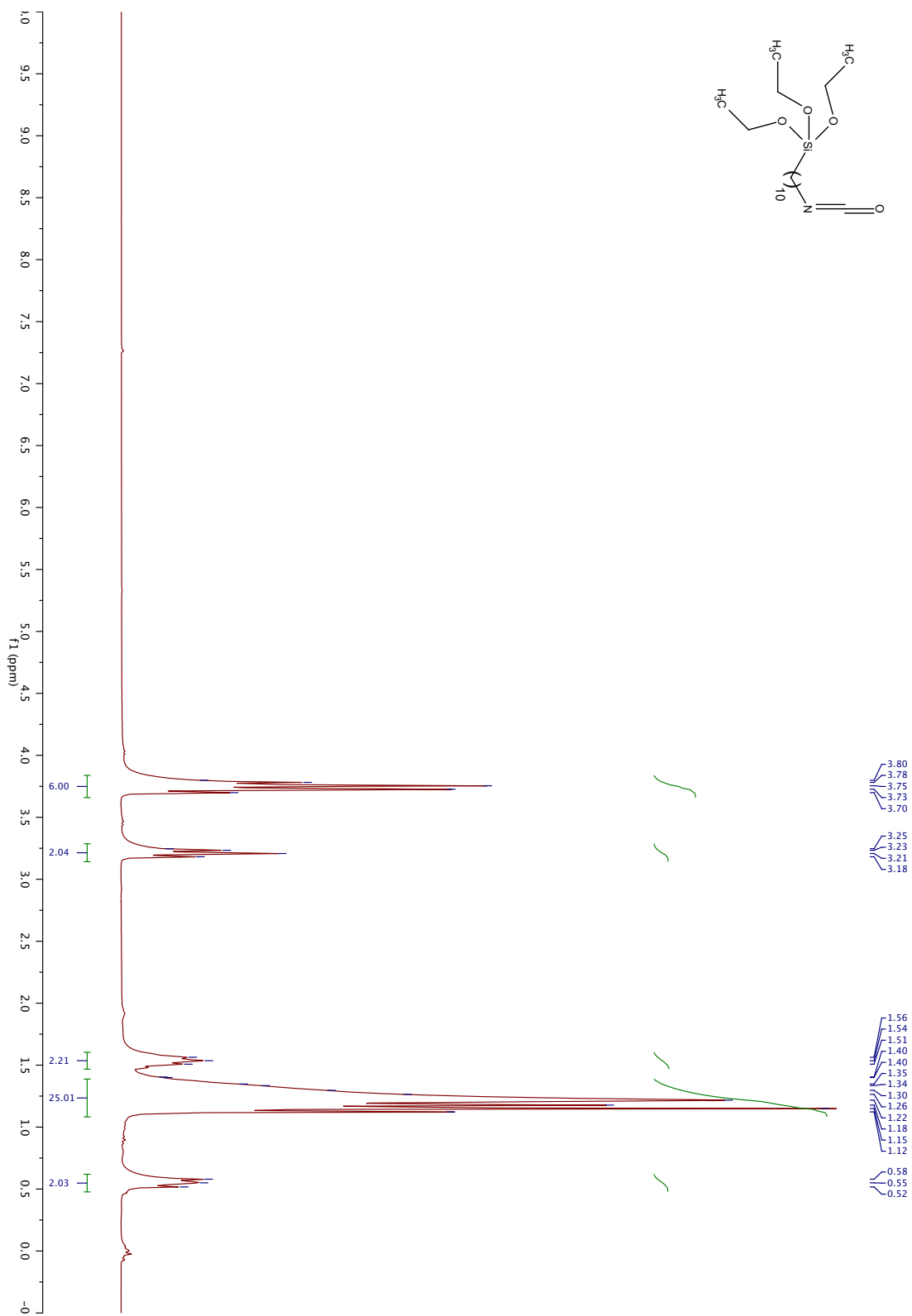Compound **2-5b** (250 MHz, CDCl$_3$)

Compound **2-6** (250 MHz, CDCl$_3$)
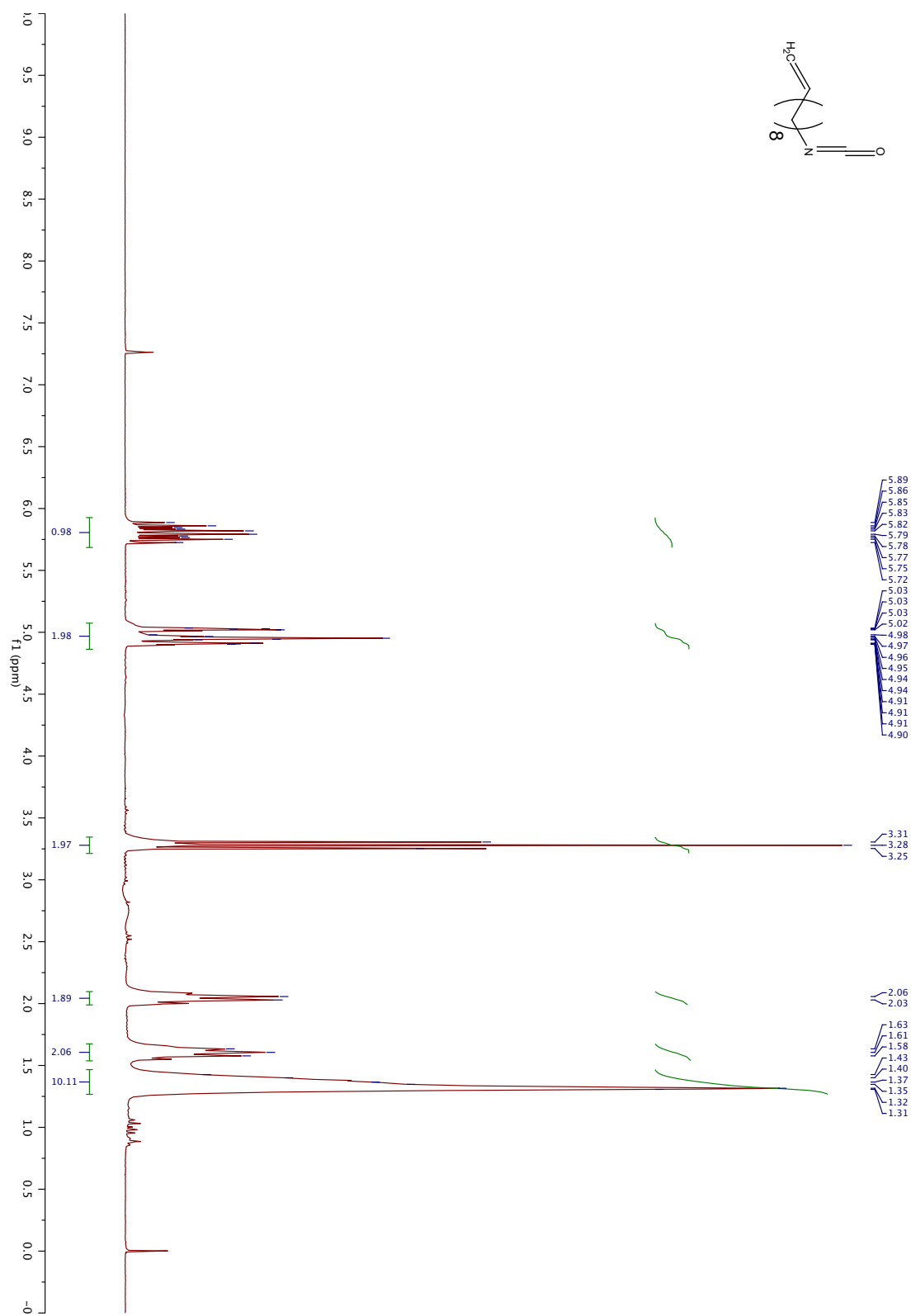
Compound **2-7** (250 MHz, CDCl₃)

94

Compound **2-8** (250 MHz, CDCl$_3$)
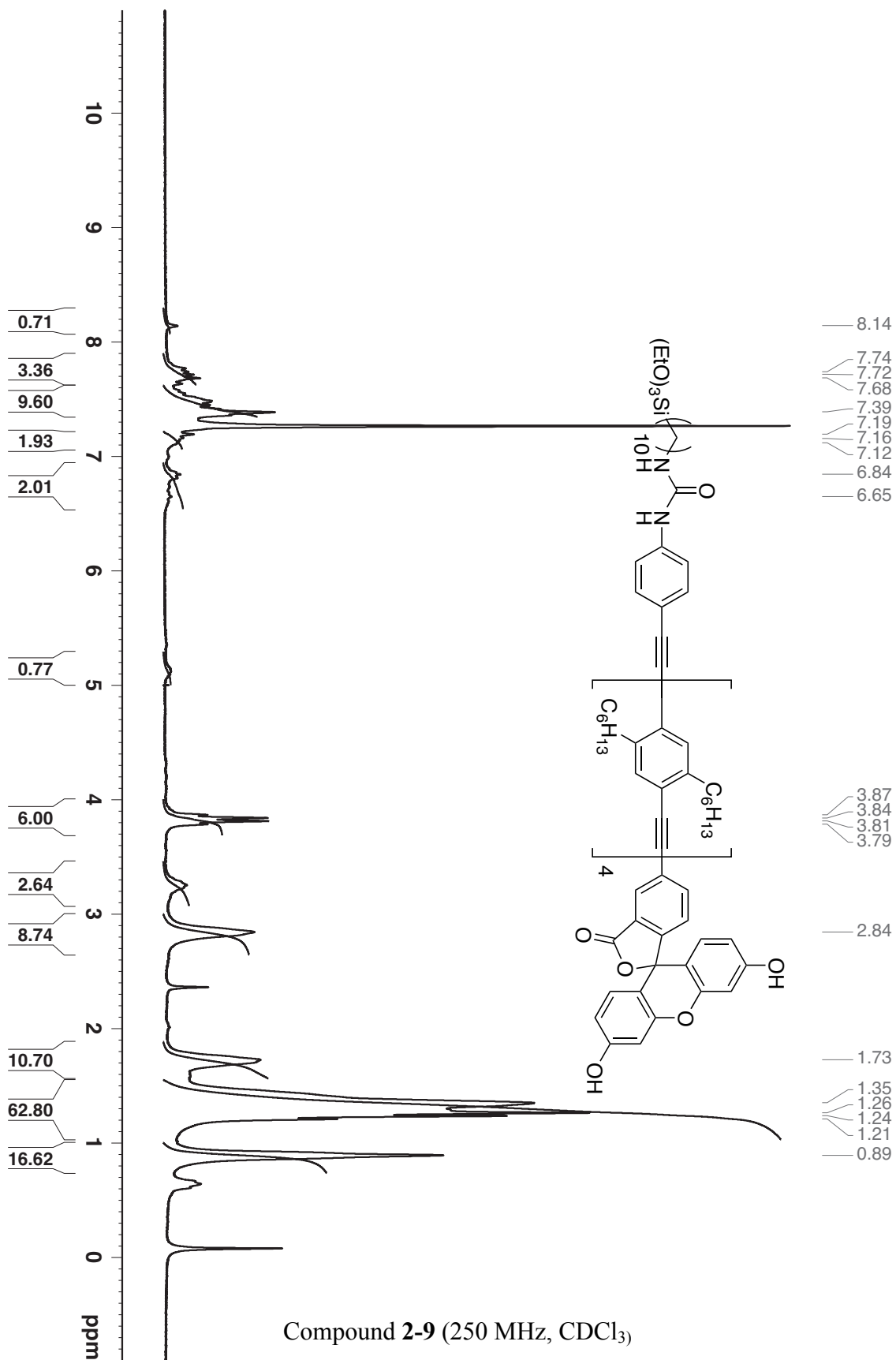
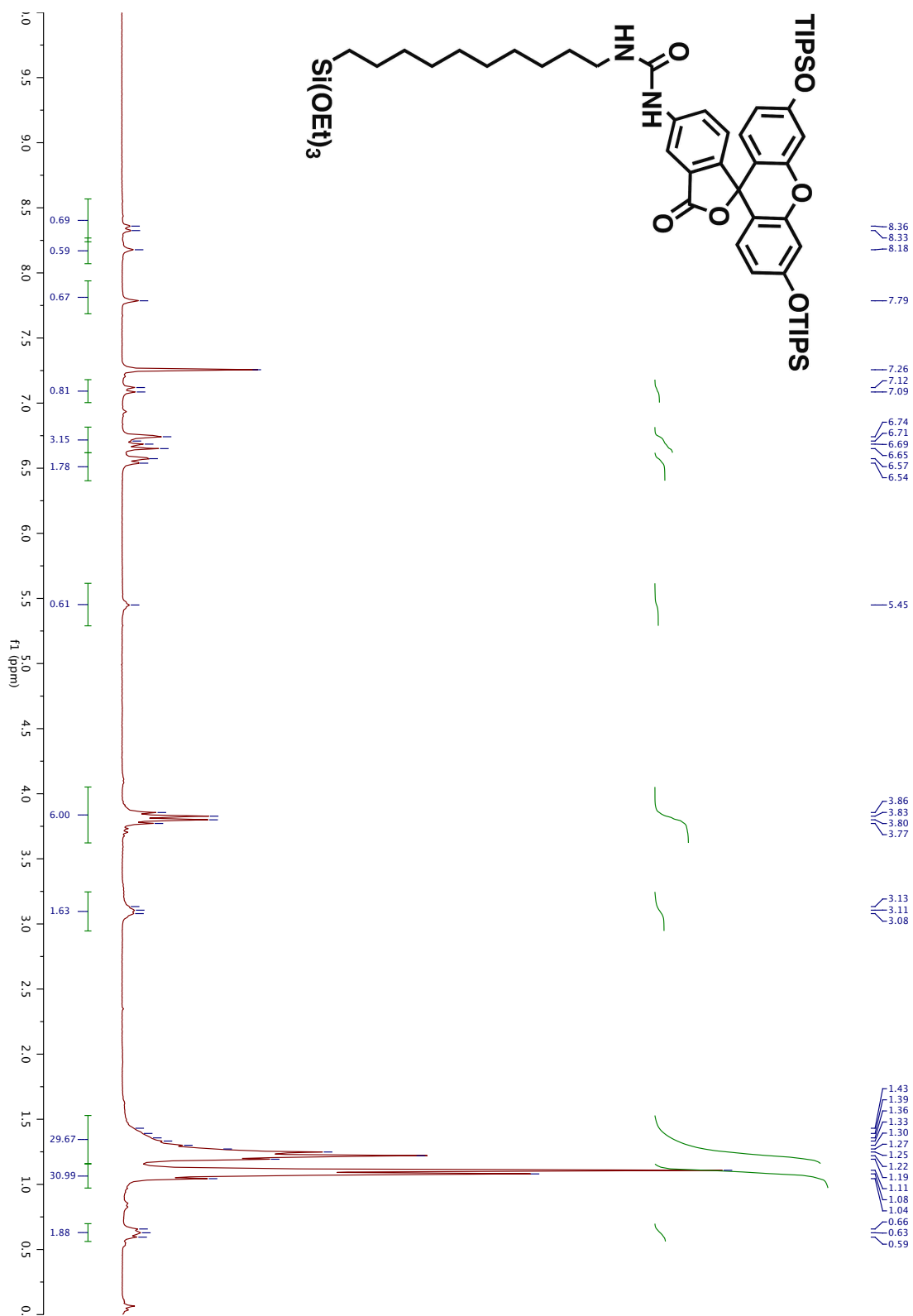Compound **2-9** (250 MHz, CDCl$_3$)
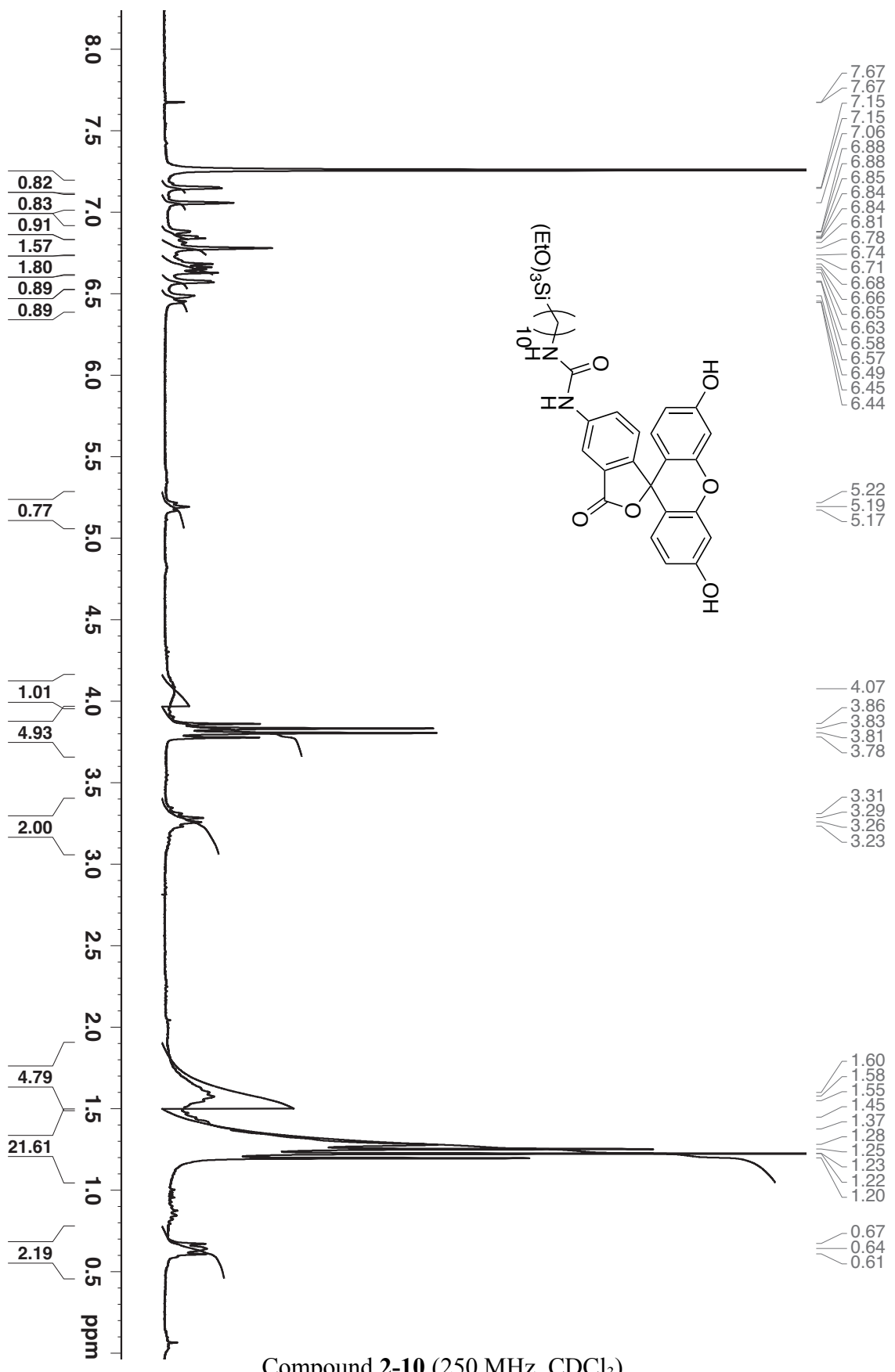
Compound **2-10** (250 MHz, CDCl₃)

7.5 1.16 / 8.92

7.0

6.5 1.17

6.0

5.5

5.0 0.51

4.5

4.0 8.15

3.5 2.76

3.0 14.47

2.5

2.0

1.5 17.52

1.0 78.09 / 24.00

0.5 2.85

ppm

7.37
7.36
7.34

3.84
3.84
3.82
3.81

3.31

2.84
2.82
2.82
2.81

1.71
1.70
1.62

1.21

(EtO)$_3$Si

10 H

N

O

N
H

C$_6$H$_{13}$

C$_6$H$_{13}$

4

H
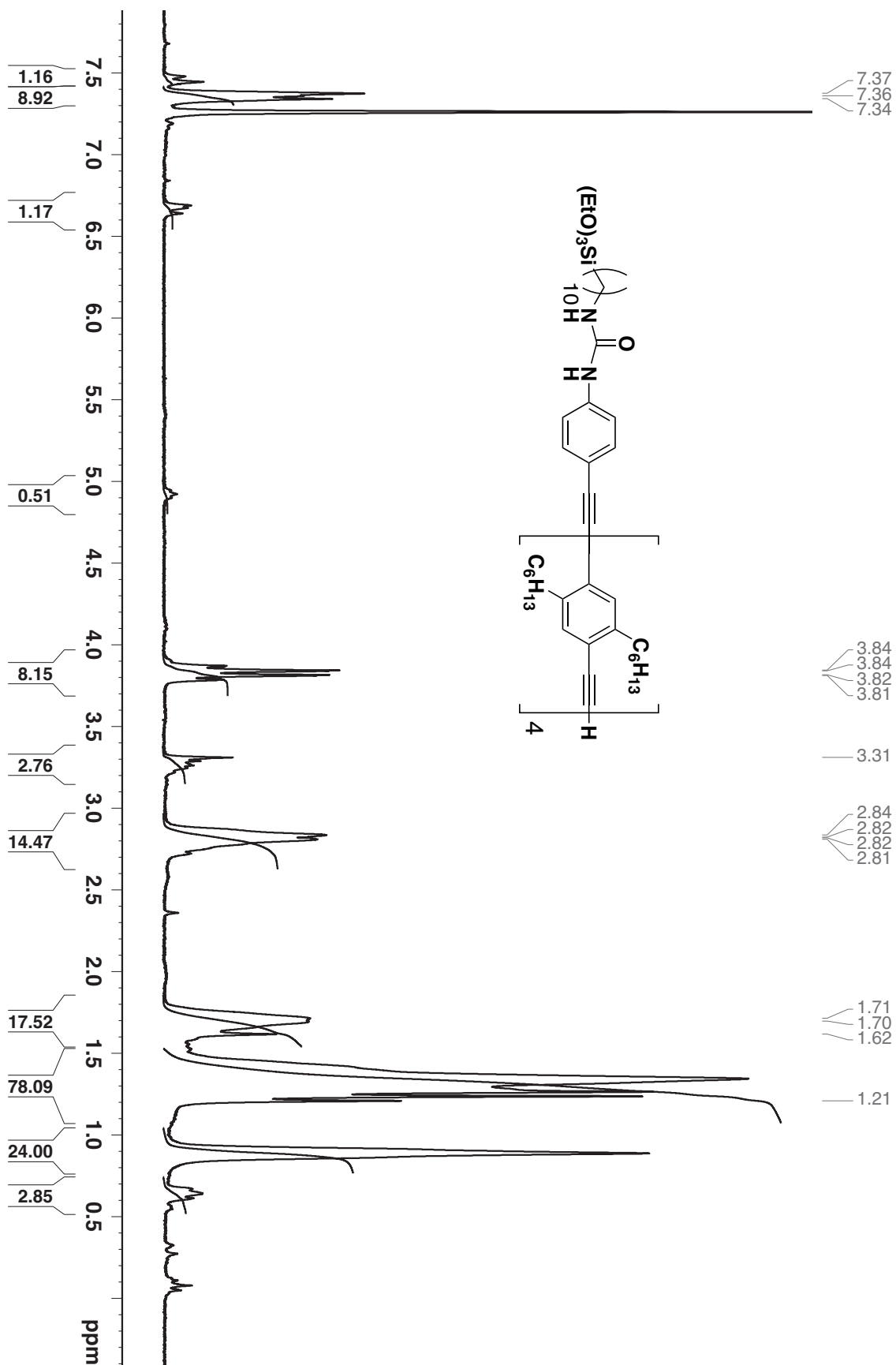
Compound **2-11** (250 MHz, CDCl$_3$)

98
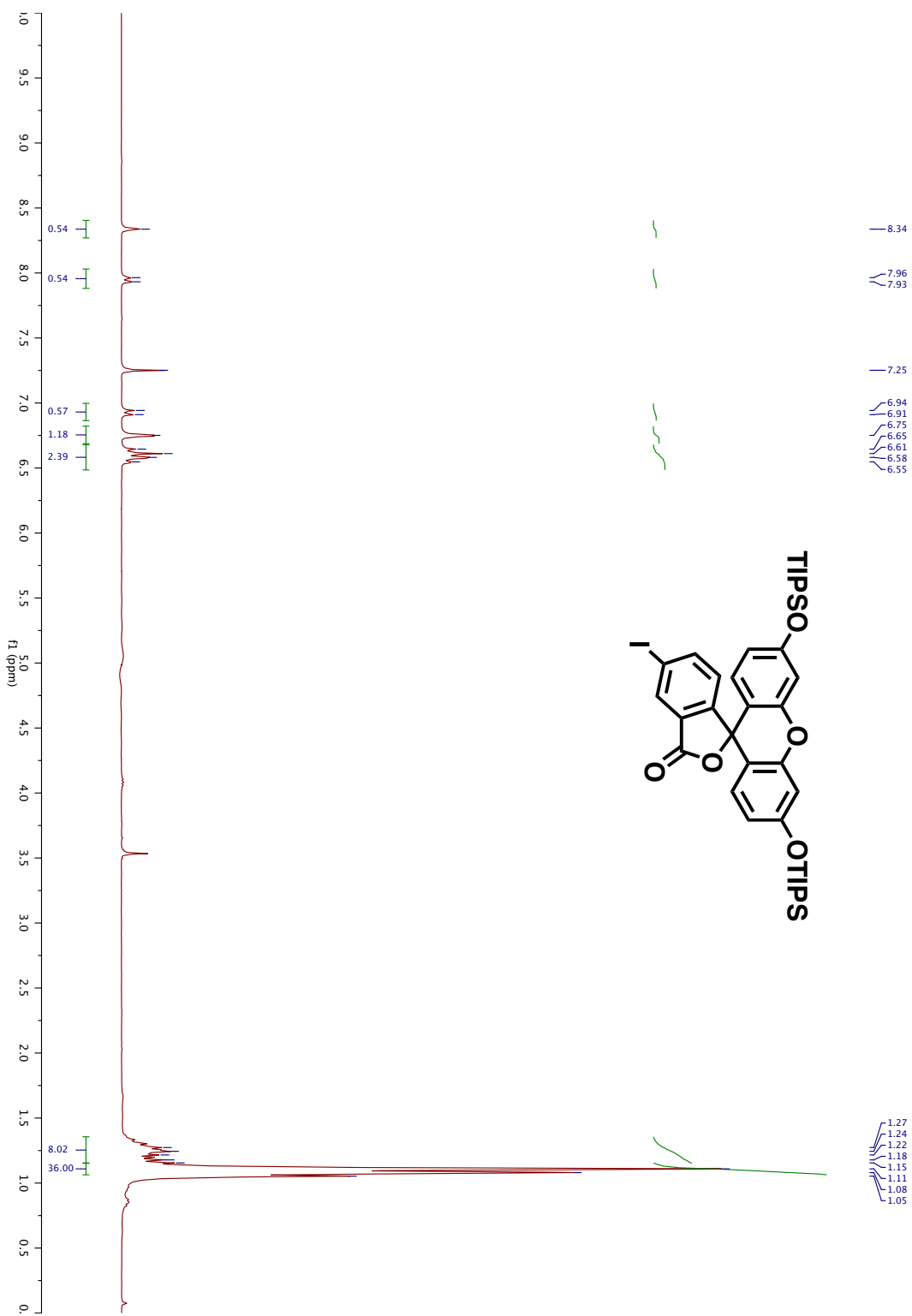
Compound **2-A** (250 MHz, CDCl₃)
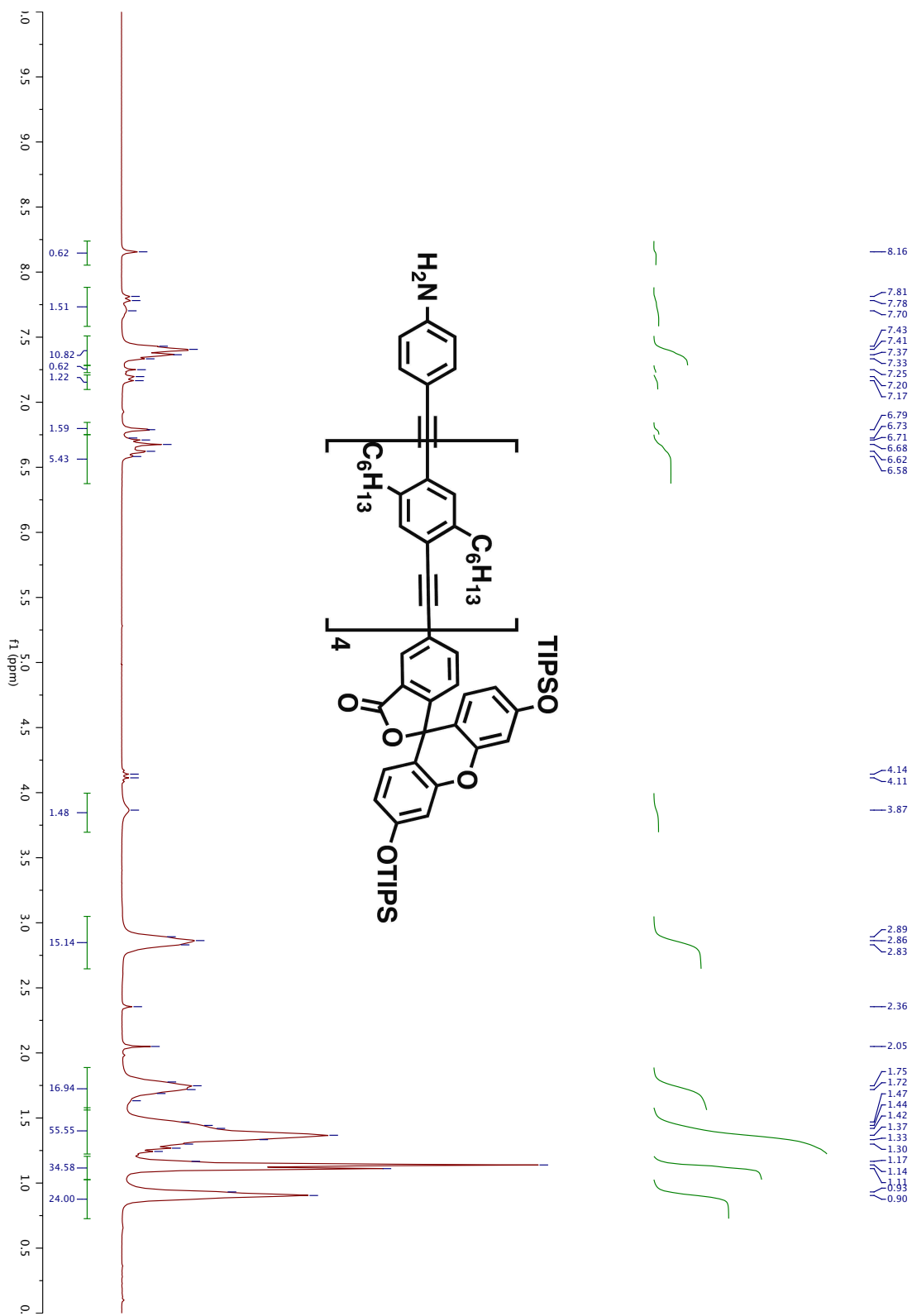
Compound **2-B** (250 MHz, CDCl₃)

Compound **2-C** (250 MHz, CDCl$_3$)
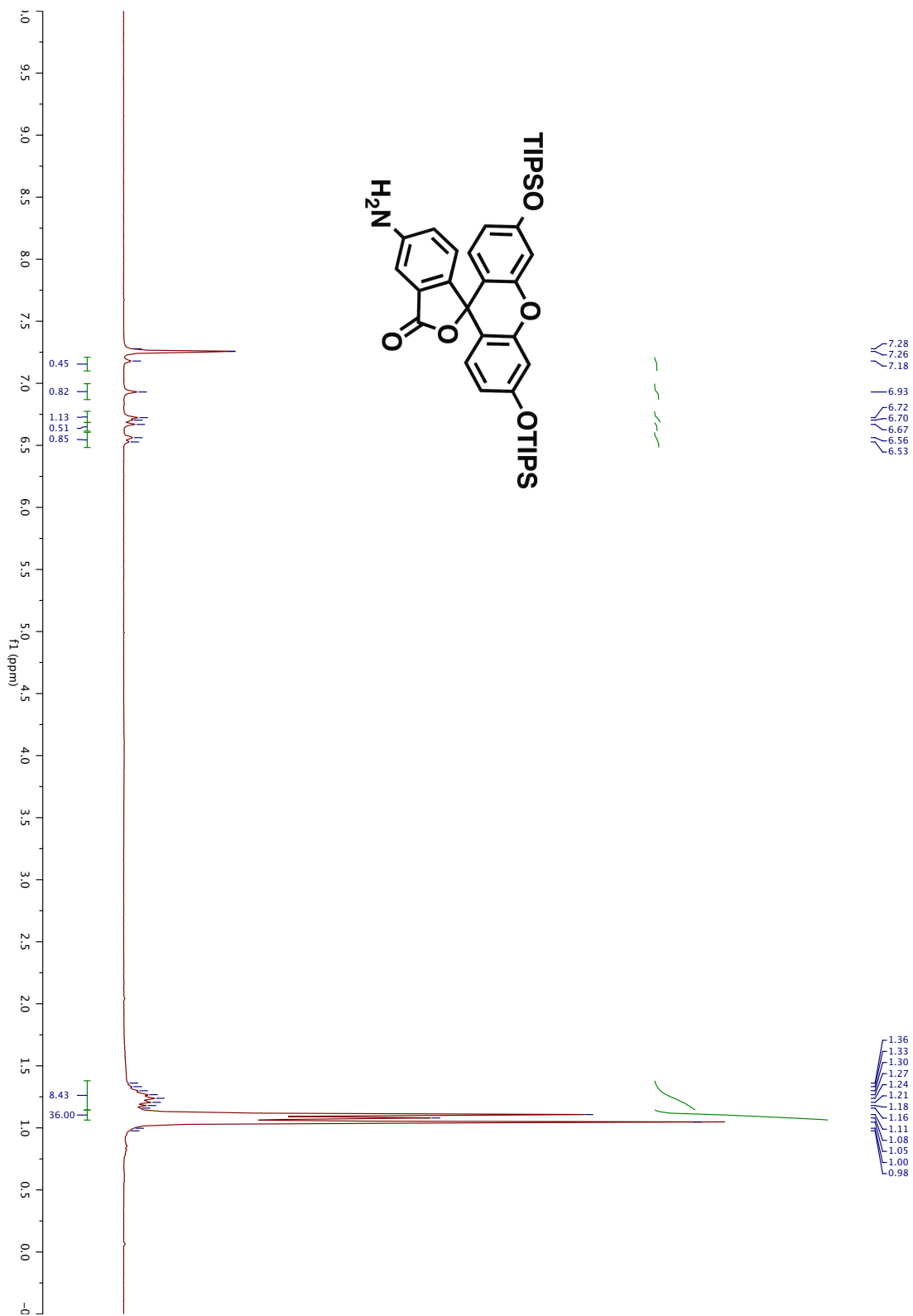
Compound **3-1** (250 MHz, CDCl₃)

Compound **3-2** (250 MHz, CDCl$_3$)

053 – 1,6-dimethoxynaphthalene/2
1H – acetone – 3/9/10

8.13
8.09

7.36
7.34
7.24
7.23
7.13
7.12
7.09
7.08
6.80
6.78
6.76

4.00
3.98
3.90

0.69
1.44
0.78
0.74
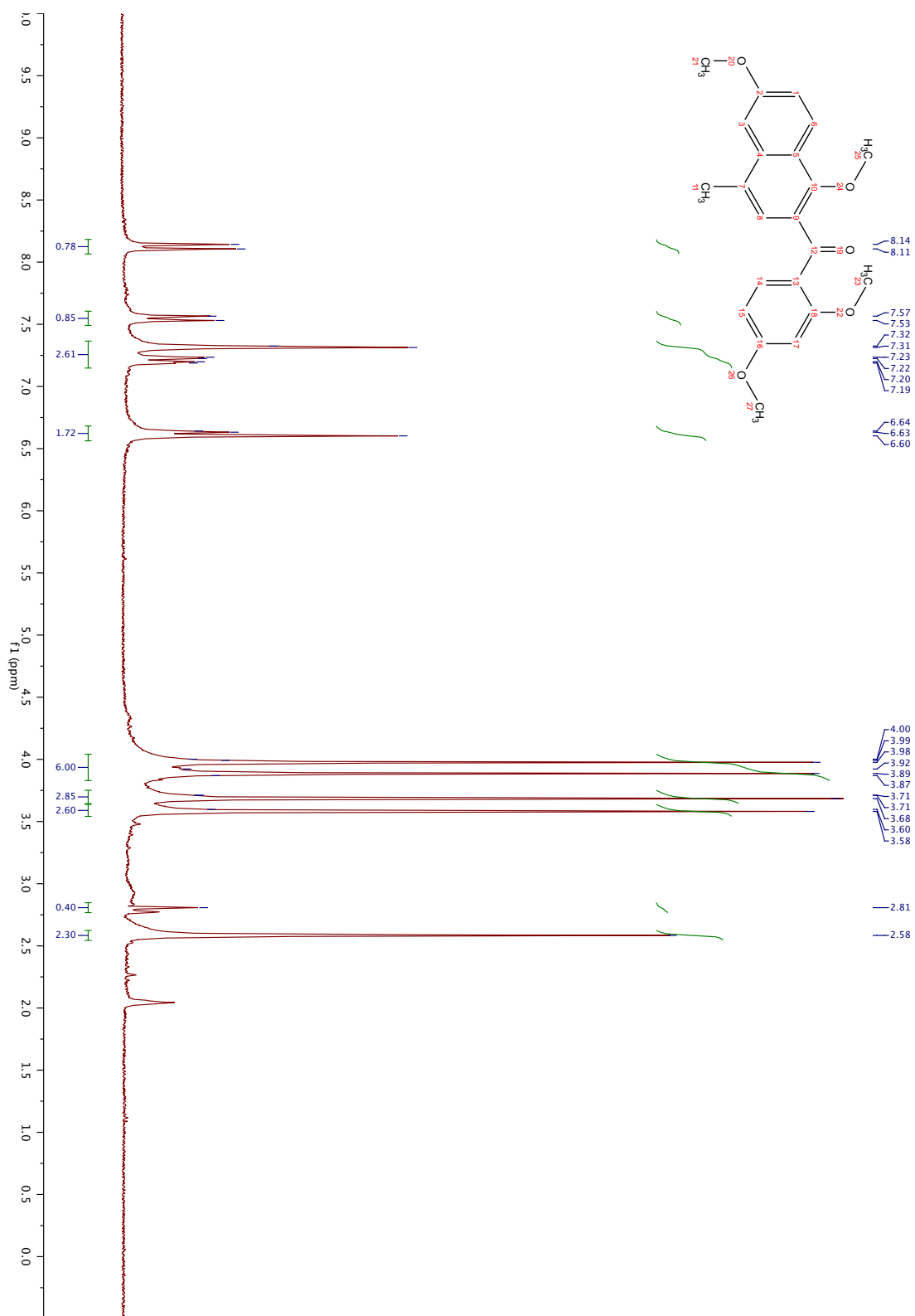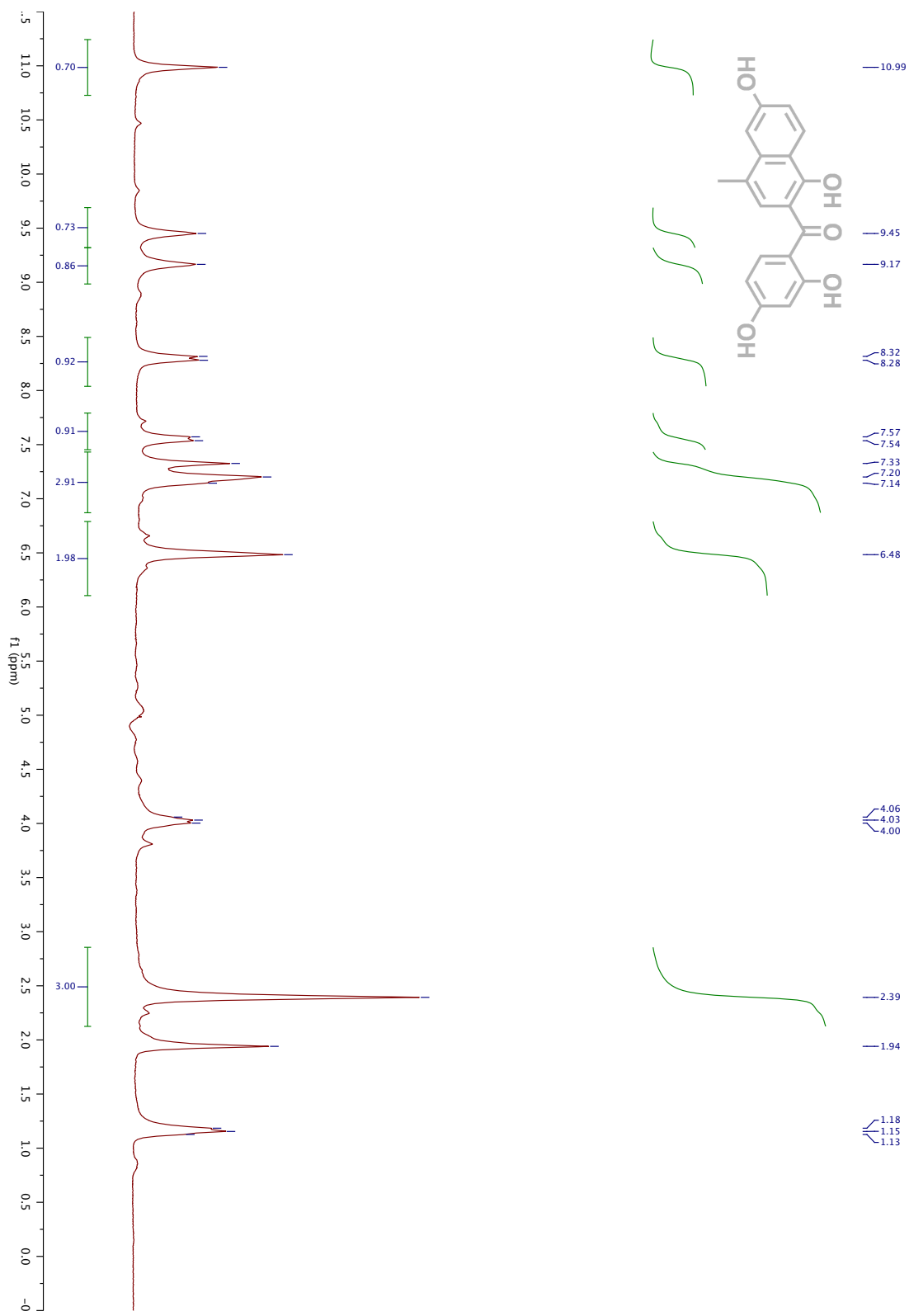0.74
6.00

f1 (ppm)
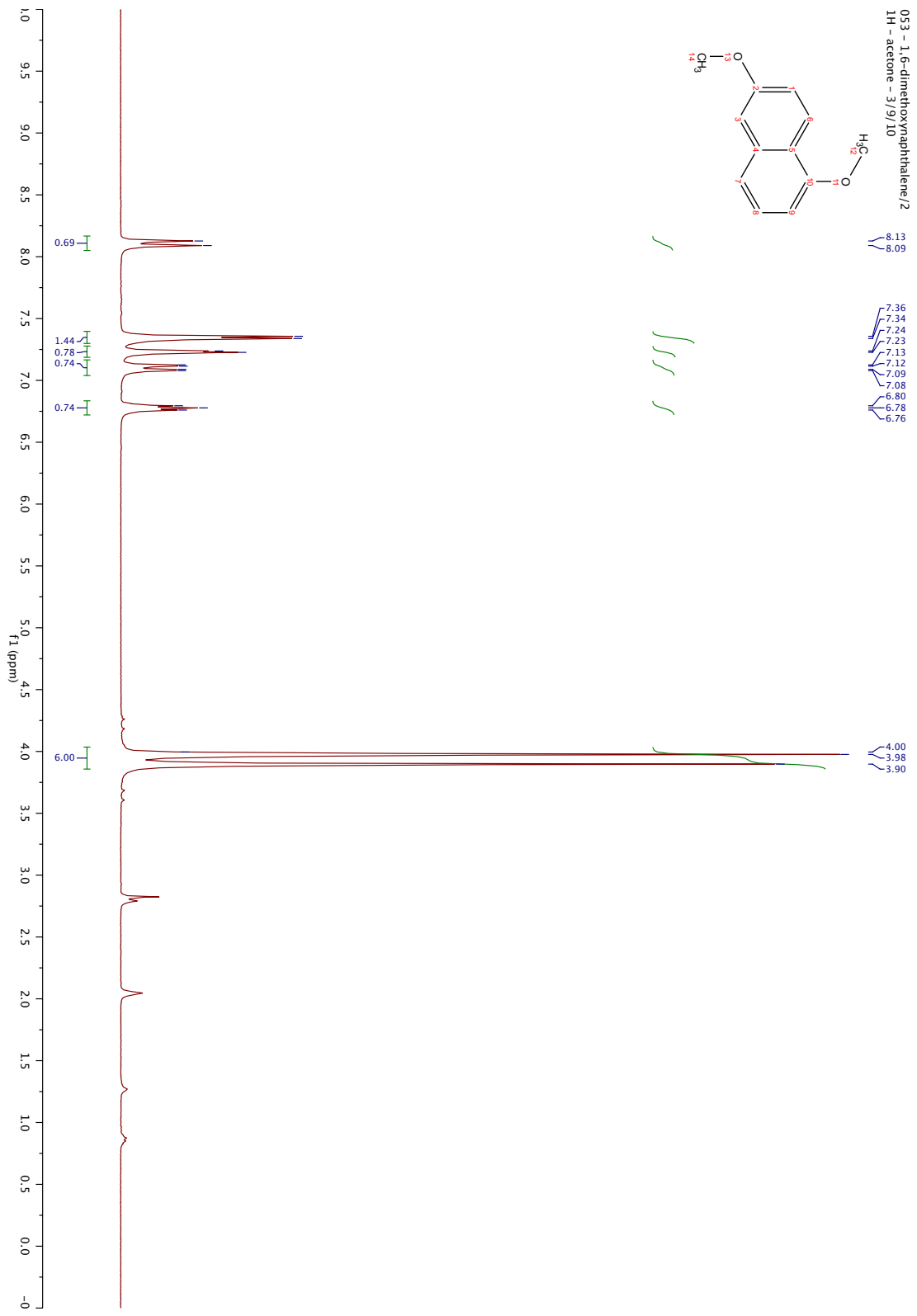
Compound **4-1** (250 MHz, acetone-d6)
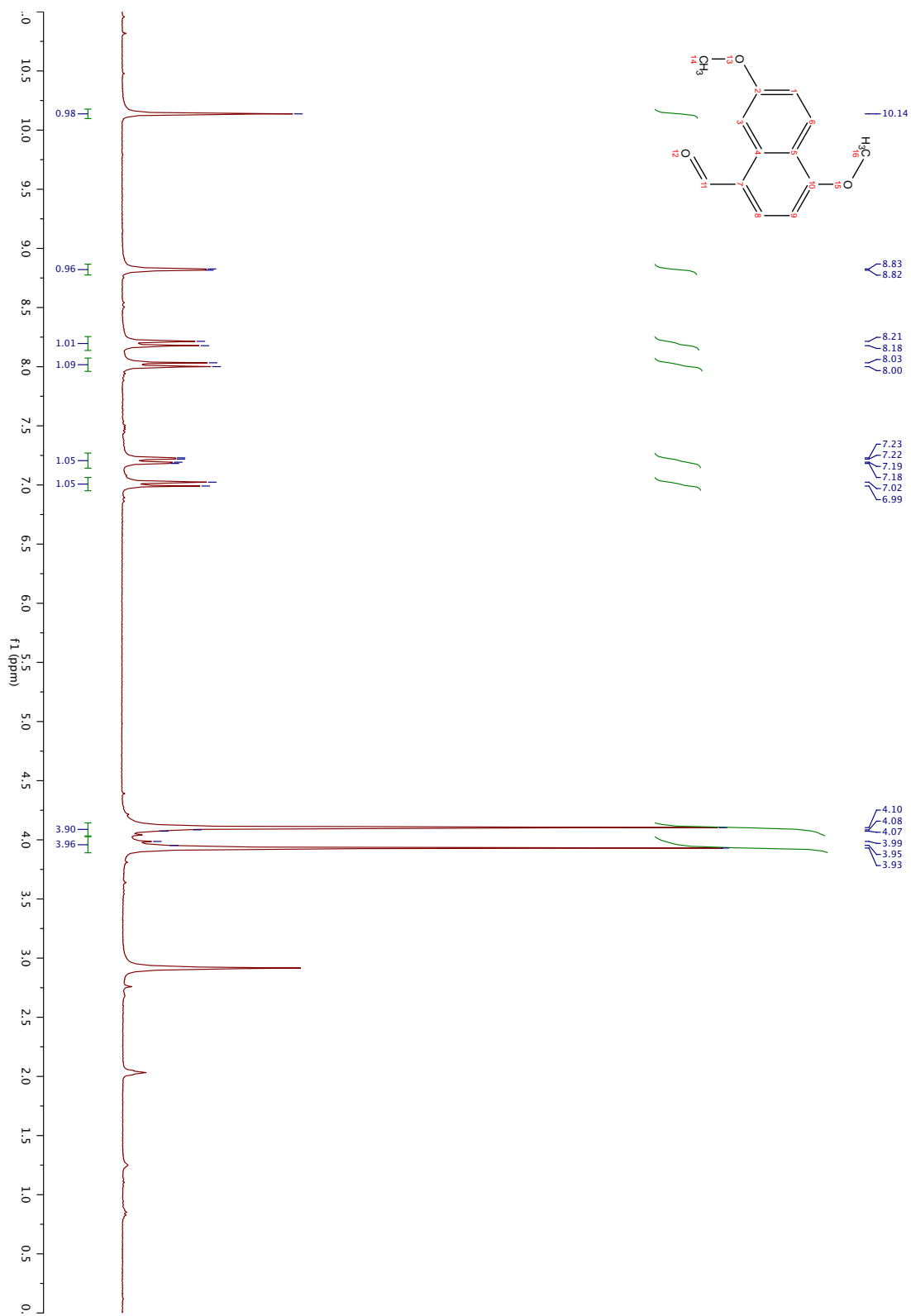
Compound **4-2** (250 MHz, acetone-d6)
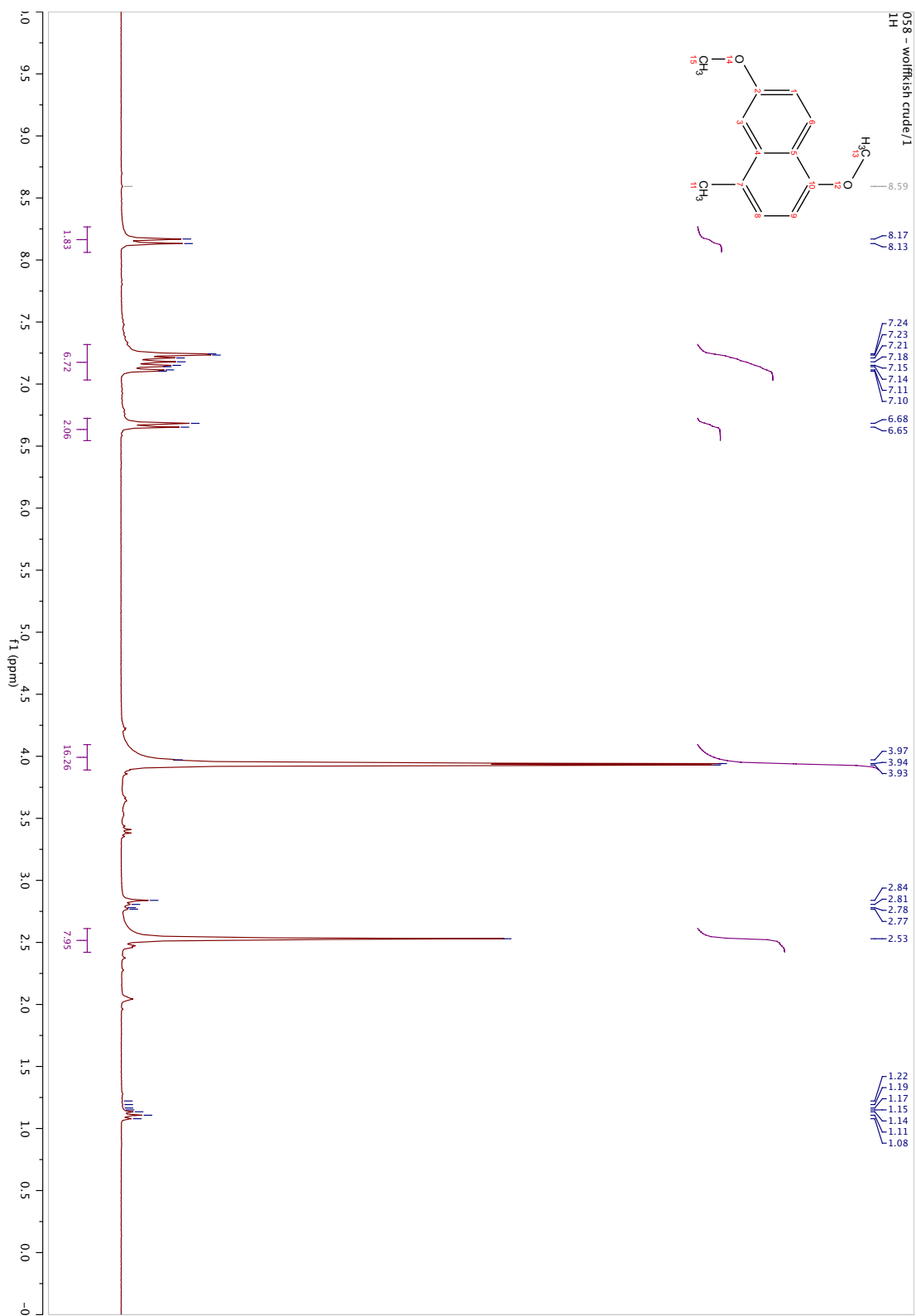
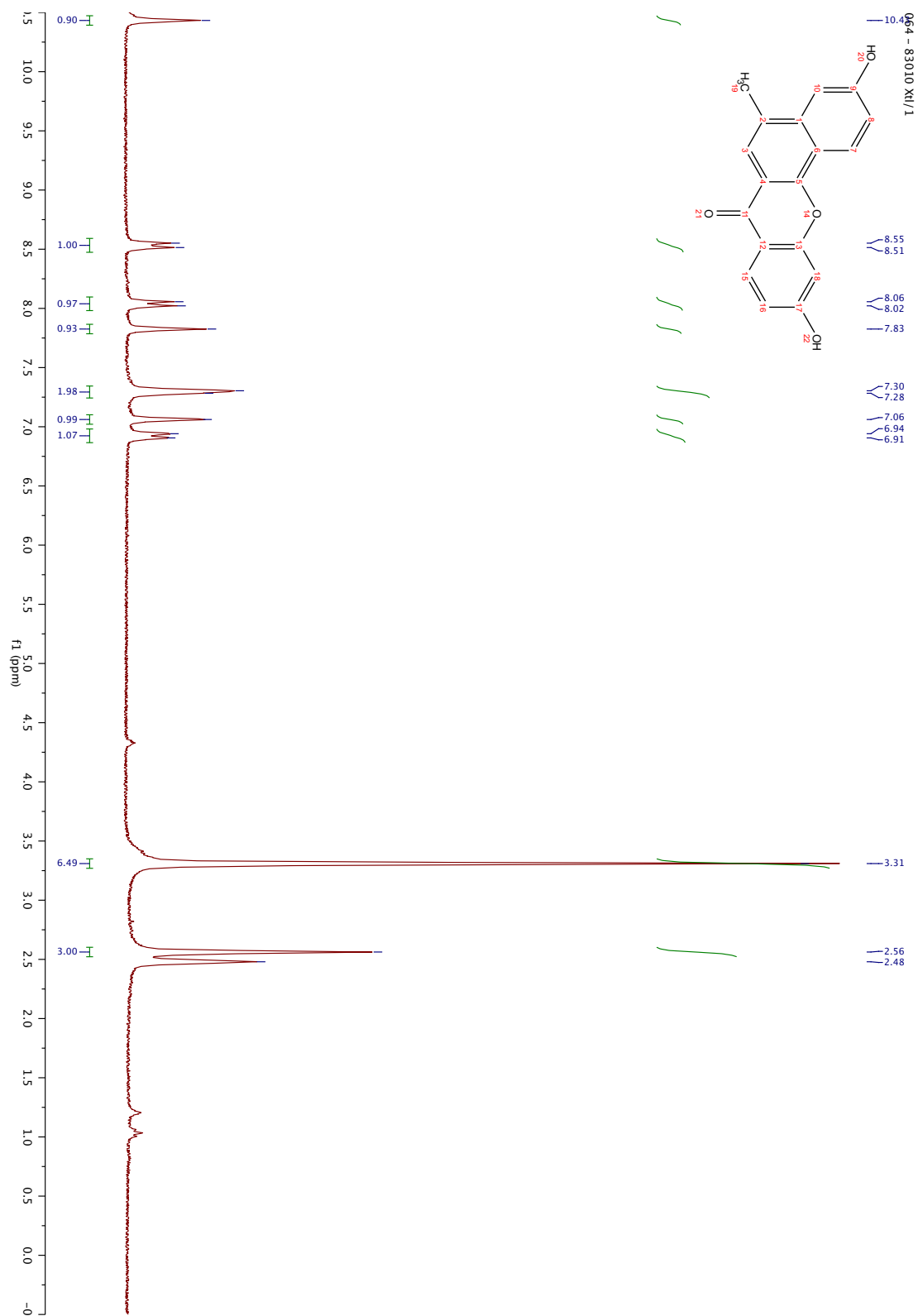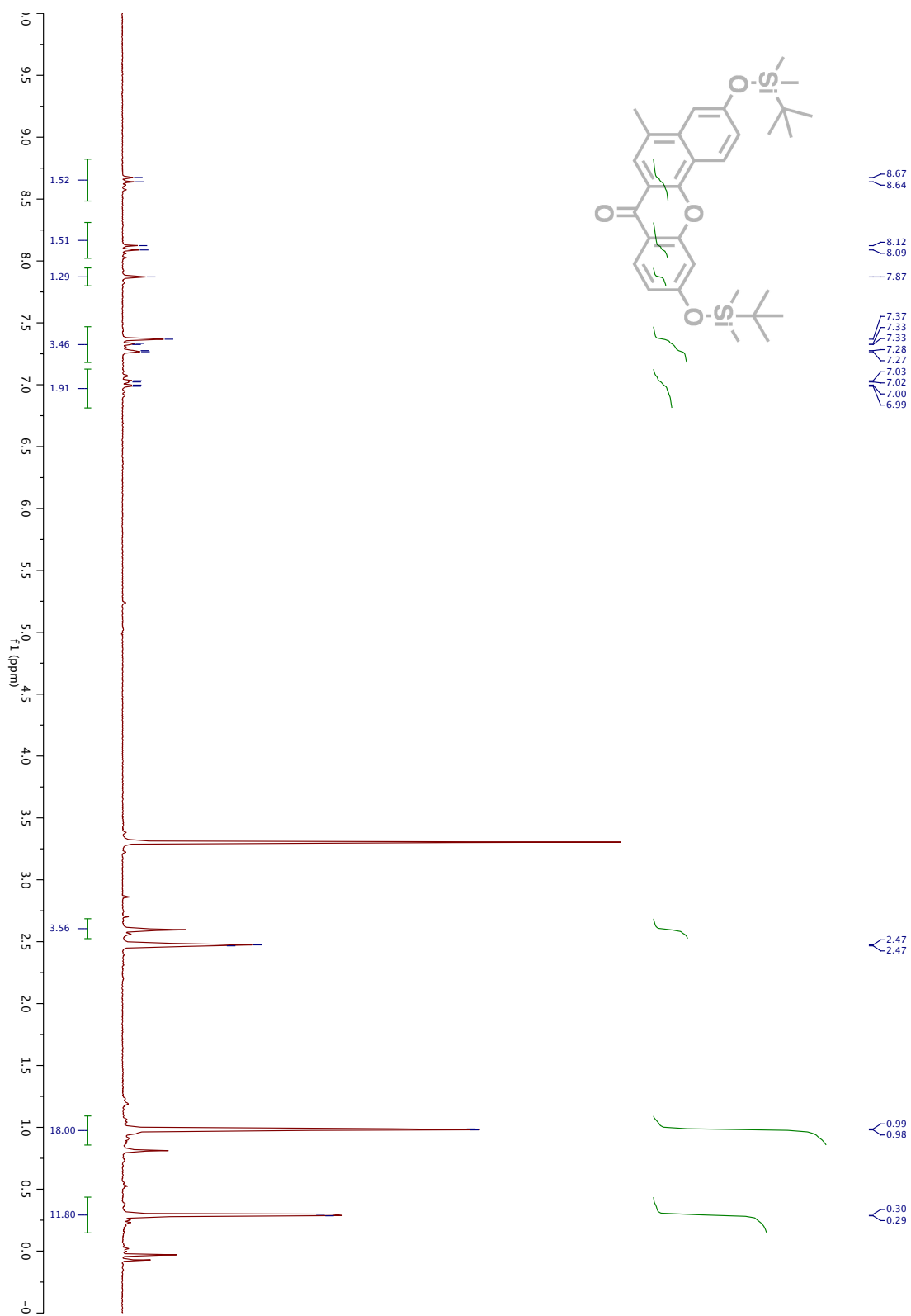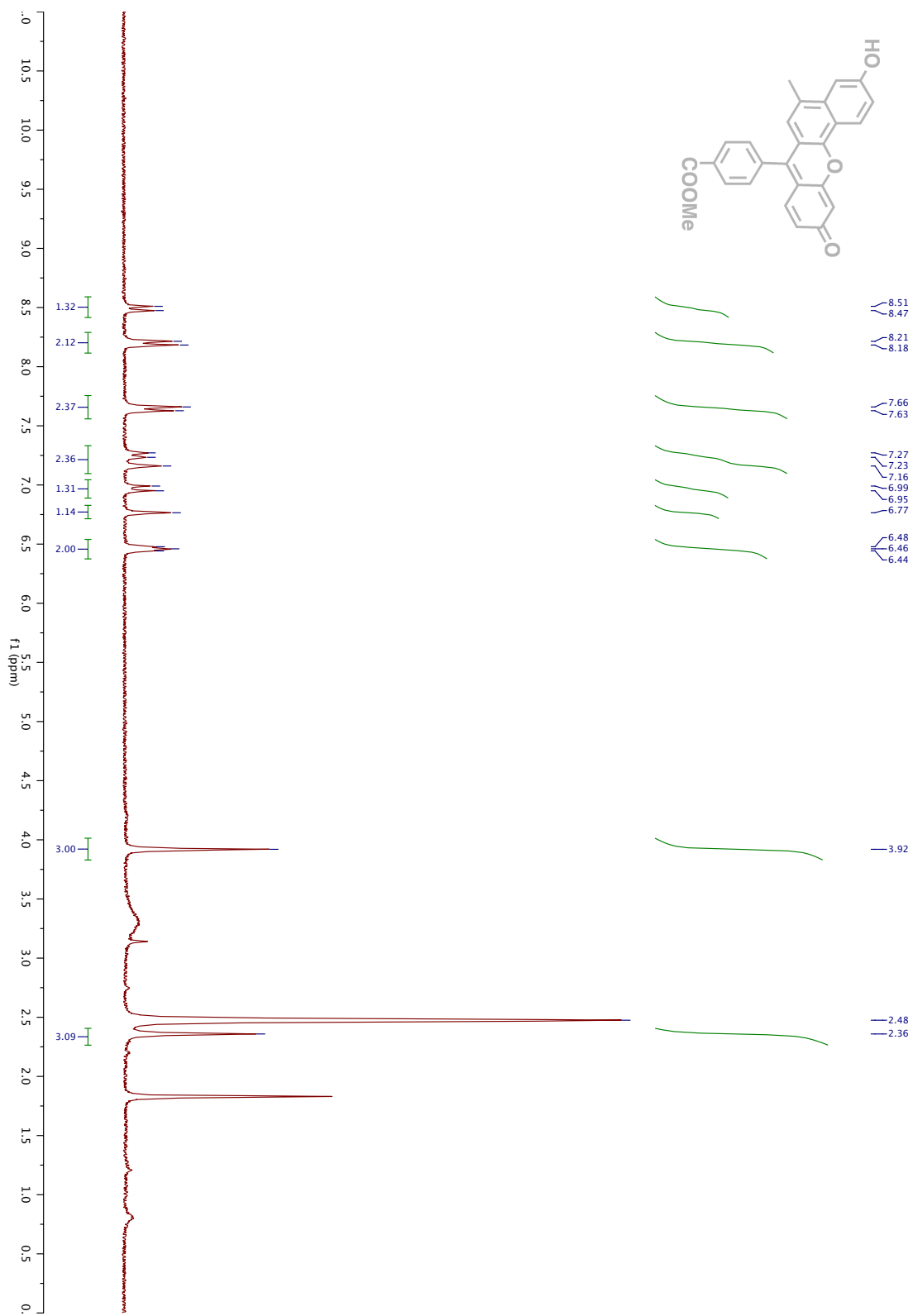Compound **4-3** (250 MHz, acetone-d6)

106

Compound **4-4** (250 MHz, acetone-d6)

Compound **4-5** (crude NMR, 250 MHz, acetone-d6)

Compound **4-6** (250 MHz, DMSO-d6)

Compound **4-7** (250 MHz, CDCl₃)

8.67
8.64

8.12
8.09

7.87

7.37
7.33
7.33
7.28
7.27
7.03
7.02
7.00
6.99

2.47
2.47

0.99
0.98

0.30
0.29

1.52
1.51
1.29
3.46
1.91
3.56
18.00
11.80

Compound **4-8** (250 MHz, DMSO-d6)

111
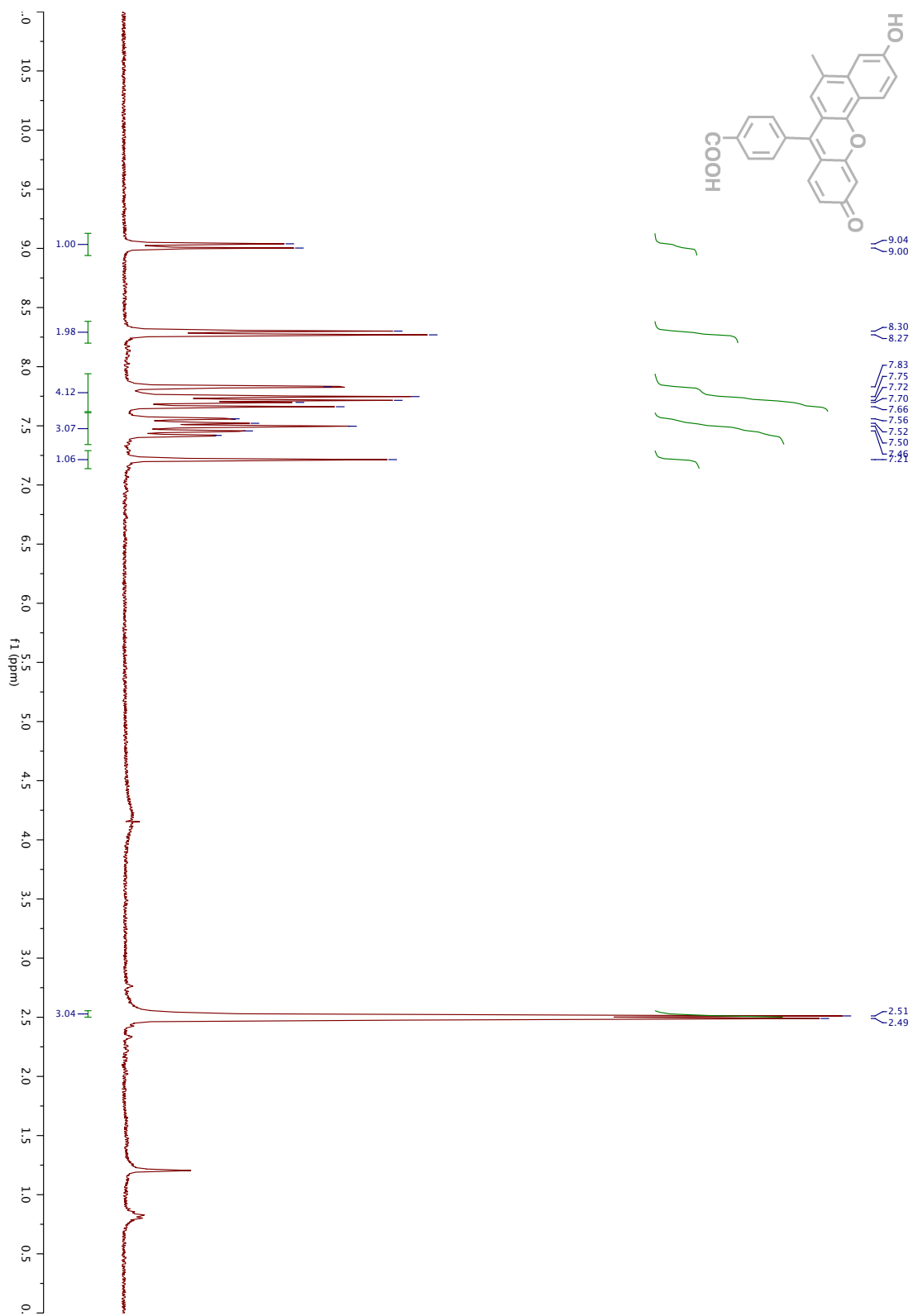
Compound **4-9** (250 MHz, DMSO-d6)

112

VITA

Brian Gerard Imsick was born in 1986 in New York City. At the age of 7, he received his first Periodic Table of the Elements and Organic Structure Model kit. From that point on, he was confident that he desired to study Organic Chemistry. After graduating from high school, he enrolled in Randolph-Macon College in Ashland, Virginia as a Chemistry major. He began his research career in the lab of Professor John D. Thoburn. In June 2008, he graduated with a Bachelor of Science in Chemistry with a thesis titled, "A Dynamic Nuclear Magnetic Resonance Study of *S*-Methyl-*N,N*-Dimethyl Dithiocarbamate" with a side of organic synthesis of novel chiroptical molecular switches based upon dithiocarbamate-iminodithiolane interconversion. He then moved to Baton Rouge, Louisiana to attend Louisiana State University. He joined the laboratory of Professor Evgueni E. Nesterov and contributed to the development of new ratiometric fluorescent sensing materials based on surface-immobilized conjugated oligomers. Brian is a candidate for the Doctor of Philosophy in Organic Chemistry which will be awarded in August 2013 with a dissertation entitled, "Conjugated Organic Functional Materials for Chemical Sensing and Imaging Applications"